Quantification of maxillary ontogenetic processes using surface histology and geometric morphometrics

Der Fakultät für Lebenswissenschaften

der Universität Leipzig

eingereichte

D I S S E R T A T I O N

zur Erlangung des akademischen Grades

Doctor rerum naturalium

(Dr. rer. nat.)

vorgelegt

von *Mag. rer. nat.* Alexandra Schuh

geboren am 25. September 1991 in Colmar, Frankreich

Dekan:	Prof. Dr. Marc Schoenwiesner
Gutachter:	Prof. Dr. Jean-Jacques Hublin Prof. Dr. Antonio Rosas

Tag der Verteidigung: 2. Juli 2021

Acknowledgements

Firstly, I want to express my deep gratitude to Jean-Jacques Hublin who offered me a PhD position in the Department of Human Evolution, and provided me with a productive environment to conduct a PhD. I would also like to thank him for his support throughout the years.

I am also incredibly grateful to my supervisor Sarah Freidline-Stimman, for her unlimited support, her patience, and trust. I would like to thank her for believing in me, and mentoring me not only on the professional, but also on the personal level.

I would also like to thank Kornelius Kupzcik and Philipp Gunz who took an active part in my supervision. To Kornelius, thank you for supporting my application, and for welcoming me to your team. To Philipp, thank you for the support, and all the great scientific insights and inspiration.

This work would not have been possible without the precious help of Silke Streiber, Heiko Temming, Lukas Westphal, Candy Felber, Uta Schwartz, Cornelia Schicke, and David Plotsky. Thank you for all the administrative and technical assistance.

I would like to thank my collaborators, and all the curators who guaranteed access to the collections: Jean-Luc Kahn, Catherine Feja, Niels Lynnerup, Chiara Villa, Wilhelmina Seconna, Victoria Gibbons, David Morris, Ana Luisa Santos, Antonio Rosas, Ildiko Pap, Sandor Evinger, Jean-Jacques Cleyet-Merle, Bruno Maureille, Michel Toussaint, Gregory Abrams and Dominique Bonjean. In particular, thank you to the Scladina team for your warm welcome in Belgium.

I would like to express my thanks to all the persons I had discussions with, who gave me significant insights and help during this PhD: Roger Mundry, Colleen Stephens, Philipp Mitteroecker, Stefan Schlager, Ellen Schulz-Kornas, Maximilian Bemmann, Simon Neubauer, Stephanie Melillo, Viviana Toro Ibacache, Sélim Natahi and Thomas Davies. In particular, I would like to deeply thank Zewdi Tsegai for her comments on this thesis and help with the English, as well as teaching me how to use the CT scanner, and, of course, her friendship. Her kindness has been inspiring me throughout these years. Very special thanks go to my French colleague Adeline Le Cabec, for her enthusiasm, scientific tips, inspiration as well as friendship. Finally, I thank Inga Bergmann for translating the summary of this thesis.

Thank you to all the members of the Department of Human Evolution for the stimulating and welcoming environment. Being part of the Max Planck family has been a huge honor. In particular, I would like to thank all the PhD students met throughout these years: Helen Fewlass, Thomas Davies, Julia Van Beesel, Alexa Benson, Stefanie Stelzer, Inga Bergmann, Frido Welker, Sarah Pederzani, Nicolas Bourgon, Michael Hein, Virginie Sinet-Mathiot, Zineb Moubtahij, Hajar

Alichane and Dorothea Mylopotamitaki. Thank you for creating such a friendly atmosphere. I am sincerely grateful for having been able to work in such an amazing, international environment.

During these years, I have met incredible people that I would like to acknowledge here. Helen Fewlass, Adam Van Casteren, Thomas Davies, Elena Zavala, Laurits Skov and Mikaela Lui. Each one of you has taken part of my "evolution" as a person. Thank you for your true friendship, for all these incredible moments all together in Leipzig (and Berlin!). I do not know what I would have done without you! I would also like to say a very special thank you to David Reher, a very special person and dear friend.

These years in Germany have been full of beautiful moments that I will never forget. Living abroad has always been a goal, as well as speaking several languages. Leipzig is an incredible city that will leave deep marks. I have been lucky to meet incredible new persons, such as my favourite fellow dancers: Christina, Oli, and Sophie. Christina, thank you for this beautiful new friendship, our coffees each Sunday and making me practice my German. To the best dance teacher ever: Mandy, thank you for your energy and giving me back my smile during difficult moments. Many thanks to the Cape Town family, for welcoming me to your house as if we knew each other since forever! This had made my trips to South Africa very special.

To my French friends Marie, Max, Caroline and Aurélien, thank you for our "apéros Skype" during a way too long lockdown. Thank you Marie and Max for all the joy that you have brought in my life for almost 8 years. Marie, I am still counting on discovering new European cities with you once this pandemic is over!

To two very special persons, Déborah Klintz and Marion Stentz. Thank you Marion for 19 years of friendship, and your presence in difficult moments, always believing that I will finally start a PhD. I am so happy that we have continued to evolve in such similar ways. To Déborah, thank you for always bringing me back to real life, a life full of laughers and red wine. Thank you for your energy and craziness, as well as your happiness in every little thing.

To the Natahi/Ottavi family, there are no words to describe how grateful I am for everything you have done for me. In particular, thank you Okba and Marie-Ange for bringing so much joy around you.

To my parents, Claude and Catherine Schuh, I would like to say that everything is possible when there is love and trust. Thank you for making me become who I am today.

Finally, but most importantly, thank you Sélim Natahi for all the happiness you have brought in my life since we met.

BIBLIOGRAPHISCHE DARSTELLUNG

Alexandra Schuh

Quantification of maxillary ontogenetic processes using surface histology and geometrics morphometrics

Fakultät für Lebenswissenschaften

Universität Leipzig

Dissertation

i-vi + 1 - 132 Seiten, 310 Literaturangaben, 25 Abbildungen, 14 Tabellen

This thesis investigates the variability of ontogenetic maxillary bone modeling patterns in humans (*Homo sapiens*) and chimpanzees (*Pan troglodytes*). Along with sutural growth, bone modeling is the microscopic process by which bones grow in size and model their shape. It results from the simultaneous cellular activities of bone formation (produced by the osteoblasts) and bone resorption (produced by the osteoclasts) on bone surfaces. The study of these activities can bring new insights into our understanding of maxillary, and, more generally, facial ontogeny. However, bone modeling variability remains poorly understood. Using surface histology, we developed quantitative methods to objectively compare and visualize bone modeling patterns. In parallel, geometric morphometric methods were used to capture and quantify maxillary shape changes. Both methods were used for the first time together in an integrative approach. A large sample of *H. sapiens* individuals ranging from birth to adulthood, and originating from three geographically distinct areas (Greenland, Western Europe and South Africa), was used to infer the variation in maxillary bone modeling at the intraspecific level. We found that human populations express similar bone modeling patterns, with only subtle differences in the location of bone resorption. Moreover, differences in developmental trajectories were identified. This suggests that population differences in maxillary morphology stem from changes in timing and/or rates of the osteoblastic and osteoclastic activities. Adult individuals show similar maxillary bone modeling patterns to subadults, with both cellular activities expressed at reduced intensities. All human populations express high amounts of bone resorption throughout ontogeny, and high inter-individual variation. In contrast, we find low amounts of bone resorption and a low inter-individual variation in chimpanzees, which results in the anterior projection of their maxilla. In chimpanzees, resorption is predominant in the premaxilla, which has been found in some species of *Australopithecus* and *Paranthropus*. Other similarities in the location of bone resorption, mostly close to the sutures, suggest the preservation of shared ontogenetic patterns between the humans and chimpanzees. The low intraspecific variation in the location of bone resorption found in both species suggests that species-specific bone modeling patterns can be inferred from a limited number of individuals. This will allow future studies to discuss the bone modeling patterns in fossils for which subadult individuals are scarce.

Table of Contents

ALEXANDRA SCHUH

QUANTIFICATION OF MAXILLARY ONTOGENETIC PROCESSES USING SURFACE HISTOLOGY AND GEOMETRIC MORPHOMETRICS

Fakultät für Lebenswissenschaften, Universität Leipzig

Angefertigt am Max Planck Institut für Evolutionäre Anthropologie, Leipzig

Kumulative Dissertation *Leipzig, 2020*

SUMMARY

The overarching theme of the present work concerns the evolution and ontogeny of the human face, with a specific focus on the maxilla. Theories and questions related to the subject are introduced in the following section, as well as the main subject of this thesis: the microscopic development of facial features, or bone modeling. Finally, the major outcomes of the present work are summarized in the last section.

Introduction

The face of present day humans, or *Homo sapiens*, is unique compared to our extinct *Homo* relatives and can be confidently traced back to skeletal material dated to around 300 ka (thousands of years) from the site of Jebel Irhoud in Morocco (Hublin et al., 2017). In particular, the midface (the part comprised between the eyebrows and the mandible) is smaller and more vertically oriented (or orthognathic; e.g., Day & Stringer, 1982; Franciscus & Trinkaus, 1995; Bastir et al., 2010; Holton et al., 2011). Among midfacial bones, the maxilla contains important anatomical information that is valuable for reconstructing phylogenetic relationships. One key feature is the canine fossa, a depression of the maxillary body. This feature, often described as unique to *H. sapiens*, has also been attributed to *H. antecessor*, a juvenile fossil dated between 949 and 772 ka (Duval et al., 2018). This has led some researchers to place this species as a direct ancestor to *H. sapiens* (Bermudez de Castro et al., 1997; Arsuaga et al., 1999). However, due to its complex shape

and ambiguous definition, the use of the canine fossa in determining phylogenetic relationships has been questioned (e.g., Maureille, 1994; Lahr, 1996; Maddux & Franciscus, 2009).

Although all members of *H. sapiens* share the same combination of facial features, their midfacial morphology is highly variable (e.g., Howells, 1973), particularly in the maxilla. Differences in maxillary morphology can be found in the degree of projection of the premaxilla (e.g., Mooney & Siegel, 1986; McCollum, 2008), in the degree of curvature of the canine fossa (e.g., Freidline et al., 2015), as well as in variations in height and width of the nasal aperture (e.g., Holton, 2012). According to some authors, epigenetic factors such as climate and diet have driven facial morphological variability in human populations (e.g., Evteev et al., 2013; Butaric & Maddux, 2016; Cui & Leclercq, 2017; Hubbe et al., 2009; Gonzalez -Jose et al., 2005; Noback & Harvati, 2015; Stynder et al., 2007; von Cramon-Taubadel, 2011; Brachetta-Aporta, 2019a). However, their precise role remains unclear. Studies focusing on facial ontogeny (i.e., growth and development) have shown that adult facial features are built through differential, population-specific patterns of size and shape changes during pre- and post-natal ontogeny, as well as changes in rates and timings of development (e.g., O'Higgins & Vidarsdóttir, 1999; Vidarsdóttir et al., 2002; Bulygina et al., 2006; Freidline et al., 2015). Thus, focusing on the patterns of growth and development of facial features will help to clarify the role of genetic and epigenetic factors in shaping the human face.

In the 1960's, Donald Enlow investigated for the first time human facial bone ontogeny at the microscopic level. His work led to the discovery of a fundamental process, called bone modeling (first named bone "remodeling"[1]; Enlow, 1962). Bone modeling results from the uncoupled cellular activities of bone formation and resorption that respectively add and remove bone on a surface. Along with sutural growth in the cranium (Rice , 2008), it is the process by which a bone grows in size and models its shape. Moreover, it is the compensatory mechanism by which alignment between bones is maintained during ontogeny. The expression of the cells responsible for bone formation and resorption (the osteoblasts and osteoclasts, respectively) is regulated by complex cascades of molecular and chemical signals (e.g., Delmas, 1995; Kini & Nandeesh, 2012). These are partly monitored by the osteocytes (the cells embedded within the cortical bone), which are known to be sensitive to mechanical stimuli (e.g., Huiskes et al., 2000).

Using histological sections of human maxillae, Enlow and Bang (1965) observed the presence of a large resorptive field on the outer bone surface. The authors proposed that this area of bone resorption must play an important role in the development of the characteristic face of *H. sapiens*, making the first link between bone modeling and the development of morphological features. Expanding their observations to more individuals of various ages, Kurihara and co-authors (1980) repeatedly found a similar result. However, they observed that in each individual the size of the resorptive field varies (i.e., resorption is more or less extended across the surface). The authors

[1] In the present work, we follow Frost' definition (1987, 1990, 2003) which separates bone modeling and remodeling in two different processes. Bone remodeling results from the sequential activities of bone resorption and formation on a similar location on a bone layer (either periosteal or endosteal). It is involved in several functions, such as bone renewal, repair of damages as well as homeostasis, and does not affect the shape of the bone (e.g., Barak, 2019; Parfitt, 1984); Hadjidakis & Androulakis, 2006; Schulte et al., 2013).

concluded that individual morphological variation must then relate to the location and extent of the latter. The analysis of facial ontogeny through the study of bone modeling patterns thus represents a promising way to investigate morphological variability among extant species. This will in turn improve our knowledge of extinct species' ontogenetic patterns. Indeed, it might be that seemingly homologous adult features develop via distinct ontogenetic trajectories, and instead are homoplastic. By representing the interface between genetic and morphological data, the analysis of the cellular activity offers new insights into the paleobiology of hominin facial evolution and can add valuable phylogenetic information.

The development of methods such as histology on dry bone surfaces facilitated bone modeling studies (Boyde & Hobdell, 1969a, b; Boyde, 1972; Boyde & Jones, 1996; Bromage, 1984, 1985). A relatively large body of research has since investigated the bone modeling patterns of different extant (Enlow, 1966a; Duterloo & Enlow, 1970; Johnson et al., 1976; Kurihara et al., 1980; Walters & O'Higgins, 1992; O'Higgins & Jones, 1998; O'Higgins et al., 1991, 2001; Wealthall, 2002; Mowbray, 2005; Kranioti et al., 2009; Martínez-Maza et al., 2013, 2015; Freidline et al., 2017; Brachetta-Aporta et al., 2014, 2019a, b) and extinct species (Bromage, 1989; McCollum, 1999, 2008; Martínez-Maza et al., 2011; Brachetta-Aporta et al., 2017; Lacruz et al., 2013, 2015a, b). Altogether, these studies suggest that bone modeling patterns are species specific (e.g., Rosas & Martínez-Maza, 2010). However, O'Higgins and co-authors (1991) as well as Martínez-Maza and co-authors (2015) observed strong similarities in the bone modeling patterns of closely related species. This might imply that some developmental processes are conserved and shared among taxa, and could reflect canalization, the developmental conservation of morphological traits (e.g., Waddington, 1942; Hallgrímsson et al., 2002). It is, however, still unclear which aspects of bone modeling patterns are specific and which are shared among closely related species (such as between Neanderthals and *H. sapiens*; although see Rosas and Martínez-Maza (2010) and Lacruz et al., 2015a).

A new way to investigate these questions is by looking at both bone modeling and morphology together in an integrative approach. As new bone is added on a surface (and resorbed on the other side), this creates a displacement of this area called "cortical drift" (Enlow, 1962; 1966b). The combination of all displacements during ontogeny thus results in macro-scale changes in morphology (i.e., shape). Although the analysis of bone modeling provides information about the location of these displacements on the bone, it does not allow for their visualization. This can, however, be achieved with the use of geometric morphometric techniques (e.g., Bookstein, 1997; Gunz et al., 2005; Mitteroecker & Gunz, 2009). Geometric morphometric methods have been specifically developed for the quantification and visualization of shape changes, and provide powerful tools for ontogenetic analyses (e.g., Vidarsdóttir et al., 2002; Mitteroecker et al., 2004, 2005; Mitteroecker & Bookstein, 2009; Bastir et al., 2006; Freidline et al., 2012, 2013, 2015). In a series of studies using both geometric morphometric and surface histology techniques, O'Higgins and Dryden (1992), as well as O'Higgins and Jones (1998) and O'Higgins and co-authors (2001), showed that the location of bone resorption is largely similar between individuals throughout ontogeny in several primate species. As suggested by the authors, this could indicate that

intraspecific shape changes mostly result from changes in cellular rates rather than differences in bone modeling patterns. Using both techniques in an exploratory investigation of human facial bone modeling patterns, Freidline and co-authors (2017) observed that bone modeling patterns reflect the variation observed at the morphological level, indicating a direct link between microscopic and macroscopic changes.

Together, these influential studies have brought about new developments in the investigation of facial ontogeny. However, as surface histology is a relatively time-consuming method, previous studies lack large ontogenetic samples. This has hampered the possibility of evaluating inter- and intraspecific variability of bone modeling patterns, as well as our understanding of facial development in fossil hominins. In order to gain a better understanding of this variability, the need to develop quantitative methods is of primary importance. Moreover, the use of quantitative instead of qualitative data will also improve the visualization (and thus, the comparison) of the bone modeling patterns, which has long represented a methodological challenge.

Aims of the thesis

The aims of the present thesis are to analyze and quantify the bone modeling patterns of large ontogenetic samples of extant species. This is done by:

(1) Developing novel methods for the quantification and visualization of bone modeling patterns
(2) Applying these techniques to a large number of *H. sapien*s individuals from an ontogenetic series to infer the intra- and inter-population variability of bone modeling patterns
(3) Comparing the results obtained for *H. sapiens* to the bone modeling patterns of chimpanzees (*Pan troglodytes),* a species whose facial projection diverges from humans

This work will, for the first time, determine which aspects of bone modeling are unique to *H. sapiens,* as well as which are shared with other species. This will in turn represent a framework for future studies of fossil hominins. As discussed above, many facial features that distinguish species are located in the midface, and more particularly on the maxilla. For example, in Neanderthals the maxillary body is inflated and the nasal aperture is more projected than in *H. sapiens,* resulting in their unique midfacial prognathism. We thus concentrated our analyses on the latter.

Summary of the results

This dissertation comprises three first-authored peer-reviewed research papers. Chapter 1 was published in the Journal of Anatomy (Schuh et al., 2019), Chapter 2 in the American Journal of Physical Anthropology (Schuh et al., 2020), and Chapter 3 is currently under review in the Journal of Human Evolution.

Chapter 1. Ontogeny of the human maxilla: a study of intra-population variability combining surface bone histology and geometric morphometrics

In this first chapter, new methods for the quantification and visualization of bone modeling patterns are presented and applied to an ontogenetic sample of 47 French individuals of known age (ranging from birth to 12 years) and sex. We tested if (1) bone resorption increases with age as stated by previous authors (Enlow & Bang, 1965; Kurihara et al., 1980; Martínez-Maza et al., 2013); (2) the variability of bone modeling patterns reflects morphological variability (Freidline et al., 2017); (3) areas of bone formation face the direction of growth (i.e., anterior displacements) as proposed by Enlow (1962) and Enlow and Bang (1965). The strength of the methodological approach relies on the direct quantification of bone resorption using images of the bone surface acquired with a digital optical microscope (Smart Zoom 5, Zeiss).

As the bone enlarges in width and length from the first to the twelfth year, the location of bone resorption on the maxilla is highly similar in all individuals, which confirms preliminary investigations of other primate species (O'Higgins & Jones, 1998; Martínez-Maza et al., 2015). This area of bone resorption is present close to the fronto-, zygomatico-, and inter-maxillary sutures, as well as on most of the maxillary arcade. This suggests that on the population level, differences in maxillary morphology are found in the rates of the cellular activities rather than in bone modeling, and that maxillary development is highly constrained from early ontogeny. Furthermore, no difference between sexes could be found in our sample; for conclusive results, this would have to be tested on a larger sample. The average percentage of bone resorption (%BR) increases between birth and 2.5 years (from 23.5 to 43.1%), then stabilizes to about one third of the total surface. This indicates that bone resorption is a rather constant process, although it shows a high variation among individuals of similar ages. Moreover, we found that regions of high morphological variation, such as the frontal process, correspond to areas of predominant bone formation. In contrast, less variable areas such as the maxillary arcade show predominant bone resorption. This might suggest that regions of higher biomechanical demands are more constrained during growth. Finally, confirming Enlow's findings (1962) we found correspondences between the direction of growth (anterior versus posterior displacements), and bone modeling patterns (formation and resorption, respectively). This could potentially be used to predict the direction of growth in fossil specimens for which bone modeling patterns are unknown.

Chapter 2. Intraspecific variability in human maxillary bone modeling patterns during ontogeny

This chapter investigates the intraspecific variability of the maxillary bone modeling patterns to address whether population differences in maxillary morphology relate to differences in the bone modeling patterns during growth. An unprecedentedly large ontogenetic sample of 145 *H. sapiens* individuals (including adults) from three geographically distinct areas (Greenland, Western Europe and South Africa) was used. Similar methods as employed in Chapter 1 were applied to the sample. The joint analysis, or covariation, of the morphological and bone modeling changes was investigated using Partial Least Squares (PLS) analysis (Rohlf & Corti, 2000). This allowed for the visualization of both changes in morphology and bone modeling together in an integrative approach.

We found that population differences in maxillary morphology arise from differential degrees of shape change throughout ontogeny, leading to divergent developmental trajectories. Greenlandic Inuit are more advanced in their development, suggesting differences in the timings and/or rates of development during both pre- and postnatal phases. At the microscopic scale, we found that all human populations share a similar general bone modeling pattern, with predominant bone formation in the frontal process and bone resorption in the maxillary arcade. Only slight differences could be observed. The region of highest bone resorption in Western Europeans and South Africans is mostly located on top of the canine bulb, while it is found close to the inter-maxillary suture in the Inuit sample. These results suggest that only minor differences in bone modeling result in important shape differences between human populations, and once again indicates that the main differences lie in the rates and/or timings of the cellular activities. The PLS analysis showed that all human populations share a similar pattern of covariation with, again, slight differences in the way maxillary morphology and bone modeling covary, mostly in Inuit. Finally, adult individuals show similar bone modeling patterns to subadults, however, expressed at lower intensities. This suggests that patterns of bone modeling are maintained throughout life.

Chapter 3. Prognathism versus orthognathism: new insights into the dynamics behind maxillary bone modeling

This chapter investigates the interspecific variability of the bone modeling patterns by comparing maxillary ontogenetic patterns of chimpanzees (*P. troglodytes*) and *H. sapiens*. Both species show opposite facial projections (prognathic versus orthognathic, respectively), for which fossil hominins show various intermediate degrees (e.g., Bastir et al., 2004). Thus, a better understanding of the ontogenetic mechanisms leading to maxillary projection can bring new insights into the evolution of the hominin face.

An ontogenetic sample of 33 chimpanzees (from birth to adulthood) was employed and compared to the Western European sample included in Chapter 2. Calendar ages and sexes are known for

both species, and similar methods to those in Chapters 1 and 2 were used. We find that the human and chimpanzee maxillary bone modeling patterns differ in many aspects. Chimpanzees express on average lower amounts of bone resorption than humans throughout ontogeny, as well as less variation within age groups. Thus, maxillary prognathism in the chimpanzee mostly develops from high amounts of bone formation, such as seen in other non-human primates studied so far (Enlow, 1966; O'Higgins, et al., 1991; Walter & O'Higgins, 1992; O'Higgins & Jones, 1998; Wealthall, 2002; Martínez-Maza et al., 2015). In the chimpanzee, bone resorption is found close to the sutures, and is predominant in the premaxilla. The postnatal development of the canine eminence in chimpanzees is accompanied by an increase in bone formation, which remains predominant in this area until adulthood. This represents a key difference between the human and chimpanzee maxillary bone modeling pattern. It is thus likely that alterations of the upper canine/premolar honing complex, a derived trait shared by all hominins, was concomitant with changes in the bone modeling patterns of this area. Using Partial Least Squares analysis, we show that the covariation between bone modeling and shape is low in both species, and shows a similar pattern up until adolescence. This suggests that during maxillary ontogeny, bone modeling is a highly stable process, and that most morphological changes are obtained via changes in rates and/or timing of development of the cellular activities. Finally, although both bone modeling patterns differ, some similarities in the location of bone resorption suggest the preservation of a shared ontogenetic pattern between the two species.

Bibliography

Arsuaga, J.-L., Martínez, I., Lorenzo, C., Gracia, A., Mun, A., & Alonso, O. (1999). The human cranial remains from Gran Dolina lower Pleistocene site (Sierra de Atapuerca, Spain). *Journal of Human Evolution, 37*(3-4), 431-457.

Barak, M.M. (2019). Bone modeling or bone remodeling: That is the question. *American Journal of Physical Anthropology, 172*(2), 153-155.

Bastir, M., & Rosas, A. (2004). Facial heights: evolutionary relevance of postnatal ontogeny for facial orientation and skull morphology in humans and chimpanzees. *J Hum Evol, 47*(5), 359-381.

Bastir, M., Rosas, A., Lieberman, D.E., & O'Higgins, P. (2008). Middle cranial fossa anatomy and the origin of modern humans. *Anat Rec (Hoboken), 291*(2), 130-140.

Bastir, M., Rosas, A., & O'Higgins, P. (2006). Craniofacial levels and the morphological maturation of the human skull. *J Anat, 209*(5), 637-654.

Bastir, M., Rosas, A., Stringer, C., Cuetara, J.M., Kruszynski, R., Weber, G.W., Ross, C.F., & Ravosa, M.J. (2010). Effects of brain and facial size on basicranial form in human and primate evolution. *J Hum Evol, 58*(5), 424-431.

Bermúdez de Castro, J.M., Arsuaga, J.L., Carbonell, E., Rosas, A., Martínez, I., & Mosquera, M. (1997). A Hominid from the Lower Pleistocene of Atapuerca, Spain: Possible Ancestor to Neandertals and Modern Humans. *276*(5317), 1392-1395.

Bookstein, F.L. (1997). Landmark methods for forms without landmarks: morphometrics of group differences in outline shape. *Medical Image Analysis, 1*(3), 225-243.

Boyde, A. (1972). Scanning electron microscope studies of bone. In G. H. Bourne (Ed.), *The Biochemistry and physiology of bone*. New York: Academic Press.

Boyde, A., & Hobdell, M.H. (1969a). Scanning electron microscopy of Lamellar bone. *Z. Zellforsch., 93*, 213-231.

---. (1969b). Scanning Electron Microscopy of Primary Membrane Bone. *Z.Zellfotsch., 99*, 98-108.

Boyde, A., & Jones, S. (1996). Scanning Electron Microscopy of Bone: Instrument, Specimen, and Issues. *Microscopy Research and Technique, 32*, 92-120.

Brachetta-Aporta, N., Gonzalez, P.N., & Bernal, V. (2017). A quantitative approach for analysing bone modelling patterns from craniofacial surfaces in hominins. *Journal of Anatomy*, n/a-n/a.

---. (2019a). Integrating data on bone modeling and morphological ontogenetic changes of the maxilla in modern humans. *Annals of Anatomy - Anatomischer Anzeiger, 222*, 12-20.

Brachetta-Aporta, N., Gonzalez, P.N., & Bernal, V. (2019b). Variation in facial bone growth remodeling in prehistoric populations from southern South America. *169*(3), 422-434.

Brachetta Aporta, N., Martínez-Maza, C., Gonzalez, P.N., & Bernal, V. (2014). Bone modeling patterns and morphometric craniofacial variation in individuals from two prehistoric human populations from Argentina. *Anat Rec (Hoboken), 297*(10), 1829-1838.

Bromage, T.G. (1984). Interpretation of Scanning Electron Microscopic Images of Abraded Forming Bone Surfaces. *American Journal of Physical Anthropology, 64*, 161-178.

Bromage, T.G. (1985). Systematic inquiry of in tests of negative/positive replica combinations for SEM. *Journal of Microscopy, 137*(2), 209-216.

---. (1989). Ontogeny of the early hominin face. *Journal of Human Evolution, 18*, 751-773.

Bulygina, E., Mitteroecker, P., & Aiello, L. (2006). Ontogeny of facial dimorphism and patterns of individual development within one human population. *Am J Phys Anthropol, 131*(3), 432-443.

Butaric, L.N., & Maddux, S.D. (2016). Morphological Covariation between the Maxillary Sinus and Midfacial Skeleton among Sub-Saharan and Circumpolar Modern Humans. *American Journal of Physical Anthropology, 160*(3), 483-497.

Cui, Y., & Leclercq, S. (2017). Environment-Related Variation in the Human Mid-Face. *The Anatomical Record, 300*(1), 238-250.

Day, M., & Stringer, C. (1982). L'Homo erectus et la place de l'homme de Tautavel permi les hominides fossiles. In: Centre National de la Recherche Scientifique, Nice, France.

Delmas, P.D. (1995). Biochemical markers of bone turnover. *Acta Orthopaedica Scandinavica, 66*(sup266), 176-182.

Duterloo, H.S., & Enlow, D.H. (1970). A comparative study of cranial growth in Homo and Macaca. *American Journal of Anatomy, 127*(4), 357-367.

Duval, M., Grün, R., Parés, J.M., Martín-Francés, L., Campaña, I., Rosell, J., Shao, Q., Arsuaga, J.L., Carbonell, E., & Bermúdez de Castro, J.M. (2018). The first direct ESR dating of a hominin tooth from Atapuerca Gran Dolina TD-6 (Spain) supports the antiquity of Homo antecessor. *Quaternary Geochronology, 47*, 120-137.

Enlow, D.H. (1962). A Study of the Post-Natal Growth and Remodeling of Bone. *American Journal of Anatomy, 110*(2), 79-101.

Enlow, D.H. (1966a). A comparative study of facial growth in Homo and Macaca. *American Journal of Physical Anthropology, 24*(3), 293-307.

---. (1966b). A morphogenetic analysis of facial growth. *American journal of orthodontics, 52*(4), 283-299.

Enlow, D.H., & Bang, D.D.S. (1965). Growth and remodeling of the human maxilla. *American journal of orthodontics, 51*(6), 446-464.

Evteev, A., Cardini, A.L., Morozova, I., & O'Higgins, P. (2013). Extreme climate, rather than population history, explains mid-facial morphology of northern asians. *American Journal of Physical Anthropology, 153*(3), 449-462.

Franciscus, R.G., & Trinkaus, E. (1995). Determinants of retromolar space presence in Pleistocene Homo mandibles. *Journal of Human Evolution, 28*(6), 577-595.

Freidline, S.E., Gunz, P., Harvati, K., & Hublin, J.-J. (2013). Evaluating developmental shape changes in Homo antecessor subadult facial morphology. *Journal of Human Evolution, 65*(4), 404-423.

Freidline, S.E., Gunz, P., Harvati, K., & Hublin, J.J. (2012). Middle Pleistocene human facial morphology in an evolutionary and developmental context. *J Hum Evol, 63*(5), 723-740.

Freidline, S.E., Gunz, P., & Hublin, J.J. (2015). Ontogenetic and static allometry in the human face: contrasting Khoisan and Inuit. *Am J Phys Anthropol, 158*(1), 116-131.

Freidline, S.E., Gunz, P., Jankovic, I., Harvati, K., & Hublin, J.J. (2012). A comprehensive morphometric analysis of the frontal and zygomatic bone of the Zuttiyeh fossil from Israel. *J Hum Evol, 62*(2), 225-241.

Freidline, S.E., Martínez-Maza, C., Gunz, P., & Hublin, J.J. (2017). Exploring Modern Human Facial Growth at the Micro- and Macroscopic Levels. In C. J. Percival & J. T. Richtsmeier (Eds.), *Buidling bones*. Cambridge: Cambridge University Press.

Frost, H.M. (1987). Bone "mass" and the "mechanostat": A proposal. *The Anatomical Record, 219*(1), 1-9.

Frost, H.M. (1990). Skeletal structural adaptations to mechanical usage (SATMU): 1. Redefining Wolff's law: the bone modeling problem. *The Anatomical Record, 226*(4), 403-413.

Frost, H.M. (2003). Bone's Mechanostat: A 2003 Update. *The Anatomical Record, 275*(A), 1081-1101.

Gonzalez-Jose, R., Ramirez-Rozzi, F., Sardi, M., Martínez-Abadias, N., Hernandez, M., & Pucciarelli, H.M. (2005). Functional-cranial approach to the influence of economic strategy on skull morphology. *Am J Phys Anthropol, 128*(4), 757-771.

Gunz, P., Mitteroecker, P., & Bookstein, F. (2005). Semilandmarks in three dimensions. In D. E. Slice (Ed.), *Modern Morphometrics in Physical Anthroplogy*. New York: Kluwer Press.

Hadjidakis, D.J., & Androulakis, I.I. (2006). Bone remodeling. *Annals of the New York Academy of Sciences, 1092*(1), 385-396.

Hallgrímsson, B., Willmore, K., & Hall, B.K. (2002). Canalization, developmental stability, and morphological integration in primate limbs. *American Journal of Physical Anthropology, Suppl 35*, 131-158.

Holton, N.E., Franciscus, R.G., Marshall, S.D., Southard, T.E., & Nieves, M.A. (2011). Nasal Septal and Premaxillary Developmental Integration: Implications for Facial Reduction in Homo. *The Anatomical Record, 294*(1), 68-78.

Holton, N.E., Franciscus, R.G., Nieves, M.A., Marshall, S.D., Reimer, S.B., Southard, T.E., Keller, J.C., & Maddux, S.D. (2010). Sutural growth restriction and modern human facial evolution: an experimental study in a pig model. *Journal of Anatomy, 216*(1), 48-61.

Holton, N.E., Yokley, T.R., & Figueroa, A. (2012). Nasal septal and craniofacial form in European- and African-derived populations. *Journal of Anatomy, 221*(3), 263-274.

Howells, W. (1973). *Cranial Variation in Man: A Study by Multivariate Analysis of Patterns of Difference among Recent Human Populations*. Cambridge: MA: Harvard University Press.

Hubbe, M., Hanihara, T., & Harvati, K. (2009). Climate Signatures in the Morphological Differentiation of Worldwide Modern Human Populations. *292*(11), 1720-1733.

Hublin, J.-J., Ben-Ncer, A., Bailey, S.E., Freidline, S.E., Neubauer, S., Skinner, M.M., Bergmann, I., Le Cabec, A., Benazzi, S., Harvati, K., & Gunz, P. (2017). New fossils from Jebel Irhoud, Morocco and the pan-African origin of Homo sapiens. *Nature, 546*, 289.

Huiskes, R., Ruimerman, R., Van Lenthe, G.H., & Janssen, J.D. (2000). Effects of mechanical forces on maintenance and adaptation of form in trabecular bone. *Nature, 405*(6787), 704-706.

Johnson, P.A., Atkinson, P.J., & Moore, W.J. (1976). The development and structure of the chimpanzee mandible. *Journal of Anatomy, 122*(2), 467-477.

Kini, U., & Nandeesh, B.N. (2012). Physiology of Bone Formation, Remodeling, and Metabolism. 29-57.

Kranioti, E.F., Rosas, A., Garcia-Vargas, S., Estalrrich, A., Bastir, M., & Pena-Melian, A. (2009). Remodeling patterns of occipital growth: a preliminary report. *Anat Rec (Hoboken), 292*(11), 1764-1770.

Kurihara, S., Enlow, D.H., & Rangel, R.D. (1980). Remodeling Reversals in Anterior Parts of the Human Mandible and Maxilla. *The Angle Orthodontics, 50*(2), 98-106.

Lacruz, R.S., Bromage, T.G., O'Higgins, P., Arsuaga, J.L., Stringer, C., Godinho, R.M., Warshaw, J., Martínez, I., Gracia-Tellez, A., de Castro, J.M., & Carbonell, E. (2015a). Ontogeny of the maxilla in Neanderthals and their ancestors. *Nat Commun, 6*, 8996.

Lacruz, R.S., Bromage, T.G., O'Higgins, P., Toro-Ibacache, V., Warshaw, J., & Berger, L.R. (2015b). Distinct growth of the nasomaxillary complex in Au. sediba. *Sci Rep, 5*, 15175.

Lacruz, R.S., de Castro, J.M., Martinon-Torres, M., O'Higgins, P., Paine, M.L., Carbonell, E., Arsuaga, J.L., & Bromage, T.G. (2013). Facial morphogenesis of the earliest europeans. *PLOS ONE, 8*(6), e65199.

Lahr, M.M. (1996). *The evolution of modern human diversity: a study of cranial variation* (Vol. 18): Cambridge University Press.

Maddux, S.D., & Franciscus, R.G. (2009). Allometric scaling of infraorbital surface topography in Homo. *J Hum Evol, 56*(2), 161-174.

Martínez-Maza, C., Freidline, S.E., Strauss, A., & Nieto-Diaz, M. (2015). Bone Growth Dynamics of the Facial Skeleton and Mandible in Gorilla gorilla and Pan troglodytes. *Evolutionary Biology, 43*(1), 60-80.

Martínez-Maza, C., Rosas, A., Garcia-Vargas, S., Estalrrich, A., & de la Rasilla, M. (2011). Bone remodelling in Neanderthal mandibles from the El Sidron site (Asturias, Spain). *Biol Lett, 7*(4), 593-596.

Martínez-Maza, C., Rosas, A., & Nieto-Diaz, M. (2013). Postnatal changes in the growth dynamics of the human face revealed from bone modelling patterns. *J Anat, 223*(3), 228-241.

Maureille, B. (1994). *La face chez Homo erectus et Homo sapiens: recherche sur la variabilité morphologique et métrique, Anthropologie.* Ph. D. Dissertation, Uni-versité de Bordeaux 1,

McCollum, M.A. (1999). The Robust Australopithecine Face: A Morphogenetic Perspective. *Science, 284*(5412), 301-305.

---. (2008). Nasomaxillary remodeling and facial form in robust Australopithecus: a reassessment. *J Hum Evol, 54*(1), 2-14.

Mitteroecker, P., & Bookstein, F. (2009). The ontogenetic trajectory of the phenotypic covariance matrix, with examples from craniofacial shape in rats and humans. *Evolution, 63*(3), 727-737.

Mitteroecker, P., & Gunz, P. (2009). Advances in Geometric Morphometrics. *Evolutionary Biology, 36*(2), 235-247.

Mitteroecker, P., Gunz, P., Bernhard, M., Schaefer, K., & Bookstein, F.L. (2004). Comparison of cranial ontogenetic trajectories among great apes and humans. *J Hum Evol, 46*(6), 679-697.

Mitteroecker, P., Gunz, P., & Bookstein, F.L. (2005). Heterochrony and geometric morphometrics: a comparison of cranial growth in Pan paniscus versus Pan troglodytes. *Evolution & Development, 7*(3), 244-258.

Mitteroecker, P., Gunz, P., Weber, G.W., & Bookstein, F.L. (2004). Regional dissociated heterochrony in multivariate analysis. *Annals of Anatomy - Anatomischer Anzeiger, 186*(5), 463-470.

Mooney, M.P., & Siegel, M.I. (1986). Developmental relationship between premaxillary-maxillary suture patency and anterior nasal spine morphology. *Cleft Palate J, 23*(2), 101-107.

Mowbray, K. (2005). Surface bone histology of the occipital bone in humans and chimpanzees. *Anat Rec B New Anat, 283*(1), 14-22.

Noback, M.L., & Harvati, K. (2015). The contribution of subsistence to global human cranial variation. *Journal of Human Evolution, 80*, 34-50.

O'Higgins, P., Bromage, T.G., Johnson, D.R., Moore, W.J., & McPhie, P. (1991). A Study of Facial Growth in the Sooty Mangabey *Cercocebus atys*. *Folia Primatologica, 56*(2), 86-94.

O'Higgins, P., Chadfield, P., & Jones, N. (2001). Facial growth and the ontogeny of morphological variation within and between the primates Cebus apella and Cercocebus torquatus. *Journal of Zoology, 254*, 337-357.

O'Higgins, P., & Dryden, I. (1992). Studies of craniofacial development and evolution. *Archaeology in Oceania, 27*(3), 105-112.

O'Higgins, P., & Jones, N. (1998). Facial growth in Cercocebus torquatus: an application of three-dimensional geometric morphometric techniques to the study of morphological variation. *Journal of Anatomy, 193*(2), 251-272.

O'Higgins, P., & Vidarsdóttir, U.E. (1999). New approaches to the quantitative analysis of craniofacial growth and variation. In C. U. Press (Ed.), *Human growth in the past: studies from bones and teeth* (pp. 128-160).

Parfitt, A. (1984). The cellular basis of bone remodeling: the quantum concept reexamined in light of recent advances in the cell biology of bone. *Calcified Tissue International, 36*(1), S37-S45.

Rice, D. (2008). *Craniofacial Sutures: Development, Disease, and Treatment.* (R. DP Ed. Vol. 12). Basel: Karger.

Rohlf, F.J., & Corti, M. (2000). Use of Two-Block Partial Least-Squares to Study Covariation in Shape. *Systematic Biology, 49*(4), 740-753.

Rosas, A., & Martínez-Maza, C. (2010). Bone remodeling of the Homo heidelbergensis mandible; the Atapuerca-SH sample. *J Hum Evol, 58*(2), 127-137.

Rosas, A., Martínez-Maza, C., Bastir, M., García-Tabernero, A., Lalueza-Fox, C., Huguet, R., Ortiz, J.E., Julià, R., Soler, V., de Torres, T., Martínez, E., Cañaveras, J.C., Sánchez-Moral, S., Cuezva, S., Lario, J., Santamaría, D., de la Rasilla, M., & Fortea, J. (2006). Paleobiology and comparative morphology of a late Neandertal sample from El Sidrón, Asturias, Spain. *Proceedings of the National Academy of Sciences, 103*(51), 19266-19271.

Schuh, A., Gunz, P., Villa, C., Kupczik, K., Hublin, J.J., & Freidline, S.E. (2020). Intraspecific variability in human maxillary bone modeling patterns during ontogeny. *American Journal of Physical Anthropology, 173*(4), 655-670.

Schuh, A., Kupczik, K., Gunz, P., Hublin, J.-J., & Freidline, S.E. (2019). Ontogeny of the human maxilla: a study of intra-population variability combining surface bone histology and geometric morphometrics. *Journal of Anatomy, 235*(2), 233-245.

Schulte, F.A., Ruffoni, D., Lambers, F.M., Christen, D., Webster, D.J., Kuhn, G., & Muller, R. (2013). Local mechanical stimuli regulate bone formation and resorption in mice at the tissue level. *PLOS ONE, 8*(4), e62172.

Stynder, D.D., Ackermann, R.R., & Sealy, J.C. (2007). Craniofacial variation and population continuity during the South African Holocene. *134*(4), 489-500.

Vidarsdóttir, U.E., O'Higgins, P., & Stringer, C. (2002). A geometric morphometric study of regional differences in the ontogeny of the modern human facial skeleton. *Journal of Anatomy, 201*, 211-229.

von Cramon-Taubadel, N. (2011). Global human mandibular variation reflects differences in agricultural and hunter-gatherer subsistence strategies. *Proceedings of the National Academy of Sciences, 108*(49), 19546-19551.

Waddington, C.H. (1942). Canalization of the development and the inheritance of acquired characters. *Nature, 150*, 563.

Walters, M., & O'Higgins, P. (1992). *Factors influencing craniofacial growth: a scanning electron microscope study of high resolution facial replicas.* Paper presented at the Proc Australas Soc Hum Biol.

Wealthall, R.J. (2002). Surface remodelling of the facial skeleton in juvenile Macaca mulatta: implications for sexual dimorphism. *Folia Primatologica, 73*(1), 49-53.

ALEXANDRA SCHUH

QUANTIFIZIERUNG VON ONTOGENETISCHEN PROZESSEN DER MAXILLA MIT HILFE DER OBERFLÄCHENHISTOLOGIE SOWIE DER GEOMETRISCHEN MORPHOMETRIE

Fakultät für Lebenswissenschaften, Universität Leipzig

Angefertigt am Max-Planck-Institut für evolutionäre Anthropologie, Leipzig

Kumulative Dissertation *Leipzig, 2020*

ZUSAMMENFASSUNG

Das übergreifende Thema der vorliegenden Arbeit ist die Evolution und Ontogenese des menschlichen Gesichts, mit einem besonderen Fokus auf die Maxilla. Neben Theorien und Fragen wird im Folgenden das Hauptthema vorgestellt: die Entwicklung von Gesichtszügen auf mikroskopischer Ebene, auch als Knochenumbau bezeichnet. Im letzten Abschnitt werden die wichtigsten Ergebnisse zusammengefasst.

Einleitung

Das Gesicht des heutigen Menschen, des *Homo sapiens*, ist einzigartig im Vergleich zu unseren ausgestorbenen *Homo* Verwandten und kann zuverlässig bis auf Skelettmaterial von Jebel Irhoud in Marokko (etwa 300.000 Jahre alt) zurückverfolgt werden (Hublin et al., 2017). Besonders unser Mittelgesicht (der Teil zwischen den Augenbrauen und dem Unterkiefer) ist kleiner und vertikaler ausgerichtet (oder orthognath; z.B. Day & Stringer, 1982; Franciscus & Trinkaus, 1995; Bastir et al., 2010; Holton et al., 2011). Unter den Mittelgesichtsknochen enthält die Maxilla wichtige anatomische Informationen, die für die Rekonstruktion phylogene-tischer Beziehungen wertvoll sind. Ein Schlüsselmerkmal ist die Fossa Canina, eine Vertiefung im Oberkieferkörper. Dieses Merkmal, das oft als einzigartig für *H. sapiens* beschrieben wird, wurde auch *H. antecessor* zugeschrieben, einem juvenilen Fossil, welches zwischen 949 und 772 ka v.h. datiert wurde (Duval et al., 2018). Einige Forscher fühlten sich veranlasst, diese Art als direkten Vorfahren von *H. sapiens* anzusehen (Bermudez de Castro et al., 1997; Arsuaga et al., 1999). Aufgrund seiner komplexen Form und mehrdeutigen Definition wurde jedoch die Verwendung der Fossa Canina

bei der Bestimmung stammesgeschichtlicher Beziehungen in Frage gestellt (z. B. Maureille, 1994; Lahr, 1996; Maddux & Franciscus, 2009).

Obwohl jeder *H. sapiens* die gleiche Kombination von Gesichtszügen aufweist, ist seine Mittelgesichtsmorphologie sehr variabel (z.B. Howells, 1973), insbesondere die des Ober-kiefers. Unterschiede in der Kiefermorphologie finden sich im Projektionsgrad des Zwischen-kieferbeins (z.B. Mooney & Siegel, 1986; McCollum, 2008), im Krümmungsgrad der Fossa Canina (z.B. Freidline et al., 2015), sowie in Höhen- und Breitenschwankungen der Nasen-öffnung (z.B. Holton, 2012). Einigen Autoren zufolge bestimmen epigenetische Faktoren wie Klima und Ernährung die morphologische Variabilität der Gesichter in menschlichen Popula-tionen (z.B. Evteev et al., 2013; Butaric & Maddux, 2016; Cui & Leclercq, 2017; Hubbe et al., 2009; Gonzalez -Jose et al., 2005; Noback & Harvati, 2015; Stynder et al., 2007; von Cramon-Taubadel, 2011; Brachetta-Aporta, 2019a). Ihre genaue Rolle bleibt jedoch unklar. Studien der Gesichtsontogenese (d. h. Wachstum und Entwicklung) haben gezeigt, dass die Gesichtszüge von Erwachsenen auf Grundlage bevölkerungsspezifischer Größen- und Formveränderungen während der vor- und postnatalen Ontogenese sowie durch Verschiebungen im Entwicklungs-zeitplan entstehen (z.B. O'Higgins & Vidarsdóttir, 1999; 2002: Vidarsdóttir et al.; Bulygina et al., 2006; Freidline et al., 2015). Folglich wird das Erforschen der Wachstums- und Entwicklungsmuster von Gesichtszügen dazu beitragen die Rolle genetischer und epigenetischer Faktoren bei der Gestaltung des menschlichen Gesichts zu erkennen.

In den 1960er Jahren untersuchte Donald Enlow erstmals die Ontogenese menschlicher Gesichtsknochen auf mikroskopischer Ebene. Seine Arbeit führte zur Entdeckung eines grundlegenden Prozesses, genannt Knochenumbau (zunächst "Knochenremodellierung" genannt[1]; Enlow, 1962). Knochenumbau bezeichnet die voneinander abgekoppelten zellulären Aktivitäten der Knochenbildung und Resorption, welche an einer bereits bestehenden Oberfläche Knochenmasse hinzufügen bzw. entfernen. Ebenso wie das suturale Schädel-wachstum (Rice, 2008) bewirkt dieser Prozess ein Größenwachstum des Knochens bei gleich-zeitiger Formveränderung. Es ist jedoch auch ein Kompensationsmechanismus, durch den die Ausrichtung zwischen den Knochen während der gesamten Entwicklung aufrechterhalten werden kann. Die Ausprägung von Zellen, die für die Knochenbildung und Resorption verantwortlich sind (Osteoblasten bzw. Osteoklasten), wird durch komplexe Abfolgen molekularer und chemischer Signale reguliert (z. B. Delmas, 1995; Kini & Nandeesh, 2012). Diese werden teilweise von den Osteozyten (Zellen im kortikalen Knochen) überwacht, die bekanntermaßen empfindlich auf mechanische Reize reagieren (z.B. Huiskes et al., 2000).

Mit Hilfe histologischer Dünnschliffe menschlicher Oberkiefer entdeckten Enlow und Bang (1965) einen großen resorptiven Bereich auf der äußeren Knochenoberfläche. Sie vermuteten, dass dieser eine wichtige Rolle bei der Entwicklung des charakteristischen Gesichts von *H. sapiens*

[1] In der vorliegenden Arbeit folgen wir Frosts Definition (1987,1990,2003), welche eine Trennung zwischen Knochenumbau und –remodellierung vorsieht. Letztere erfolgt durch fortlaufende Knochenresorption und -formation an ähnlicher oder gleichbleibender Stelle einer Knochenschicht (entweder periostal oder endostal) Dies hat mehrere Funktionen, beispielsweise Knochener-neuerung, -reparatur oder Homöostase, wobei die Knochenform unverändert bleibt (Barak, 2019; Parfitt, 1984; Hadjidakis & Androulakis, 2006; Schulte et al., 2013).

spielen muss und stellten damit die erste Verbindung zwischen Knochenumbau und der Ausprägung morphologischer Merkmale her. Kurihara et al. (1980) weiteten ihre Beobachtungen auf mehr Individuen unterschiedlichen Alters aus und gelangten wiederholt zu ähnlichen Ergebnissen. Sie stellten jedoch fest, dass bei jedem Einzelnen die Größe des resorptiven Feldes variiert (d. h. Resorption dehnt sich mal mehr, mal weniger auf der Oberfläche aus). Die Autoren kamen zu dem Schluss, dass die individuelle morphologische Variation deshalb von Lage und Ausmaß dieses Feldes abhängen muss. Die Analyse der Gesichtsontogenese durch die Untersuchung von Knochenumbaumustern stellt somit eine vielversprechende Möglichkeit dar, die morphologische Variabilität bei bestehenden Arten zu untersuchen. Dies wird wiederum unser Wissen über die Ontogenese ausgestorbener Arten erweitern. Tatsächlich könnte es sein, dass sich scheinbar homologe Erwachsenenmerkmale über unterschiedliche ontogenetische Bahnen entwickeln, und stattdessen homoplastisch sind. Als Schnittstelle zwischen genetischen und morphologischen Daten bietet die Analyse zellulärer Aktivitäten neue Einblicke in die Paläobiologie der homininen Gesichtsevolution und kann wertvolle stammesgeschichtliche Informationen beitragen.

Die Entwicklung von Methoden wie der Histologie auf trockenen Knochenoberflächen erleichterte Knochenumbaustudien (Boyde & Hobdell, 1969a, b; Boyde, 1972; Boyde & Jones, 1996; Bromage, 1984, 1985). Ein relativ großer Teil der Forschung hat seitdem die Knochenumbaumuster verschiedener bestehender (Enlow, 1966a; Duterloo & Enlow, 1970; Johnson et al., 1976; Kurihara et al., 1980; Walters & O'Higgins, 1992; O'Higgins & Jones, 1998; O'Higgins et al., 1991, 2001; Wealthall, 2002; Mowbray, 2005; Kranioti et al., 2009; Martínez-Maza et al., 2013, 2015; Freidline et al., 2017; Brachetta-Aporta et al., 2014, 2019a, b) und ausgestorbener Arten (Bromage, 1989; McCollum, 1999, 2008; Martínez-Maza et al., 2011; Brachetta-Aporta et al., 2017; Lacruz et al., 2013, 2015a, b) untersucht. Insgesamt deuten diese Studien darauf hin, dass Knochenumbaumuster artspezifisch sind (z.B. Rosas & Martínez-Maza, 2010). O'Higgins und Co-Autoren (1991) sowie Martínez-Maza und Co-Autoren (2015) beobachteten jedoch starke Ähnlichkeiten zwischen Knochenumbaumustern eng verwandter Arten. Dies könnte bedeuten, dass einige Entwicklungsprozesse über Artgrenzen hinweg beibehalten werden, was wiederum auf Kanalisierung hindeutet: die Erhaltung morphologischer Merkmale während der Ontogenese (z. B. Waddington, 1942; Hallgrímsson et al., 2002). Es ist jedoch noch unklar, welche Aspekte der Knochenumbaumuster spezifisch sind und welche eng verwandten Arten gemein sind (z. B. zwischen Neandertalern und *H. sapiens*; jedoch siehe Rosas und Martínez-Maza (2010) und Lacruz et al. 2015a).

Eine neue Möglichkeit, diese Fragen zu untersuchen, besteht darin, sowohl Knochenumbau als auch Morphologie in einem integrativen Ansatz gemeinsam zu betrachten. Da neuer Knochen auf einer Seite der Oberfläche hinzugefügt wird (und auf der anderen Seite resorbiert wird), entsteht eine Verschiebung dieses Bereichs, die als "kortikaler Drift" bezeichnet wird (Enlow, 1962; 1966b). Die Kombination aller Verschiebungen während der Ontogenese führt somit zu makroskopischen Veränderungen in der Morphologie (d.h. Form). Obwohl die Knochenumbauanalyse Informationen über die Lage dieser Verschiebungen auf dem Knochen liefert, ist eine Visualisierung nicht möglich. Dies kann jedoch mit der geometrischen Morphometrie erreicht werden (z.B. Bookstein, 1997; Gunz et al., 2005; Mitteroecker & Gunz,

2009). Dieser Ansatz wurde speziell für die Quantifizierung und Visualisierung von Formänderungen entwickelt und bietet leistungsfähige Methoden für ontogenetische Analysen (e.g., Vidarsdóttir et al., 2002; Mitteroecker et al., 2004, 2005; Mitteroecker & Bookstein, 2009; Bastir et al., 2006; Freidline et al., 2012, 2013, 2015). In einer Reihe von Studien, die sowohl geometrisch morphometrische als auch oberflächenhistologische Techniken verwenden, zeigten O'Higgins und Dryden (1992), O'Higgins und Jones (1998) als auch O'Higgins und Co-Autoren (2001), dass bei mehreren Primatenarten die Lage der Knochenresorption zwischen Individuen während ihrer gesamten Ontogenese weitgehend ähnlich ist. Wie von den Autoren vorgeschlagen, könnte dies darauf hindeuten, dass intraspezifische Formänderungen meist auf Veränderungen der Zellraten und nicht auf Unterschiede in den Knochenumbaumustern zurückzuführen sind. Freidline und Co-Autoren (2017) zeigten anhand beider Techniken in einer explorativen Untersuchung, dass Knochenumbaumuster im menschlichen Gesicht die auf morphologischer Ebene beobachtete Variation widerspiegeln, was auf einen direkten Zusammenhang zwischen mikroskopischen und makroskopischen Veränderungen hindeutet.

Zusammen betrachtet, haben diese einflussreichen Studien neue Entwicklungen in der Untersuchung der Gesichtsontogenese hervorgebracht. Da die Oberflächenhistologie jedoch eine relativ zeitaufwändige Methode ist, fehlen früheren Studien große ontogenetische Proben. Dies hat die Möglichkeit, inter- und intraspezifische Variabilität von Knochenumbaumustern sowie die Gesichtsentwicklung bei fossilen Homininen zu verstehen, beeinträchtigt. Für ein besseres Verständnis dieser Variabilität, ist die Notwendigkeit quantitative Methoden zu entwickeln, von vorrangiger Bedeutung. Darüber hinaus wird die Verwendung quantitativer anstelle von qualitativer Daten auch die Visualisierung (und damit den Vergleich) von Knochenumbaumustern verbessern, was seit langem eine methodische Herausforderung darstellt.

Ziele der These

Ziel der vorliegenden Abschlussthese ist es, die Knochenumbaumuster großer ontogenetischer Serien bestehender Arten zu analysieren und zu quantifizieren. Dies geschieht durch:

(1) Entwicklung neuartiger Methoden zur Quantifizierung und Visualisierung von Knochenumbaumustern
(2) Anwendung dieser Techniken an umfangreichen ontogenetischen *H. sapiens* Reihen, um die Intra- und Interpopulationsvariabilität von Knochenumbaumustern abzuleiten
(3) Vergleich der für *H. sapiens* erzielten Ergebnisse mit den Knochenumbaumustern von Schimpansen (*Pan troglodytes)*, einer Art, deren Gesichtsprojektion vom Menschen abweicht

Diese Arbeit wird erstmalig die Aspekte des Knochenumbaus bestimmen, welche einzigartig für *H. sapiens* sind sowie jene, welche mit anderen Arten übereinstimmen. Dies wird einen geeigneten Rahmen für zukünftige Studien fossiler Homininen bieten. Wie oben diskutiert, befinden sich viele

artunterscheidende Gesichtszüge im Mittelgesicht und vor allem an der Maxilla. Zum Beispiel wirkt der Oberkieferkörper bei Neandertalern im Vergleich zu *H. sapiens* recht aufgebläht und die Nasenöffnung tritt deutlich hervor, was zu ihrer einzigartigen Mittelgesichtsprognathie führt. Folglich fokussieren wir unsere Analysen auf Letztere.

Zusammenfassung der Ergebnisse

Diese Dissertation umfasst drei als Erstautor verfasste Peer-Review-Forschungsarbeiten. Kapitel 1 wurde im Journal of Anatomy (Schuh et al., 2019), Kapitel 2 im American Journal of Physical Anthropology (Schuh et al., 2020) veröffentlicht, und Kapitel 3 wird derzeit durch das Journal of Human Evolution geprüft.

Kapitel 1. Ontogenese der menschlichen Maxilla: eine Studie über Intrapopulationsvariabilität mit Hilfe von Knochenoberflächenhistologie und geometrischer Morphometrie

In diesem ersten Kapitel werden neue Methoden zur Quantifizierung und Visualisierung von Knochenumbaumustern vorgestellt und auf eine ontogenetische Stichprobe von 47 französischen Personen bekannten Alters (von der Geburt bis zu 12 Jahren) und Geschlecht angewendet. Wir haben getestet, ob (1) Knochenresorption mit dem Alter zunimmt, wie von früheren Autoren angegeben (Enlow & Bang, 1965; Kurihara et al., 1980; Martínez-Maza et al., 2013); (2) die Variabilität der Knochenumbaumuster die morphologische Variabilität widerspiegelt (Freidline et al., 2017); (3) Knochenbildungsareale der Wachstumsrichtung (d. h. Verschiebung nach vorn) gegenüberliegen, wie von Enlow (1962) sowie Enlow und Bang (1965) vorgeschlagen. Die Stärke des methodischen Ansatzes beruht auf der direkten Resorp-tionsquantifizierung anhand von Bildern der Knochenoberfläche, die mit einem digitalen optischen Mikroskop (Smart Zoom 5, Zeiss) aufgenommen wurden.

Da sich der Knochen vom ersten bis zum zwölften Lebensjahr in Breite und Länge vergrößert, befinden sich Knochenresorptionsareale bei allen Individuen an fast der gleichen Stelle, was Voruntersuchungen anderer Primatenarten bestätigt (O'Higgins & Jones, 1998; Martínez-Maza et al., 2015). Diese Areale sind im Falle der Maxilla in der Nähe der Stirnbein, Jochbein- und Zwischenoberkiefernähte sowie auf einem Großteil des Zahnbogens verteilt. Dies deutet darauf hin, dass auf der Populationsebene Unterschiede in der Oberkiefer-morphologie eher auf unterschiedlichen Zellraten als auf Knochenumbau beruhen und dass maxilläres Wachstum maßgeblich durch frühe Entwicklungsphasen vorbestimmt ist. Darüber hinaus konnte in unserer Stichprobe kein Unterschied zwischen den Geschlechtern gefunden werden; für schlüssige Ergebnisse müsste dies an einer größeren Probe getestet werden. Der durchschnittliche Prozentsatz

der Knochenresorption (%BR) steigt zwischen der Geburt und 2,5 Jahren (von 23,5 auf 43,1%), stabilisiert sich dann auf etwa ein Drittel der Gesamtfläche. Dies deutet darauf hin, dass Knochenresorption ein eher konstanter Prozess ist, welcher jedoch sehr variabel bei Individuen ähnlichen Alters sein kann. Darüber hinaus befanden wir Regionen mit hoher morphologischer Variation, wie z. B. den Stirnbeinfortsatz, als Hotspots der Knochenbildung. Im Gegensatz dazu waren weniger variable Bereiche wie der Zahnbogen eher resorptiv. Dies könnte darauf hindeuten, dass hohe biomechanische Anforderungen wachstumsbeschränkend wirken. Schließlich, Enlows Befunde (1962) bestätigend, fanden wir Übereinstimmungen zwischen der Wachstumsrichtung (Verschiebung nach vorn oder hinten) und Knochenumbaumustern (Bildung bzw. Resorption). Dies könnte möglicherweise genutzt werden, um die Wachstumsrichtung fossiler Homininen vorherzusagen, für welche Knochenumbaumuster unbekannt sind.

Kapitel 2. Intraspezifische Variabilität in menschlichen Oberkieferknochenumbau-mustern während der Ontogenese

Dieses Kapitel untersucht die intraspezifische Variabilität der Oberkieferknochenumbaumuster um festzustellen, ob Bevölkerungsunterschiede in der Morphologie mit Unterschieden in Knochenumbaumustern während des Wachstums zusammenhängen. Es wurde eine nie dagewesene Stichprobengröße von 145 *H. sapiens* Individuen (einschließlich Erwachsener) aus drei geografisch unterschiedlichen Gebieten (Grönland, Westeuropa und Südafrika) verwendet, wobei ähnliche Methoden wie in Kapitel 1 angewandt wurden. Die gemeinsame Analyse bzw. Kovariation der morphologischen und Knochenumbauveränderungen wurde mit der Partiellen kleinsten Quadrate (PLS) Methode untersucht (Rohlf & Corti, 2000). Dies ermöglichte deren Visualisierung in einem integrativen Ansatz.

Wir fanden heraus, dass Bevölkerungsunterschiede in der Oberkiefermorphologie durch unterschiedlich starke Formveränderungen während der Ontogenese entstehen und damit auf unterschiedlichen Entwicklungsbahnen beruhen. Die grönländischen Inuit sind in ihrer Entwicklung weiter fortgeschritten, was auf Unterschiede in zeitlichen Abläufen und/oder Entwicklungsraten sowohl in prä- als auch postnatalen Phasen hindeutet. Auf mikroskopischer Ebene stellten wir ein gleichartiges Knochenumbaumuster bei allen menschlichen Populationen fest, mit vorherrschender Knochenbildung im Stirnbeinfortsatz und Knochenresorption im Zahnbogen. Es konnten nur geringfügige Unterschiede beobachtet werden. Bei Westeuropäern und Südafrikanern befindet sich die Region mit der höchsten Knochenresorption meist direkt über dem Eckzahn, während sie bei den Inuit nahe der intermaxillären Naht zu finden ist. Dies lässt vermuten, dass bereits geringe Unterschiede im Knochenumbau zu prägnanten Formunterschieden zwischen menschlichen Populationen führen, und es wird einmal mehr gezeigt, dass die Hauptunterschiede in zeitlichen Abläufen und Zellraten liegen. Die PLS-Analyse zeigte bei allen menschlichen Populationen ein ähnliches Muster der Kovariation mit wiederum leichten Unterschieden in der Art und Weise wie Oberkiefermorphologie und knochenumbau kovarieren, vor allem bei Inuit. Schließlich haben erwachsene Individuen ähnliche Knochenumbaumuster wie Juvenile, jedoch bei

geringerer Intensität. Dies lässt darauf schließen, dass Knochenumbaumuster im Laufe des Lebens beibehalten werden.

Kapitel 3. Prognathie versus Orthognathie: Neue Einblicke in die Dynamik hinter dem Oberkieferknochenumbau

Dieses Kapitel untersucht durch den Vergleich der ontogenetischen Muster zwischen Schimpansen (*Pan troglodytes verus*) und Menschenoberkiefer die interspezifische Variabi-lität der Knochenumbaumuster. Beide Arten zeigen entgegengesetzte Gesichtsprojektionen (prognath bzw. orthognath), für welche fossile Homininen verschiedene Zwischengrade aufweisen (Bastir et al., 2004). Ein besseres Verständnis der ontogenetischen Mechanismen, die zu einer Oberkieferprojektion führen, kann neue Erkenntnisse über die Evolution des Homininengesichts bringen.

Eine ontogenetische Stichprobe von 33 Schimpansen (von der Geburt bis zum Erwachsenenalter) wurde verwendet und mit den Westeuropäern aus Kapitel 2 verglichen. Kalendarisches Alter und Geschlecht sind für beide Arten bekannt, und es wurden ähnliche Methoden wie in den Kapiteln 1 und 2 verwendet. Wir stellen fest, dass sich die Umbaumuster des menschlichen und Schimpansenoberkieferknochens in vielen Aspekten unterscheiden. Schimpansen weisen während ihrer gesamten Ontogenese im Durchschnitt eine geringere Knochenresorption als Menschen auf, sowie weniger Variation innerhalb der Altersgruppen. So entwickelt sich Oberkieferprognathie beim Schimpansen meist durch verstärkte Knochen-bildung, wie auch schon bei anderen bisher untersuchten nichtmenschlichen Primaten beobachtet (Enlow, 1966; O'Higgins, et al., 1991; Walter & O'Higgins, 1992; O'Higgins & Jones, 1998; Wealthall, 2002; Martínez-Maza et al., 2015). Beim Schimpansen findet Knochenresorption nahe der Nähe statt und besonders im Zwischenkieferbein. Die postnatale Entwicklung der Eckzahn-Eminenz bei Schimpansen geht einher mit zunehmender Knochenbildung, welche in diesem Bereich bis ins Erwachsenenalter hinein vorherrschend bleibt. Dies stellt einen entscheidenden Unterschied zwischen menschlichem Oberkiefer-knochenumbaumuster und dem des Schimpansen dar. Es ist daher wahrscheinlich, dass Veränderungen des oberen Eckzahn/Prämolar-Honen-Komplexes, ein abgeleitetes Merkmal aller Homininen, mit Veränderungen im Knochenumbaumuster dieses Bereichs einhergehen. Anhand der PLS-Analyse zeigen wir, dass die Kovariation zwischen Knochenumbau und Form bei beiden Arten gering ist und ein ähnliches Muster bis zur Pubertät aufweist. Dies deutet darauf hin, dass ontogenetischer Knochenumbau ein sehr stabiler Prozess ist und dass die meisten morphologischen Veränderungen von Entwicklungsraten und/oder zeitpunkten der zellulären Aktivitäten abhängen. Schlussendlich unterscheiden sich Knochenumbaumuster zwischen Schimpansen und Menschen zwar, jedoch deutet eine ähnliche Lage von Knochen-resorptionsarealen auf die Erhaltung eines gemeinsamen ontogenetischen Musters hin.

Literatur

Arsuaga, J.-L., Martínez, I., Lorenzo, C., Gracia, A., Mun, A., & Alonso, O. (1999). The human cranial remains from Gran Dolina lower Pleistocene site (Sierra de Atapuerca, Spain). *Journal of Human Evolution, 37*(3-4), 431-457.

Barak, M.M. (2019). Bone modeling or bone remodeling: That is the question. *American Journal of Physical Anthropology, 172*(2), 153-155.

Bastir, M., & Rosas, A. (2004). Facial heights: evolutionary relevance of postnatal ontogeny for facial orientation and skull morphology in humans and chimpanzees. *J Hum Evol, 47*(5), 359-381.

Bastir, M., Rosas, A., Lieberman, D.E., & O'Higgins, P. (2008). Middle cranial fossa anatomy and the origin of modern humans. *Anat Rec (Hoboken), 291*(2), 130-140.

Bastir, M., Rosas, A., & O'Higgins, P. (2006). Craniofacial levels and the morphological maturation of the human skull. *J Anat, 209*(5), 637-654.

Bastir, M., Rosas, A., Stringer, C., Cuetara, J.M., Kruszynski, R., Weber, G.W., Ross, C.F., & Ravosa, M.J. (2010). Effects of brain and facial size on basicranial form in human and primate evolution. *J Hum Evol, 58*(5), 424-431.

Bermúdez de Castro, J.M., Arsuaga, J.L., Carbonell, E., Rosas, A., Martínez, I., & Mosquera, M. (1997). A Hominid from the Lower Pleistocene of Atapuerca, Spain: Possible Ancestor to Neandertals and Modern Humans. *276*(5317), 1392-1395.

Bookstein, F.L. (1997). Landmark methods for forms without landmarks: morphometrics of group differences in outline shape. *Medical Image Analysis, 1*(3), 225-243.

Boyde, A. (1972). Scanning electron microscope studies of bone. In G. H. Bourne (Ed.), *The Biochemistry and physiology of bone*. New York: Academic Press.

Boyde, A., & Hobdell, M.H. (1969a). Scanning electron microscopy of Lamellar bone. *Z. Zellforsch., 93*, 213-231.

---. (1969b). Scanning Electron Microscopy of Primary Membrane Bone. *Z.Zellfotsch., 99*, 98-108.

Boyde, A., & Jones, S. (1996). Scanning Electron Microscopy of Bone: Instrument, Specimen, and Issues. *Microscopy Research and Technique, 32*, 92-120.

Brachetta-Aporta, N., Gonzalez, P.N., & Bernal, V. (2017). A quantitative approach for analysing bone modelling patterns from craniofacial surfaces in hominins. *Journal of Anatomy*, n/a-n/a.

---. (2019a). Integrating data on bone modeling and morphological ontogenetic changes of the maxilla in modern humans. *Annals of Anatomy - Anatomischer Anzeiger, 222*, 12-20.

Brachetta-Aporta, N., Gonzalez, P.N., & Bernal, V. (2019b). Variation in facial bone growth remodeling in prehistoric populations from southern South America. *169*(3), 422-434.

Brachetta Aporta, N., Martínez-Maza, C., Gonzalez, P.N., & Bernal, V. (2014). Bone modeling patterns and morphometric craniofacial variation in individuals from two prehistoric human populations from Argentina. *Anat Rec (Hoboken), 297*(10), 1829-1838.

Bromage, T.G. (1984). Interpretation of Scanning Electron Microscopic Images of Abraded Forming Bone Surfaces. *American Journal of Physical Anthropology, 64*, 161-178.

Bromage, T.G. (1985). Systematic inquiry of in tests of negative/positive replica combinations for SEM. *Journal of Microscopy, 137*(2), 209-216.

---. (1989). Ontogeny of the early hominin face. *Journal of Human Evolution, 18*, 751-773.

Bulygina, E., Mitteroecker, P., & Aiello, L. (2006). Ontogeny of facial dimorphism and patterns of individual development within one human population. *Am J Phys Anthropol, 131*(3), 432-443.

Butaric, L.N., & Maddux, S.D. (2016). Morphological Covariation between the Maxillary Sinus and Midfacial Skeleton among Sub-Saharan and Circumpolar Modern Humans. *American Journal of Physical Anthropology, 160*(3), 483-497.

Cui, Y., & Leclercq, S. (2017). Environment-Related Variation in the Human Mid-Face. *The Anatomical Record, 300*(1), 238-250.

Day, M., & Stringer, C. (1982). L'Homo erectus et la place de l'homme de Tautavel permi les hominides fossiles. In: Centre National de la Recherche Scientifique, Nice, France.

Delmas, P.D. (1995). Biochemical markers of bone turnover. *Acta Orthopaedica Scandinavica, 66*(sup266), 176-182.

Duterloo, H.S., & Enlow, D.H. (1970). A comparative study of cranial growth in Homo and Macaca. *American Journal of Anatomy, 127*(4), 357-367.

Duval, M., Grün, R., Parés, J.M., Martín-Francés, L., Campaña, I., Rosell, J., Shao, Q., Arsuaga, J.L., Carbonell, E., & Bermúdez de Castro, J.M. (2018). The first direct ESR dating of a hominin tooth from Atapuerca Gran Dolina TD-6 (Spain) supports the antiquity of Homo antecessor. *Quaternary Geochronology, 47*, 120-137.

Enlow, D.H. (1962). A Study of the Post-Natal Growth and Remodeling of Bone. *American Journal of Anatomy, 110*(2), 79-101.

Enlow, D.H. (1966a). A comparative study of facial growth in Homo and Macaca. *American Journal of Physical Anthropology, 24*(3), 293-307.

---. (1966b). A morphogenetic analysis of facial growth. *American journal of orthodontics, 52*(4), 283-299.

Enlow, D.H., & Bang, D.D.S. (1965). Growth and remodeling of the human maxilla. *American journal of orthodontics, 51*(6), 446-464.

Evteev, A., Cardini, A.L., Morozova, I., & O'Higgins, P. (2013). Extreme climate, rather than population history, explains mid-facial morphology of northern asians. *American Journal of Physical Anthropology, 153*(3), 449-462.

Franciscus, R.G., & Trinkaus, E. (1995). Determinants of retromolar space presence in Pleistocene Homo mandibles. *Journal of Human Evolution, 28*(6), 577-595.

Freidline, S.E., Gunz, P., Harvati, K., & Hublin, J.-J. (2013). Evaluating developmental shape changes in Homo antecessor subadult facial morphology. *Journal of Human Evolution, 65*(4), 404-423.

Freidline, S.E., Gunz, P., Harvati, K., & Hublin, J.J. (2012). Middle Pleistocene human facial morphology in an evolutionary and developmental context. *J Hum Evol, 63*(5), 723-740.

Freidline, S.E., Gunz, P., & Hublin, J.J. (2015). Ontogenetic and static allometry in the human face: contrasting Khoisan and Inuit. *Am J Phys Anthropol, 158*(1), 116-131.

Freidline, S.E., Gunz, P., Jankovic, I., Harvati, K., & Hublin, J.J. (2012). A comprehensive morphometric analysis of the frontal and zygomatic bone of the Zuttiyeh fossil from Israel. *J Hum Evol, 62*(2), 225-241.

Freidline, S.E., Martínez-Maza, C., Gunz, P., & Hublin, J.J. (2017). Exploring Modern Human Facial Growth at the Micro- and Macroscopic Levels. In C. J. Percival & J. T. Richtsmeier (Eds.), *Buidling bones*. Cambridge: Cambridge University Press.

Frost, H.M. (1987). Bone "mass" and the "mechanostat": A proposal. *The Anatomical Record, 219*(1), 1-9.

Frost, H.M. (1990). Skeletal structural adaptations to mechanical usage (SATMU): 1. Redefining Wolff's law: the bone modeling problem. *The Anatomical Record, 226*(4), 403-413.

Frost, H.M. (2003). Bone's Mechanostat: A 2003 Update. *The Anatomical Record, 275*(A), 1081-1101.

Gonzalez-Jose, R., Ramirez-Rozzi, F., Sardi, M., Martínez-Abadias, N., Hernandez, M., & Pucciarelli, H.M. (2005). Functional-cranial approach to the influence of economic strategy on skull morphology. *Am J Phys Anthropol, 128*(4), 757-771.

Gunz, P., Mitteroecker, P., & Bookstein, F. (2005). Semilandmarks in three dimensions. In D. E. Slice (Ed.), *Modern Morphometrics in Physical Anthroplogy*. New York: Kluwer Press.

Hadjidakis, D.J., & Androulakis, I.I. (2006). Bone remodeling. *Annals of the New York Academy of Sciences, 1092*(1), 385-396.

Hallgrímsson, B., Willmore, K., & Hall, B.K. (2002). Canalization, developmental stability, and morphological integration in primate limbs. *American Journal of Physical Anthropology, Suppl 35*, 131-158.

Holton, N.E., Franciscus, R.G., Marshall, S.D., Southard, T.E., & Nieves, M.A. (2011). Nasal Septal and Premaxillary Developmental Integration: Implications for Facial Reduction in Homo. *The Anatomical Record, 294*(1), 68-78.

Holton, N.E., Franciscus, R.G., Nieves, M.A., Marshall, S.D., Reimer, S.B., Southard, T.E., Keller, J.C., & Maddux, S.D. (2010). Sutural growth restriction and modern human facial evolution: an experimental study in a pig model. *Journal of Anatomy, 216*(1), 48-61.

Holton, N.E., Yokley, T.R., & Figueroa, A. (2012). Nasal septal and craniofacial form in European- and African-derived populations. *Journal of Anatomy, 221*(3), 263-274.

Howells, W. (1973). *Cranial Variation in Man: A Study by Multivariate Analysis of Patterns of Difference among Recent Human Populations*. Cambridge: MA: Harvard University Press.

Hubbe, M., Hanihara, T., & Harvati, K. (2009). Climate Signatures in the Morphological Differentiation of Worldwide Modern Human Populations. *292*(11), 1720-1733.

Hublin, J.-J., Ben-Ncer, A., Bailey, S.E., Freidline, S.E., Neubauer, S., Skinner, M.M., Bergmann, I., Le Cabec, A., Benazzi, S., Harvati, K., & Gunz, P. (2017). New fossils from Jebel Irhoud, Morocco and the pan-African origin of Homo sapiens. *Nature, 546*, 289.

Huiskes, R., Ruimerman, R., Van Lenthe, G.H., & Janssen, J.D. (2000). Effects of mechanical forces on maintenance and adaptation of form in trabecular bone. *Nature, 405*(6787), 704-706.

Johnson, P.A., Atkinson, P.J., & Moore, W.J. (1976). The development and structure of the chimpanzee mandible. *Journal of Anatomy, 122*(2), 467-477.

Kini, U., & Nandeesh, B.N. (2012). Physiology of Bone Formation, Remodeling, and Metabolism. 29-57.

Kranioti, E.F., Rosas, A., Garcia-Vargas, S., Estalrrich, A., Bastir, M., & Pena-Melian, A. (2009). Remodeling patterns of occipital growth: a preliminary report. *Anat Rec (Hoboken), 292*(11), 1764-1770.

Kurihara, S., Enlow, D.H., & Rangel, R.D. (1980). Remodeling Reversals in Anterior Parts of the Human Mandible and Maxilla. *The Angle Orthodontics, 50*(2), 98-106.

Lacruz, R.S., Bromage, T.G., O'Higgins, P., Arsuaga, J.L., Stringer, C., Godinho, R.M., Warshaw, J., Martínez, I., Gracia-Tellez, A., de Castro, J.M., & Carbonell, E. (2015a). Ontogeny of the maxilla in Neanderthals and their ancestors. *Nat Commun, 6*, 8996.

Lacruz, R.S., Bromage, T.G., O'Higgins, P., Toro-Ibacache, V., Warshaw, J., & Berger, L.R. (2015b). Distinct growth of the nasomaxillary complex in Au. sediba. *Sci Rep, 5*, 15175.

Lacruz, R.S., de Castro, J.M., Martinon-Torres, M., O'Higgins, P., Paine, M.L., Carbonell, E., Arsuaga, J.L., & Bromage, T.G. (2013). Facial morphogenesis of the earliest europeans. *PLOS ONE, 8*(6), e65199.

Lahr, M.M. (1996). *The evolution of modern human diversity: a study of cranial variation* (Vol. 18): Cambridge University Press.

Maddux, S.D., & Franciscus, R.G. (2009). Allometric scaling of infraorbital surface topography in Homo. *J Hum Evol, 56*(2), 161-174.

Martínez-Maza, C., Freidline, S.E., Strauss, A., & Nieto-Diaz, M. (2015). Bone Growth Dynamics of the Facial Skeleton and Mandible in Gorilla gorilla and Pan troglodytes. *Evolutionary Biology, 43*(1), 60-80.

Martínez-Maza, C., Rosas, A., Garcia-Vargas, S., Estalrrich, A., & de la Rasilla, M. (2011). Bone remodelling in Neanderthal mandibles from the El Sidron site (Asturias, Spain). *Biol Lett, 7*(4), 593-596.

Martínez-Maza, C., Rosas, A., & Nieto-Diaz, M. (2013). Postnatal changes in the growth dynamics of the human face revealed from bone modelling patterns. *J Anat, 223*(3), 228-241.

Maureille, B. (1994). *La face chez Homo erectus et Homo sapiens: recherche sur la variabilité morphologique et métrique, Anthropologie.* Ph. D. Dissertation, Uni-versité de Bordeaux 1,

McCollum, M.A. (1999). The Robust Australopithecine Face: A Morphogenetic Perspective. *Science, 284*(5412), 301-305.

---. (2008). Nasomaxillary remodeling and facial form in robust Australopithecus: a reassessment. *J Hum Evol, 54*(1), 2-14.

Mitteroecker, P., & Bookstein, F. (2009). The ontogenetic trajectory of the phenotypic covariance matrix, with examples from craniofacial shape in rats and humans. *Evolution, 63*(3), 727-737.

Mitteroecker, P., & Gunz, P. (2009). Advances in Geometric Morphometrics. *Evolutionary Biology, 36*(2), 235-247.

Mitteroecker, P., Gunz, P., Bernhard, M., Schaefer, K., & Bookstein, F.L. (2004). Comparison of cranial ontogenetic trajectories among great apes and humans. *J Hum Evol, 46*(6), 679-697.

Mitteroecker, P., Gunz, P., & Bookstein, F.L. (2005). Heterochrony and geometric morphometrics: a comparison of cranial growth in Pan paniscus versus Pan troglodytes. *Evolution & Development, 7*(3), 244-258.

Mitteroecker, P., Gunz, P., Weber, G.W., & Bookstein, F.L. (2004). Regional dissociated heterochrony in multivariate analysis. *Annals of Anatomy - Anatomischer Anzeiger, 186*(5), 463-470.

Mooney, M.P., & Siegel, M.I. (1986). Developmental relationship between premaxillary-maxillary suture patency and anterior nasal spine morphology. *Cleft Palate J, 23*(2), 101-107.

Mowbray, K. (2005). Surface bone histology of the occipital bone in humans and chimpanzees. *Anat Rec B New Anat, 283*(1), 14-22.

Noback, M.L., & Harvati, K. (2015). The contribution of subsistence to global human cranial variation. *Journal of Human Evolution, 80*, 34-50.

O'Higgins, P., Bromage, T.G., Johnson, D.R., Moore, W.J., & McPhie, P. (1991). A Study of Facial Growth in the Sooty Mangabey *Cercocebus atys*. *Folia Primatologica, 56*(2), 86-94.

O'Higgins, P., Chadfield, P., & Jones, N. (2001). Facial growth and the ontogeny of morphological variation within and between the primates Cebus apella and Cercocebus torquatus. *Journal of Zoology, 254*, 337-357.

O'Higgins, P., & Dryden, I. (1992). Studies of craniofacial development and evolution. *Archaeology in Oceania, 27*(3), 105-112.

O'Higgins, P., & Jones, N. (1998). Facial growth in Cercocebus torquatus: an application of three-dimensional geometric morphometric techniques to the study of morphological variation. *Journal of Anatomy, 193*(2), 251-272.

O'Higgins, P., & Vidarsdóttir, U.E. (1999). New approaches to the quantitative analysis of craniofacial growth and variation. In C. U. Press (Ed.), *Human growth in the past: studies from bones and teeth* (pp. 128-160).

Parfitt, A. (1984). The cellular basis of bone remodeling: the quantum concept reexamined in light of recent advances in the cell biology of bone. *Calcified Tissue International, 36*(1), S37-S45.

Rice, D. (2008). *Craniofacial Sutures: Development, Disease, and Treatment.* (R. DP Ed. Vol. 12). Basel: Karger.

Rohlf, F.J., & Corti, M. (2000). Use of Two-Block Partial Least-Squares to Study Covariation in Shape. *Systematic Biology, 49*(4), 740-753.

Rosas, A., & Martínez-Maza, C. (2010). Bone remodeling of the Homo heidelbergensis mandible; the Atapuerca-SH sample. *J Hum Evol, 58*(2), 127-137.

Rosas, A., Martínez-Maza, C., Bastir, M., García-Tabernero, A., Lalueza-Fox, C., Huguet, R., Ortiz, J.E., Julià, R., Soler, V., de Torres, T., Martínez, E., Cañaveras, J.C., Sánchez-Moral, S., Cuezva, S., Lario, J., Santamaría, D., de la Rasilla, M., & Fortea, J. (2006). Paleobiology and comparative morphology of a late Neandertal sample from El Sidrón, Asturias, Spain. *Proceedings of the National Academy of Sciences, 103*(51), 19266-19271.

Schuh, A., Gunz, P., Villa, C., Kupczik, K., Hublin, J.J., & Freidline, S.E. (2020). Intraspecific variability in human maxillary bone modeling patterns during ontogeny. *American Journal of Physical Anthropology, 173*(4), 655-670.

Schuh, A., Kupczik, K., Gunz, P., Hublin, J.-J., & Freidline, S.E. (2019). Ontogeny of the human maxilla: a study of intra-population variability combining surface bone histology and geometric morphometrics. *Journal of Anatomy, 235*(2), 233-245.

Schulte, F.A., Ruffoni, D., Lambers, F.M., Christen, D., Webster, D.J., Kuhn, G., & Muller, R. (2013). Local mechanical stimuli regulate bone formation and resorption in mice at the tissue level. *PLOS ONE, 8*(4), e62172.

Stynder, D.D., Ackermann, R.R., & Sealy, J.C. (2007). Craniofacial variation and population continuity during the South African Holocene. *134*(4), 489-500.

Vidarsdóttir, U.E., O'Higgins, P., & Stringer, C. (2002). A geometric morphometric study of regional differences in the ontogeny of the modern human facial skeleton. *Journal of Anatomy, 201*, 211-229.

von Cramon-Taubadel, N. (2011). Global human mandibular variation reflects differences in agricultural and hunter-gatherer subsistence strategies. *Proceedings of the National Academy of Sciences, 108*(49), 19546-19551.

Waddington, C.H. (1942). Canalization of the development and the inheritance of acquired characters. *Nature, 150*, 563.

Walters, M., & O'Higgins, P. (1992). *Factors influencing craniofacial growth: a scanning electron microscope study of high resolution facial replicas.* Paper presented at the Proc Australas Soc Hum Biol.

Wealthall, R.J. (2002). Surface remodelling of the facial skeleton in juvenile Macaca mulatta: implications for sexual dimorphism. *Folia Primatologica, 73*(1), 49-53.

Chapter 1

Ontogeny of the human maxilla: a study of intra-population variability combining surface bone histology and geometric morphometrics

Journal of Anatomy

J. Anat. (2019) doi: 10.1111/joa.13002

Ontogeny of the human maxilla: a study of intra-population variability combining surface bone histology and geometric morphometrics

Alexandra Schuh,[1] Kornelius Kupczik,[2] Philipp Gunz,[1] Jean-Jacques Hublin[1] and Sarah E. Freidline[1]

[1]*Department of Human Evolution, Max Planck Institute for Evolutionary Anthropology, Leipzig, Germany*
[2]*Max Planck Weizmann Center for Integrative Archaeology and Anthropology, Max Planck Institute for Evolutionary Anthropology, Leipzig, Germany*

Abstract

Bone modeling is the process by which bone grows in size and models its shape via the cellular activities of the osteoblasts and osteoclasts that respectively form and remove bone. The patterns of expression of these two activities, visible on bone surfaces, are poorly understood during facial ontogeny in *Homo sapiens*; this is due mainly to small sample sizes and a lack of quantitative data. Furthermore, how microscopic activities are related to the development of morphological features, like the uniquely human-canine fossa, has been rarely explored. We developed novel techniques for quantifying and visualizing variability in bone modeling patterns and applied these methods to the human maxilla to better understand its development at the micro- and macroscopic levels. We used a cross-sectional ontogenetic series of 47 skulls of known calendar age, ranging from birth to 12 years, from a population of European ancestry. Surface histology was employed to record and quantify formation and resorption on the maxilla, and digital maps representing each individual's bone modeling patterns were created. Semilandmark geometric morphometric (GM) methods and multivariate statistics were used to analyze facial growth. Our results demonstrate that surface histology and GM methods give complementary results, and can be used as an integrative approach in ontogenetic studies. The bone modeling patterns specific to our sample are expressed early in ontogeny, and fairly constant through time. Bone resorption varies in the size of its fields, but not in location. Consequently, absence of bone resorption in extinct species with small sample sizes should be interpreted with caution. At the macroscopic level, maxillary growth is predominant in the top half of the bone where bone formation is mostly present. Our results suggest that maxillary growth in humans is highly constrained from early stages in ontogeny, and morphological changes are likely driven by changes in osteoblastic and osteoclastic rates of expression rather than differences in the bone modeling patterns (i.e. changes in location of formation and resorption). Finally, the results of the micro- and macroscopic analyses suggest that the development of the canine fossa results from a combination of bone resorption and bone growth in the surrounding region.

Key words: bone formation; bone modeling; bone resorption; facial growth; semilandmark geometric morphometrics.

Introduction

Bone modeling results from the simultaneous activities of osteoblasts and osteoclasts that respectively form and resorb bone surfaces (Frost, 1987). It is the main process by which bone grows in size and models its shape. In the human maxilla, bone modeling was first described in detail by Enlow & Bang (1965), who found bone formation on the posterior and superior parts of the bone, whereas the anterio-inferior region (mostly represented by the maxillary arcade) was predominantly resorptive. Studies of facial growth by Kurihara et al. (1980) and later Martinez-Maza et al. (2013) confirmed Enlow & Bang's findings and proposed that as the maxilla increases in size, the resorptive field enlarges from the anterior maxillary arcade to the zygomatic bone in order to compensate forward

Correspondence
Alexandra Schuh, Department of Human Evolution, Max Planck Institute for Evolutionary Anthropology, Deutscher Platz 6, 04103 Leipzig, Germany. E: alexandra.schuh@eva.mpg.de

Accepted for publication *20 March 2019*

displacements. The forward and downward direction of growth, combined with a generally resorptive maxilla, is typical of *H. sapiens* and results in the characteristic orthognathic face of our species (Enlow & Hans, 2008; Martinez-Maza et al. 2013). The analysis of bone modeling patterns is thus particularly relevant for ontogenetic studies, as it provides insight into the growth processes that occur at the microscopic level and can potentially inform us about ontogenetic processes that are either shared between or unique to a species.

In the last decades, an increasing number of studies have analyzed the bone modeling patterns of the craniofacial complex in extant (Enlow, 1966a,b; Duterloo & Enlow, 1970; Johnson et al. 1976; Kurihara et al. 1980; O'Higgins & Jones, 1998; O'Higgins et al. 1991, 2001; Mowbray, 2005; Kranioti et al. 2009; Martinez-Maza et al. 2013, 2015; Brachetta-Aporta et al. 2014, 2018) and extinct species (Bromage, 1985, 1989; McCollum, 1999, 2008; Martinez-Maza et al. 2011; Rosas & Martinez-Maza, 2010; Lacruz et al. 2013, 2015). With the improvements in microscopy techniques, and as the osteoblastic and osteoclastic activities leave specific marks on bone surfaces, it is possible to observe bone modeling patterns on dry bones using surface histology without employing destructive methods (Boyde & Hobdell, 1969a,b; Bromage, 1984, 1985; Boyde & Jones, 1996). Bone resorption appears to be sparser on the maxillary bone of extant species with prognathic faces (such as great apes) compared with orthognathic *Homo sapiens*, and bone modeling patterns seem to differ between species (Martinez-Maza et al. 2015; O'Higgins et al. 2001). In extinct species, Bromage (1989) and McCollum (2008) found different patterns in 'gracile' compared with 'robust' australopiths (*Paranthropus*), with resorption present in the nasomaxillary clivus in robust but not in gracile forms. Lacruz et al. (2013) compared the bone modeling patterns in the maxilla between *Homo antecessor* (ATD6-69) and an African *Homo erectus* specimen (KNM-WT 15000). These authors found that the bone modeling pattern of KNM-WT 15000 is more similar to that of australopiths, whereas ATD6-69 showed a pattern of resorption in the subnasal area similar to that seen in *H. sapiens*. Conversely, Lacruz et al. (2015) showed that the bone modeling pattern in the Neanderthal maxilla differs from *H. sapiens* by being largely bone forming, explaining their more projecting faces.

However, bone modeling studies suffer from small sample sizes, usually due to poorly preserved bone surfaces and time-consuming methodologies. Therefore, our understanding of intraspecific variability in bone modeling patterns is limited and, consequently, interpreting bone modeling patterns in our fossil ancestors is difficult. As of now, five studies have looked at facial bone modeling patterns in *H. sapiens*, creating a total sample size of fewer than 80 individuals of diverse origin and ranging in age from infancy to adulthood (Enlow & Bang, 1965; Kurihara et al. 1980; McCollum, 2008; Martinez-Maza et al. 2013). Moreover, age of death is often unknown and approximated based on dental development. Finally, bone modeling patterns are usually qualitatively assessed and mostly visualized on handmade maps (although see Brachetta-Aporta et al. 2017). Bone modeling studies thus generally suffer from a lack of quantitative data, leaving many questions on how formation and resorption are expressed during ontogeny unanswered. For example, Freidline et al. (2016) proposed that constant bone modeling patterns (i.e. less frequently changing between bone formation and resorption) may result in less morphological variation; however, this remains to be tested quantitatively. Moreover, whether bone modeling is species-specific is still unclear, as patterns of variation can be shared between closely related species such as great apes (Martinez-Maza et al. 2015). Thus, understanding the relationship between bone modeling activities and morphological development is essential, as similar morphological features shared between species may instead develop from distinct rates and patterns of growth. For example, the suprainiacfossa, a thinning of the occipital diploic layer found in Neanderthals, can be differentiated from suprainiac depressions found in other species by its developmental pattern (Balzeau & Rougier, 2010).

One way to improve some of the methodological shortcomings listed above, and better understand the link between morphological changes and bone modeling, is by marrying surface histology with geometric morphometric (GM) techniques (O'Higgins & Jones, 1998; Brachetta-Aporta et al. 2014, 2018; Martinez-Maza et al. 2015; Freidline et al. 2016). Geometric morphometrics is a set of powerful tools for the quantification of shape and form (i.e. size and shape; O'Higgins, 2000; Mitteroecker et al. 2004; Bastir & Rosas, 2004; Gunz et al. 2010, 2012; Freidline et al. 2012). Surface histology provides insights into growth processes occurring at the microscopic level, and GM methods enable the quantification and visualization of complex displacements during ontogeny that are not evident with surface histology.

The goal of this study is to quantify bone modeling variability during ontogeny in a large sample of modern human maxillae in order to better understand how the expression of microscopic processes drives morphological variation. For this purpose, we developed novel techniques for quantifying and visualizing bone modeling patterns. We use surface histology to quantify bone resorption and formation and build digital maps to visualize and compare the bone modeling patterns between individuals, as well as semilandmark geometric morphometrics (GM) to quantify morphological changes. We assessed whether the resorptive field located on the anterior maxilla increases in size during ontogeny as proposed by former studies (Enlow & Bang, 1965; Kurihara et al. 1980; Martinez-Maza et al. 2013) (hypothesis 1). Secondly, we test whether frequent changes in formation and resorption result in greater morphological variability (Freidline et al. 2016) (hypothesis 2). Finally,

surface histology and semilandmark GMs are combined in a joint analysis in order to better interpret the relationship between bone modeling patterns and morphological changes, and we test Enlow's hypothesis (1962a) that formation fields face the direction of growth (hypothesis 3).

Materials and methods

Sample

The sample is composed of 47 right maxillae from a cross-sectional growth series of French origin (Anatomical Institute of Strasbourg, France). The calendar ages range from birth to 12 years (Table 1; Rampont, 1994; Le Minor et al. 2009). So as to facilitate comparisons with other studies, the sample was divided into four age groups (AG) according to dental development following AlQahtani et al. (2010) (Table 1). Each specimen presents remarkable surface preservation, with very little missing data. Following Bromage (1989), negative molds of the right maxilla were made using a low-viscosity silicone (President Plus light body, Coltene/Whaledent AG, Switzerland) and attached to a silicone base (President microSystem regular body, Coltene/Whaledent AG, Switzerland). Each mold was delimited with a retaining wall made with an impression material used for dentistry (PROVIL novo Putty regular set), and a positive replica was generated using a transparent two-component epoxy resin Injektionsharz EP (Reckli-Chemiewerkstoff, Herne, Germany). The same individuals used for the surface histology analysis were scanned using micro-computed tomography (CT) at a resolution of 0.2–0.4 mm (BIR ACTIS 225/300). The 3D surface models of the scans were acquired using the software AVIZO (ThermoFisherScientific).

Analyses

Surface histology: quantification of bone formation and resorption

Surface histology was used to quantify the resorbing areas. Following Martinez-Maza et al. (2010, 2013), a grid of 5 x 5 mm squares was drawn on each cast. Bone formation and resorption were observed using an automated digital microscope (SmartZoom 5, Zeiss) with a 1.6x objective (zoom: 34x), and recorded following Boyde's criteria (1972). Bone formation is characterized by the pres- ence of elongated structures corresponding to mineralized collagen fiber bundles, as well as osteocyte lacunae, and bone resorption is characterized by the presence of multiple cavities known as Howship's lacunae, produced after the digestion of the bone by the osteoclasts (Fig. 1). Each 5 x 5 mm square was analyzed and the bone modeling activities were recorded on maps as follows: squares presenting both activities (i.e. bone formation and resorption) were subdivided using another grid of 2.5 x 2.5 mm so that each 'sub square' could be photographed using a higher zoom of 101x with a 5x objective (Fig. 2A). Each picture was analyzed in the software IMAGEJ 1.46r (Schneider et al. 2012). Areas of bone resorption were manually delimited, and the surface areas of the resorptive fields were calculated in IMAGEJ. From these calculations, a percentage of bone resorption was calculated for each square. Finally, a total percentage of bone resorption per specimen was obtained after summing up the results at each square and dividing this amount by the total surface of each specimen. Additionally, we calculated a mean percentage of resorption for each age group. Because of small sample sizes, statistical tests were not performed.

Table 1 Age of the specimens and sample size of each age group (AG).

Age group*	Age range (years)	Number of specimens
1	[0–0.6]	7
2	[0.7–2.5]	17
3	[3–6]	19
4	[7–12]	4
Total		47

*AG 1: No teeth emerged. AG 2: From alveolar emergence of the first deciduous tooth to the root completion of the last deciduous tooth to emerge. AG 3: Alveolar emergence of the permanent first molar until root completion. AG 4: Development of second permanent molar.

Table 2 List of homologous landmarks, curve and surface semilandmarks shown in Figure 3.

Landmarks	Label	
Superolateral nasion	sln	
Dacryon	d	
Zygoorbitale	zyo	
Inferolateral rhinion	ilr	
Anterior nasal spine	ans	
Alveolare (infradentale superius)	ids	
Zygomaxillare	zm	
Malar root origin	mro	
Maxillo-palatine suture	mps	
Curve semilandmarks		**Number - definition**
Fronto-maxillary suture	FMS	2 – superolateral nasion to dacryon
Naso-maxillary suture	NMS	6 – superolateral nasion to inferolateral rhinion
Inferior orbital margin	IOM	6 – dacryon to zygoorbitale
Nasal aperture outline	NA	6 – inferolateral rhinion to anterior nasal spine
Subnasal outline	SO	3 – nasal spine to alveolar
Zygomatico-maxillary suture	ZMS	5 – zygoorbitale to zygomaxillare
Maxillary contour	MC	4 – zygomaxillare to malar root origin
Alveolar outline	AO	8 – alveolare to maxillo-palatine suture
Surface semilandmarks		200 – covering the whole surface of the bone

Analysis of bone modeling variability

To compare and visualize the average bone modeling patterns for each age group, we first created digital maps for each specimen. The maps were computed in RSTUDIO 1.1.383 by associating the percentage of bone resorption for each square (calculated above, Fig. 2A) to a color (Fig. 2B). A percentage of 0 (red) indicates the absence of resorption, implying the presence of bone formation,

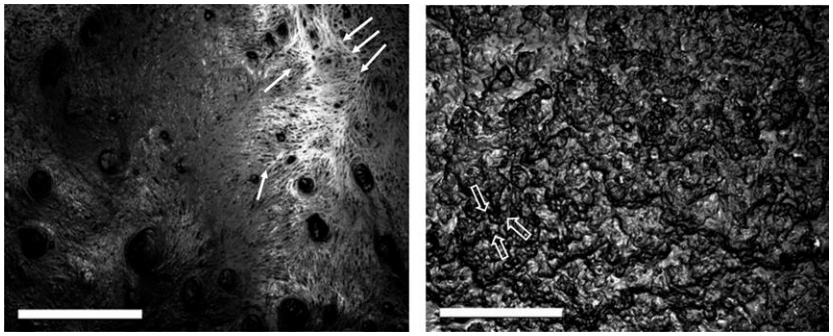

Fig. 1 Left: bone formation. Bone formation is characterized by the presence of collagen fiber bundles (white arrows) produced by the osteoblasts. Scale bar: 1 mm. Right: bone resorption. The presence of Howship's lacunae (open white arrows) indicates the digestion of the bone by the osteoclasts. Scale bar: 500 lm.

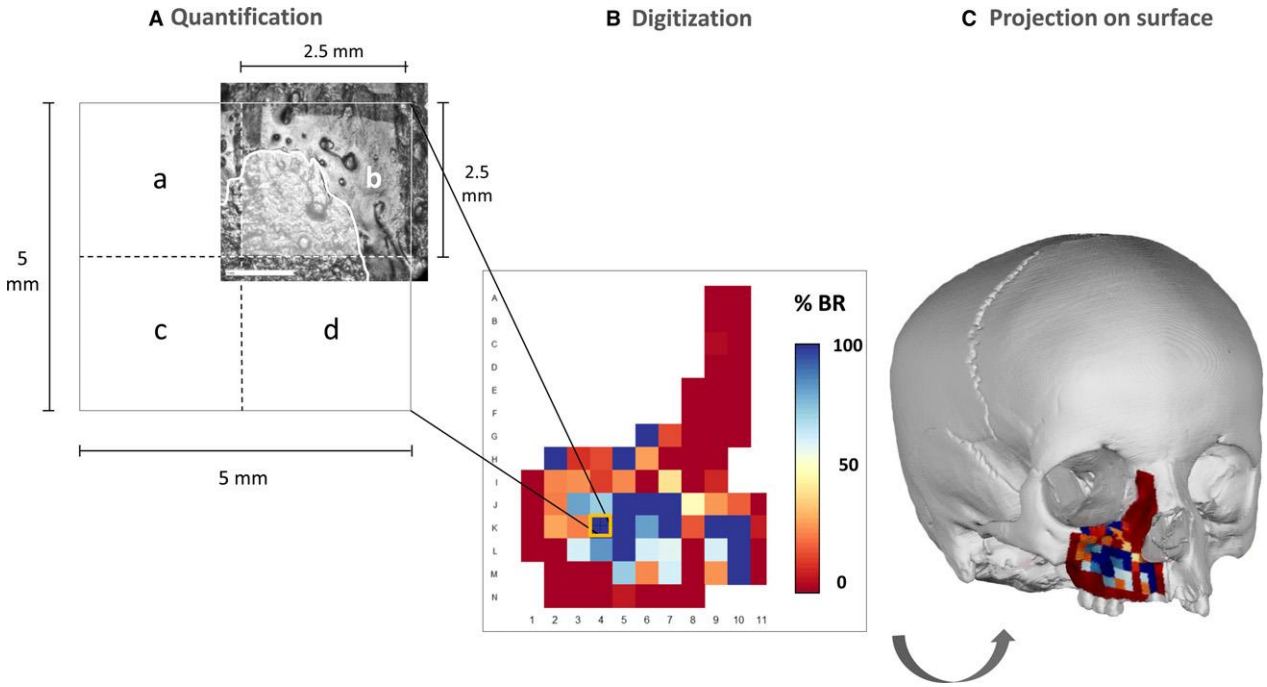

Fig. 2 Quantification of bone resorption and design of digital colored maps representing the bone modeling patterns. (A) Selection of the resorptive area in sub square b (square K4). This process was repeated in all subsquares where both formation and resorption were present in order to obtain a percentage of bone resorption (BR) per square. Scale bar: 1 mm. (B) After obtaining all percentages of BR for each square, each percent- age was associated to a color. The color scale goes from red (0% of BR, i.e. bone formation) to blue (100% BR). (C) The 2D grids were warped onto the 3D surfaces of the specimen for visualization.

and 100% (blue) denotes full resorption. To compare the maps between very young (small) and older (larger) individuals, each map was scaled to a standardized grid of 8 9 8 squares in RSTUDIO. More precisely, an 'empty' grid of 8 9 8 squares was first laid over the original one, such that the left-, right-, bottom-, and top-most edges matched. The final percentage of bone resorption for each cell of the new grid was then calculated as the average percentage of the cells of the original grid that intersected with those of the 8 9 8squaresgrid.Thecontributionofeachcelloftheoriginalgrid in the final percentage of BR was weighted by the area of intersection with the cells of the new grid, so that a large overlay between an original and a new cell weighs more in the final percentage of BR than a small overlay. We thus obtained 47 grids (one for each specimen) of similar size (8 9 8 squares), with comparable data. From these results, 'mean bone modeling maps' were computed for each age group using the average percentage at each square. To visualize the resultson 3D models, the 2D mean maps were warped onto the3D surface models of the mean configuration of each age group in GEOMAGIC STUDIO□ (Fig. 2C). We used a template of 15 land- marks registered on both objects to project the 2D map onto the 3Dmodel.

The next step was to examine and visualize the variability of the patterns. To do so, we calculated the variance of the percentagesof bone resorption in each square for the whole sample. Each variance was transformed to values between 0 and 1 before being associated with a shade of gray. Results were visualized on a 3D digital map ('variability map') using the same method as for the mean maps. Dark gray represent regions where bone resorption is highly variable (i.e. areas on the surface with frequent changes between formation and resorption) and light gray are regionsof low variability.

Analyses of form and morphological variability

To analyze the morphological changes during ontogeny, a 3D template of 249 landmarks and semilandmarks was created in VIEWBOX

(dHAL software). This template is composed of nine homologous landmarks, 40 curve semilandmarks and 200 surface semilandmarks (Fig. 3 A, B; Table 2). The landmarks and curve semilandmarks were manually placed on each specimen. The surface semilandmarks were digitized on one reference specimen and automatically warped using a thin plate spline (TPS) interpolation and projected onto the surfaces of every specimen in the sample. Coordinates of each point were extracted and loaded into R to perform the sliding process (Mitteroecker & Gunz, 2009). To establish geometric homology, the 240 semilandmarks were allowed to slide along tangents to the curves and tangent planes to the surface, minimizing the bending energy of the TPS interpolation function between each specimen and the Procrustes consensus configuration (Gunz & Mitteroecker, 2013). To compare all configurations and convert the coordinates to shape variables, a Generalized Procrustes Analysis (GPA) was performed (Rohlf & Slice, 1990; Bookstein, 1991). The GPA is a standardization of the position (translation to a common centroid) and orientation (rotation that minimizes the squared distances between pairs of corresponding landmarks) of each configuration in space, as well as the scaling to unit centroid size (computed as the square root of the sum of squared Euclidean distances from all landmarks to their centroid; Rohlf & Slice, 1990). To analyze maxillary growth, the natural logarithm of the centroid size was added as a variable to the matrix of the Procrustes coordinates following Mitteroecker et al. (2004). Using these coordinates, we performed a principal component analysis (PCA) in form (shape plus size) space. A multivariate regression analysis was performed to examine how much of the morphological variation in our sample is explained by ontogenetic allometry. To do so, we regressed all form variables on centroid size.

To later compare variability in bone modeling patterns to variability in form, the template was divided into two subsets corresponding to the upper (frontonasal) and lower (zygomatico-maxillary) parts of the maxilla bone (Fig. 3C, D), consisting of respectively 92 and 157 landmarks and semilandmarks (see Table 3 for description). The two subsets correspond to areas with absence or presence of developing teeth, respectively; we were then able to check whether underlying developing tissue can affect the variability of the bone modeling patterns. On each landmark subset, we performed separate GPAs and added the natural logarithm of the centroid size to each Procrustes matrix. Following Zelditch et al. (2012), we calculated morphological variance by summing the diagonal elements of the Procrustes variance-covariance matrix. To make the variances of the landmark subsets comparable, values were divided by the total number of landmarks in each subset following Freidline et al. (2016).

Comparison of morphological changes and bone modeling patterns

To visualize changes at both the micro- and macroscales, we combined the texture data produced by the surface histology analysis with the morphological changes highlighted by the GM analysis using the Geometric Morphometric Image Analysis (GMIA) method (Mayer et al. 2014). This method allows the comparison of morphometric and texture data in a joint analysis by performing a two- block Partial Least Squares (PLS) analysis (Bookstein, 1994; Rohlf & Corti, 2000) between datasets of different lengths and dimensions. After performing a singular value decomposition of the two-block covariance matrix, the maximum covariation between the linear

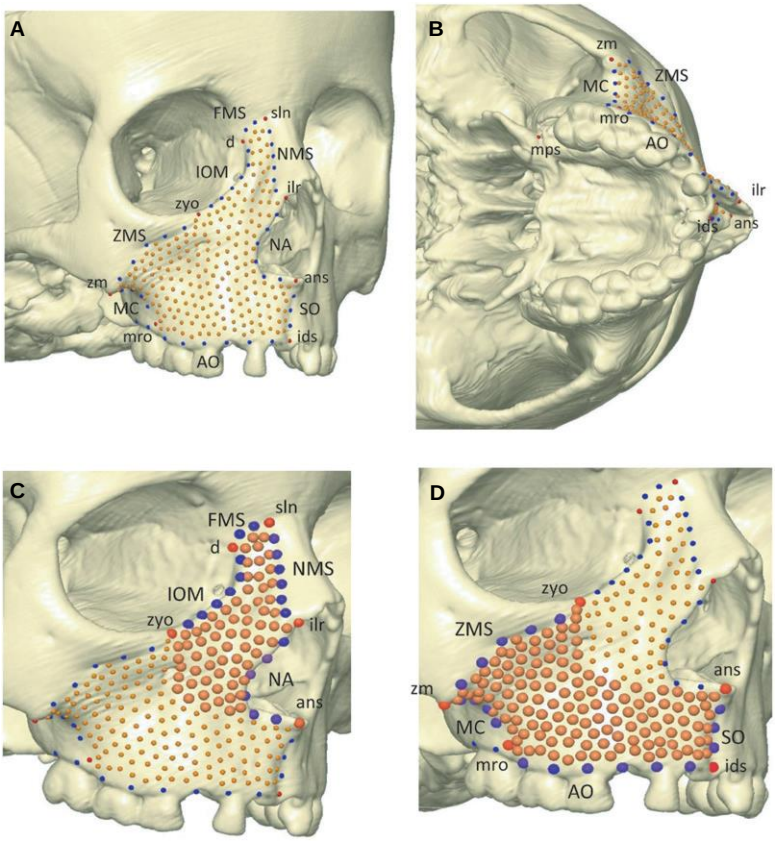

Fig. 3 (A,B) Template of the right maxilla (249 landmarks and semilandmarks) in fronto-lateral and inferior views, respectively. Red dots: landmarks (9); blue dots: curve semilandmarks (40); yellow dots: surface semilandmarks (200). Names and definitions of all points are listed in Table 2. (C,D) Landmarks and semilandmarks subsets created from the general template. (C) Upper part ('frontonasal'; 92 landmarks and semilandmarks); (D) lower part ('zygomatico-maxillary'; 157 landmarks and semilandmarks). See Table 3 for the description of the subsets.

combinations of each block can be visualized. For the texture data, missing values (representing less than 0.5% of the data) were first estimated for each age group independently in RSTUDIO using a regularized iterative PCA algorithm of the missMDA package. The matrix of Procrustes coordinates, to which the natural logarithm of the centroid size was added, was used for the morphological data. A PLS analysis was then performed on the two datasets. Results were visualized by computing extreme forms and textures on each axis (+/- 2 standard deviations from the mean). The morphological changes were visualized by warping the deformed surfaces on a standard 3D model using a TPS deformation (Bookstein, 1991; Mitteroecker & Gunz, 2009), and the extreme textures were warped onto the 3D models in GEOMAGIC using the same method cited above.

Finally, to explore how bone modeling activities and local displacements are linked, we computed distance maps to show how growth intake is distributed across the maxilla (Martinez-Maza et al. 2015; Freidline et al. 2016). Mean forms were calculated for each age group, and warped onto a reference surface. The distances between each mean form (e.g. between AG1 and 2, AG2 and 3 and AG3 and 4) were calculated and converted to a color value.

Results

Description of the maxillary bone modeling patterns

To visualize changes in the bone modeling patterns of the maxilla, we computed mean bone modeling maps representing the average pattern at each age group (Fig. 4). Our analysis shows that bone resorption is already present at early stages in our sample. It is mainly localized at the fronto-maxillary suture and the region above the lateral incisors and canine bulb in age group 1 (see mean maps AG1 on Fig. 4). The mean map for age group 2 shows an extension of the resorptive area in the maxillary arcade and zygomatic process, with increasing values of bone resorption (between 60 and 80%). In age group 3, bone resorption is mostly absent from the fronto-maxillary suture, and the top half of the bone becomes mainly bone formation. Similar to age group 3, the highest concentrations of resorption in age group 4 are predominantly in the maxillary arcade and the zygomatic process, mostly present near the zygomatico-maxillary suture, the inferior orbital margin and the anterior part of the maxillary arcade. All maps show a similar pattern throughout ontogeny, with bone resorption mainly present in the lower part of the bone, represented by the maxillary arcade and the zygomatic process. Younger age groups tend to show high concentrations of bone resorption near the fronto-maxillary suture.

Quantification of bone resorption

A total percentage of bone resorption was obtained for each individual and plotted against age (Fig. 5, top). Each individual is represented by a bar, and individuals of similar ages are represented by different shades of gray. Bone resorption first increases between birth and the first year (from ~2 to ~40%). Between 1 and 2.5 years, values fluctuate between 25 and 62%, and around 3 to 3.5 years, percentages decrease to between 5 and 10%. Values between 3 to 6 years range from 5.9 to 58.6%. Between 7 and 12 years, values vary between 17.3 and 50.6%. When only specimens of the same age are considered, differences in the percentage of bone resorption are variable, ranging from 1% (at 1.2 years) to 43% (at 6 years). These differences are uncorrelated with age and dental eruption. Box- plots representing the distribution and mean bone resorption at each age group were computed (Fig. 5, bottom). Age group 2 shows the highest mean value of bone resorption (43.1%), followed by age groups 4 (35.4%), 3 (32.6%) and 1 (24.2%).

Analysis of variability in bone resorption

Variability in the expression of bone resorption during growth was explored by computing the variance of the percentages of bone resorption in each square and represented on a map (Fig. 6). The most variable regions highlighted by this analysis are located in the top of the

Table 3 Names and number of landmarks, semilandmarks and description of each subset.

Subset	Landmarks names*–number	Curve names–number of semilandmarks	Surface semilandmarks	Description
A	d, sln, ilr, ans, zyo–5	Frontomaxillary suture (FMS)–2 Nasomaxillary suture (NMS)–6 Infero orbital margin (IOM)–6 Nasal aperture (NA)–6	67	Upper limit: Frontomaxillary suture (FMS); medial limit: Nasomaxillary suture (NMS); distal limit: Infero orbital margin (IOM); lower limit: horizontal line defined by the lower limit of the nasal aperture
B	zyo, zm, mro, ids, ans–5	Zygomatico-maxillary suture (ZMS)–5 Maxillary contour (MC)–4 Subnasal outline (SO)–3 Alveolar outline (AO)–6	134	Upper limit: horizontal line defined by the lower limit of the nasal aperture; medial limit: subnasal outline (SO); distal limit: Zygomatico-maxillary suture (ZMS) and maxillary contour (MC); lower limit: Alveolar outline (AO)

*For the names of the landmarks, refer to Table 2.

frontal process, the maxillary arcade and zygomatic process, with higher values close to the sutures. The least variable area is located in the nasal area. The map was then compared with the analysis of morphological variability within each subset defined in Table 3 (upper vs. lower part of the maxilla). The results shown in Table 4 suggest a higher morphological variability in the frontonasal subset.

Comparison of morphological and surface histology analyses

Joint analysis of form and texture

Morphological variability was analyzed by means of a PCA in form space (Fig. 7A). The first two PCs account for 87.2 and 3.2% of the total form variance, respectively. In PC 1, the youngest specimens fall along the negative values and the older specimens along the positive values. The main factor creating variability in our sample is size (i.e. ontogenetic allometry) as shown by the multivariate regression analysis ($R^2 = 0.86$). All age groups are aligned along PC 1 and only AG 4 is distinct from the other groups, with AG 1 being the most variable along this axis. Morphological changes along PC 1 mainly imply an increase in height in the superior–inferior direction. The second PC shows a slight rotation of the orbital ridge as well as an increase in the height of the bone. A second PCA was performed on the bone modeling data (Fig. 7B). The first two PCs account for respectively 29.6 and 20.2% of the total variance. This analysis shows a large overlap between age groups, particularly on PC 1. Changes along this axis are represented by an increase in bone resorption in the maxillary arcade of the bone and in the frontal process. On PC 2, the youngest specimens (AG1) are separated from the oldest (AG4). On this axis, changes are represented by an increase in bone resorption in the maxillary arcade, with an absence of bone resorption in the frontal process on the positive end. Figure 7C shows the joint analysis between form and texture by means of a PLS analysis. We show that changes in height in the superior–inferior direction are associated with an increase of BR in the maxillary arcade (correlation coefficient: 0.49). Moreover, results of this joint analysis indicate that subtle changes in the bone modeling patterns (axis 1) result in the form changes observed in our sample (axis 2).

Local displacements and bone modeling activity

To investigate how bone formation and resorption are linked to local displacements (and test whether formation fields face the forward displacement, cf. hypothesis 3), differences in growth between age groups were visualized by computing distance maps (Fig. 8). Warm colors represent forward growth between two age groups, whereas cold colors represent backward growth. Between age groups 1 and 2 (Fig. 8A), growth is homogeneous across the bone. Between age groups 2 and 3 (Fig. 8B), warm colors are present in the frontal process and the nasal area, whereas cold colors are seen in the maxillary arcade and the zygomatic process, particularly around the inferior part of the orbit. This pattern is even more apparent in the third map, which shows differences between age groups 3 and 4 (Fig. 8C). Cold colors are predominant in the infra-orbital region and the anterior part of the maxillary arcade. Again, the frontal process and the nasal area are represented by warmer colors. These results indicate differences in growth intake (direction and magnitude) between the top half of the bone (represented by the frontal process and the nasal area) and the bottom half (represented by the maxillary arcade and the zygomatic process), particularly in the infra-orbital region.

Discussion

In this study, we investigated bone modeling patterns and morphological form changes expressed in the maxilla during ontogeny, focusing on the variability of these two processes in a population of European ancestry. We quantified for the first time the activities of bone formation and resorption with histological methods, and improved the visualization of the patterns by creating digital rather than handmade maps. The remarkable preservation of the bone surfaces, as well as the use of semilandmark geometric morphometric techniques as a complementary approach, allowed us to analyze and compare changes at both the micro-and macroscopic levels at a very high resolution.

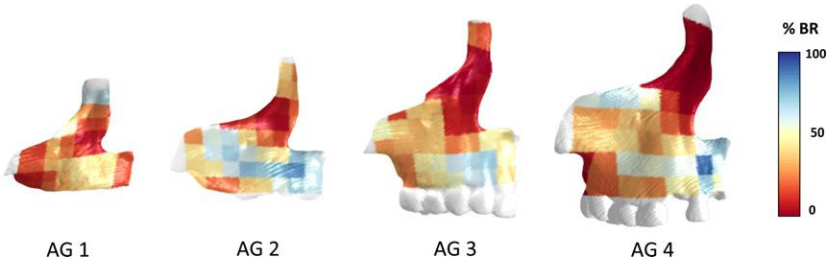

Fig. 4 Mean bone modeling maps representing the average pattern for each age group. Cold colors indicate high percentages of bone resorption (BR), warm colors indicate low percentages. AG1: age group 1; AG2: age group 2; AG3: age group 3; AG4: age group 4.

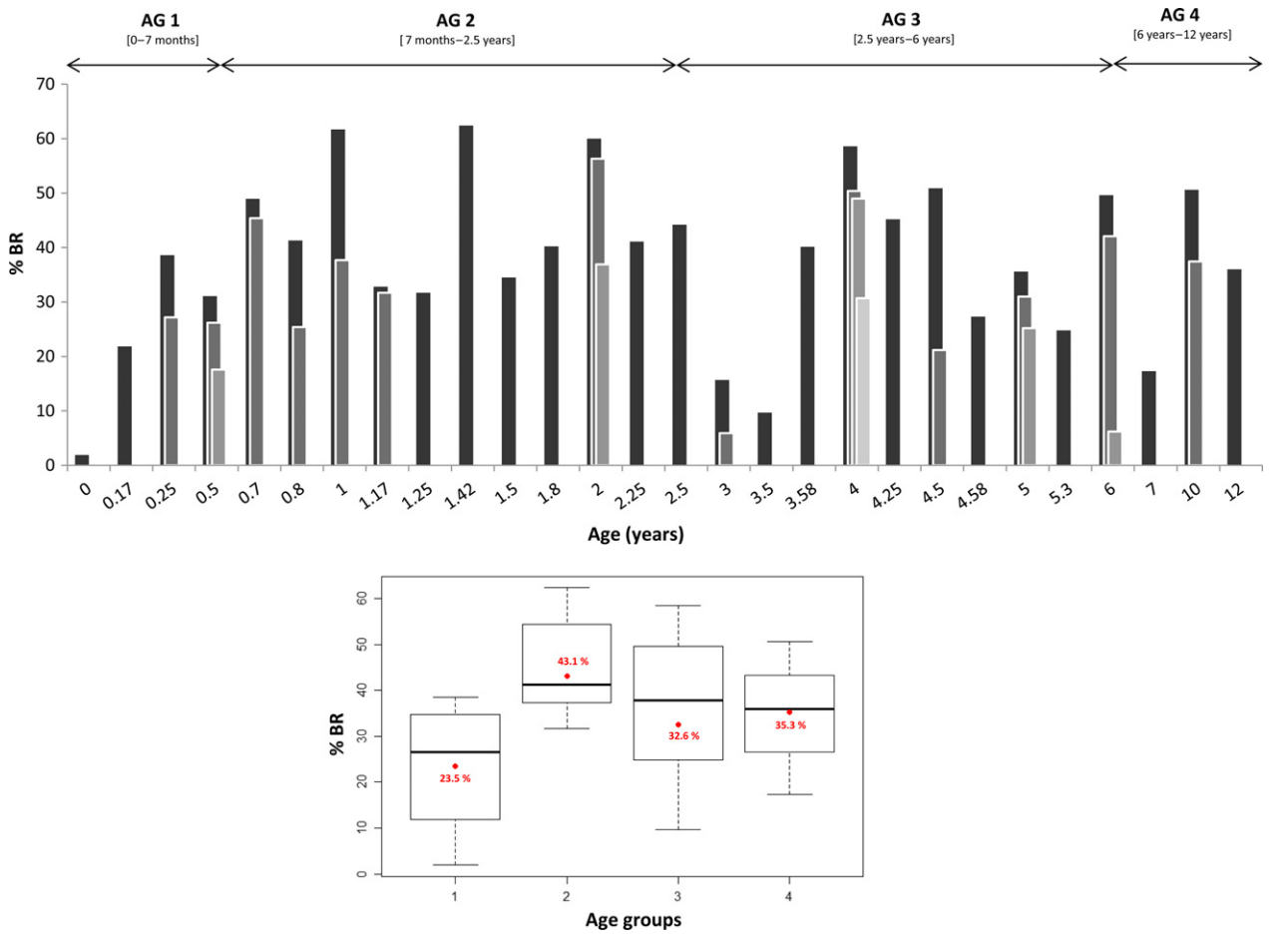

Fig. 5 (Top) Percentages of bone resorption for each individual plotted against age (in years). Each individual is represented by a bar. Individuals of similar age are shown in different shades of gray. (Bottom) Box plots representing the distribution of the percentages of bone resorption at each age group. Age group means are indicated as red dots.

Patterns of bone modeling in the human maxilla

The ontogenetic bone modeling patterns found in this study are similar to previous findings in *H. sapiens* (Enlow & Hans, 2008; Kurihara et al. 1980; McCollum, 2008; Martinez-Maza et al. 2013). In a previous study, Kurihara et al. (1980) found no sign of a resorptive activity before the age of 3 months; however, in our sample, this activity is already present at birth. The digitization of each age groups' mean map allows the observation of major changes in the bone modeling activities throughout ontogeny. Areas affected by bone resorption are mainly located in the maxillary arcade, in the inferior part of the orbital rim and in the zygomatic process (Fig. 4). We show that the top of the frontal process (around the fronto-maxillary suture) is predominantly resorptive in the youngest individuals, a pattern never reported before. However, this activity is later reduced in older specimens, becoming mostly bone forming (Fig. 4, AG4). What causes a reduction in bone resorption in the top of the frontal process is unknown but could indicate a change in the integration pattern between this area (frontal process, frontal and nasal bones) and the rest of the skull as the direction of growth changes from a backward to a forward displacement (Enlow & Hans, 2008; see also Fig. 8). The nasal area is known to mature later than other craniofacial components (Humphrey, 1998), increasing in height into adulthood (Martinez-Maza et al. 2013) probably due to its association to respiratory requirements (Bastir, 2008; Holton et al. 2016). The forward growth observed in this region associated with bone formation in our sample may thus reflect this expansion. More generally, due to the central position of the maxilla in the craniofacial complex and the biological functions it supports (vision, mastication, and respiration as mentioned above),maxillary growth is likely to be influenced by growth of the surrounding bones and soft tissues (Moss & Young, 1960; Smith et al. 2014; Goergen et al. 2017), the basicranium (Bastir et al. 2008; Bastir & Rosas, 2016) as well as the vertical expansion of the maxillary sinus ('secondary pneumatization', Smith et al. 2005) as its shape has been found to covary with the midface (Butaric & Maddux, 2016; although see O'Higgins et al. 2006). Therefore, changes in the

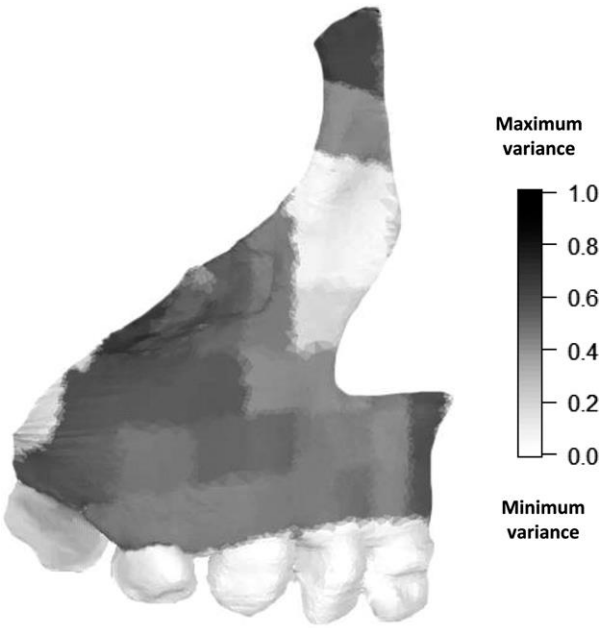

Fig. 6 Map representing the variability in bone modeling patterns in the whole sample. The variances of the percentages of BR in each square are reduced to values between 0 and 1, and represented by a shade of gray.

Table 4 Variances of form variables in the upper and lower parts of the maxilla.

	Total variance
Frontonasal	5.00E-04
Zygomatico-maxillary	1.80E-04

Expression of bone modeling patterns are certainly a response to the complex integration patterns of the craniofacial components.

Bone resorption is often predominant in areas overlaying the developing teeth bulbs in the maxillary arcade, and later near the inferior part of the orbital rim. Several studies (Enlow & Bang, 1965; Kurihara et al. 1980; Martinez-Maza et al. 2013) have reported an increase in the resorptive activity throughout postnatal ontogeny in the anterior part of the maxilla, presented as an enlarging resorptive field from the maxillary arcade to the zygomatic process. Our study, based on quantitative data, also shows an increase in bone resorption in the maxillary arcade and zygomatic regions from early to later stages; however, as the resorptive area decreases in the frontal process with time (Fig. 4), the total percentage of bone resorption in the whole bone stabilizes after 3 years and represents about a third of the total surface (Fig. 5). It is likely that in the anterior part of the bone, a combination of local (on teeth bulbs) and regional (in the zygomatic process and maxillary arcade) fields of bone resorption result in the extension of the resorptive field. As the anterior face is developing laterally and vertically ('forward and downward displacement', Enlow & Hans, 2008), the teeth also develop postero-laterally and thus, result in an expansion of the resorptive area along the arcade.

Interindividual and intrapopulation variability

The comparison of the percentages of bone resorption between specimens of similar ages (Fig. 5, top) shows a certain degree of interindividual variability in the extension of the resorptive fields, with differences between two individuals of similar ages reaching up to 43%. This suggests that although bone resorption increases in the anterior maxilla, this process is not linear (i.e. constantly increasing with time) but rather is interrupted by either accelerated growth or remodeling phases, with bone formation covering the resorptive areas in order to maintain the cortical thickness. Although males are known to have slightly larger faces at early stages in ontogeny compared with females (Bulygina et al. 2006), sexual dimorphism did not affect the bone modeling patterns found in our study, as no differences between males and females were visible (Supporting Information Fig. S1). McCollum (2008) suggested that the differences between individuals in the expression of bone resorption observed in her sample may have resulted from different ancestries of the specimens. Whether ancestry explains differences in bone modeling patterns between individuals, or populations, has never been tested. As population differences in facial morphology arise early in development (Vidarsdottir et al. 2002; Freidline et al. 2015), a comparison of specimens from populations with different ancestries will help clarify this question. Nicholas (2016) found morphological differences between European-Americans and African-Americans in the maxilla already present before birth; whether this translates into different bone modeling patterns is still unknown.

When considering variability at the population level (Fig. 6), we show that the most variable regions are found where bone resorption is the most predominant (see Fig. 4); in particular, changes between formation and resorption seem higher around the fronto-maxillary, zygomatico-maxillary and inter-maxillary sutures. Following our hypothesis (2), we expected the upper maxilla to be less variable in form than the lower maxilla, as bone formation is predominant in this area. This result could not be confirmed by our analysis of morphological variability (Table 4). Several authors (Martinez-Maza et al. 2015; Freidline et al. 2016) observed that the anterior maxilla and the mandibular ramus are morphologically and microscopically more variable in great apes, particularly in *H. sapiens*, and suggested that this was due to less functional constraints leading to greater plasticity in these regions. In the present study, average percentages of bone resorption seem to stabilize in age groups 3 and 4 once the permanent teeth are fully formed and positioned in the occlusal plane

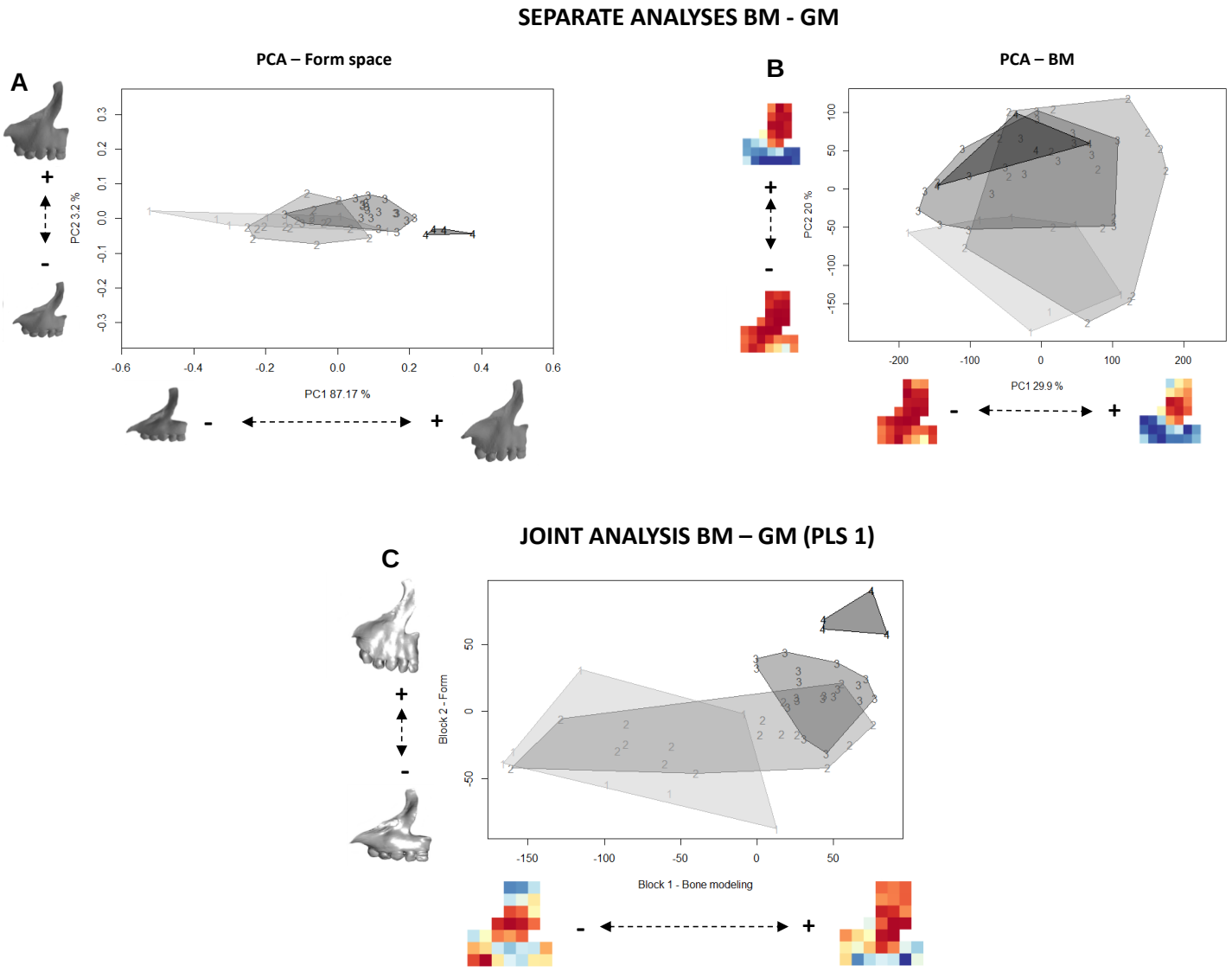

Fig. 7 (A) PCA in form space showing the morphological changes of the right maxilla during ontogeny. The three first PCs account for 90.4% of the total variance. PC 1 accounts for 87.2% and PC 2 for 3.2%. Morphological changes are represented by 3D surfaces computed at each PC extreme. (B) PCA of the bone modeling data. PC 1 accounts for 53.4 and PC 2 22.1%. Changes in the maps are represented at each PC extreme. (C) Joint analysis of morphological and bone modeling changes: on the x-axis, bone modeling data are represented and on the y-axis, form data are represented. Each age group is represented by numbers (1, 2, 3 and 4). Extremes maps and forms at each axis are shown in each plot.

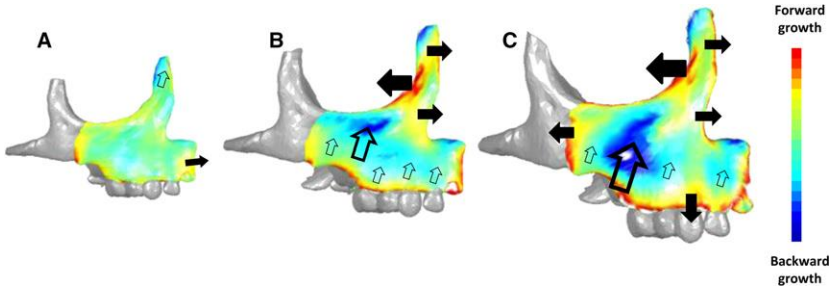

Fig. 8 Distance maps representing local displacements (i.e. growth difference/intake) of the growing maxilla. (A) Growth difference between AG 1 and 2. (B) Growth difference between AG 2 and 3. (C) Growth difference between AG 3 and 4. Warm color: forward growth; cold colors: back- ward growth. Solid black arrows: bone formation; empty black arrows: bone resorption.

(see Fig. 5). This corresponds to a reduction in morphological variability (Fig. 7A), already observed in former studies (Bulygina et al. 2006; Mitteroecker et al. 2012). Developmental canalization (Waddington, 1942) is defined as the reduction in variability of a trait despite genetic and/or environmental changes (Hallgrímsson et al. 2002). Whether more frequent changes between bone resorption and formation result in developmental canalization should be further tested with larger samples, and on other regions of the face. Our results so far suggest that the maxillary arcade, under biomechanical forces induced by the effect of mastication, expresses more frequent changes between formation and resorption, leading to less morphological variability. This would also explain why most changes between formation and resorption are found close to the sutures (Fig. 6), as they 'diffuse' mechanical loads across the skull (Popowics & Herring, 2007). Areas such as the upper face and nasal region that are under fewer functional constraints show more consistently forming fields (Martinez-Maza et al. 2013) and present higher morphological variability (Evteev et al. 2018), especially in older age groups as sexual dimorphism is inducing morphological changes in those areas (Freidline et al. 2016; Holton et al. 2016).

Although inter individual variability in the percentages of bone resorption is high, particularly in younger age groups, overall the general patterns of bone modeling remain very similar from age groups 2–4 in this European sample (Fig. 7B). The existence of a 'uniform' bone modeling pattern in post-natal ontogeny has already been observed in former studies by O'Higgins et al. (1991) in the mangabey *Cercocebus torquatus*, as well as in the common pig (*Sus scrofa*; Herring & Ochareon, 2016). We thus propose that, rather than changes in the bone modeling patterns, differences in rates and timings of development (induced by differential expressions of the osteoclastic and osteoblastic activities) may result in the morphological changes observed in our sample.

An integrative approach to studies of facial ontogeny

Growth appears to be fairly homogeneous in all parts of the bone at younger stages (Fig. 8A), although more active in areas close to the sutures. This result is in accordance with Enlow & Bang's (1965) hypothesis that sutural growth is predominant in early facial development. In the subsequent age groups (Fig. 8 B-D), backward growth is found in the lower maxilla (in the maxillary arcade and the zygomatic process), whereas forward growth is found in the upper maxilla (in the nasal area and the frontal process). Compared with the mean maps (Fig. 4), this respectively corresponds to areas that are mainly resorptive vs. areas predominantly forming bone. In particular, the difference in growth is notably low in the infraorbital region as shown by Fig. 8C. The morphology of the infraorbital plate has often been considered an important region differentiating Neanderthals and *H. sapiens* (Rak, 1986; Harvati et al. 2010). In Neanderthals, this region is often described as being flat or inflated, whereas a depression, often referred to as a canine fossa, is the condition for *H. sapiens*. According to our bone modeling maps (Fig. 4), this area shows intermediate values of bone resorption (around 50%) and high variability in the bone modeling patterns (Fig. 6). Together, these results suggest that the depression observed in modern humans does not result from bone being actively broken down only through bone resorption, but rather is created by both the growth of the surrounding areas coupled with phases of formation and resorption. This supports former findings (Maddux, 2011; Maddux & Franciscus, 2009; Freidline et al. 2012) that the canine fossa in *H. sapiens* is a byproduct of the development of the sur- rounding structures. In Neanderthals, this area is mostly represented by bone formation (Lacruz et al. 2015); however, the general pattern of variation in bone modeling is still unknown for this species. These results confirm our hypothesis (3) that bone formation faces the direction of growth, as proposed by Enlow (1963). More generally, these results are consistent with several studies (Enlow & Hans, 2008; Bjork & Skieller, 1976; Martinez-Maza et al. 2013) describing patterns of displacements in the midface in *H. sapiens*. As the whole bone is being pushed forward during development (due to the displacement of surrounded bones as well as its own growth), the resorptive area extends rapidly in the anterior part of the face in early developmental stages to 'force' the growth vector to follow a vertical direction. This pattern remains until later developmental stages, as shown by the stability in resorptive activity in all specimens.

Conclusion

In this study, we present new approaches for the quantification and visualization of the bone modeling patterns during ontogeny. We show that the typical bone modeling patterns found in our sample develop early in ontogeny, already present in the first months of postnatal life. The resorptive field located in the anterior part of the maxilla rapidly enlarges, attaining around a third of the whole sur- face by 3 years of age. This extension is, however, variable during an individual's life, with several phases of either growth intake and/or remodeling. Absence of bone resorption in isolated fossils may not indicate a unique, species-wide bone modeling pattern, as resorptive fields may have been present at earlier or later stages in ontogeny. In *H. sapiens*, the anterior resorptive field prevents forward growth of the midface, as growth is less predominant in this area than in the other parts of the bone. It is the combination of these processes (formation in the posterior part of the bone and resorption in the anterior part) and the movements of surrounding bones that leads to the specific orthognathic *H. sapiens* face. We show that surface histology and GM techniques give complementary results and

can be employed together as an integrative approach. Surface histology can inform about microstructural growth processes and GM techniques allow for the quantification of the ontogenetic changes at the macroscopic level. A better knowledge of intraspecific variability in bone modeling patterns during ontogeny and how this translates to large- scale morphological form changes is essential to improve our understanding of the evolution of hominin facial morphology.

Acknowledgements

We would like to thank Dr. Philipp Mitteroecker for reviewing this manuscript as well as one anonymous reviewer, Prof. Kahn from Strasbourg University (France) for providing us access to the Strasbourg anatomical collection, and Roger Mundry (Max Planck Institute of Evolutionary Anthropology, Leipzig, Germany) for his help generating the maps.

Author contributions

A.S. and S.F. designed the work. A.S. collected the data and performed the analyses. All authors contributed to the interpretation of the data. A.S. and S.F. wrote the article.

References

AlQahtani SJ, Hector MP, Liversidge HM (2010) Brief communication: the London atlas of human tooth development and eruption. *Am J Phys Anthropol* **142**, 481–490.

Balzeau A, Rougier H (2010) Is the suprainiac fossa a Neandertal autapomorphy? A complementary external and internal investigation. *J Hum Evol* **58**, 1–22.

Bastir M (2008) A systems-model for the morphological analysis of integration and modularity in human craniofacial evolution. *J Anthropol Sci* **86**, 37–58.

Bastir M, Rosas A (2004) Facial heights: evolutionary relevance of postnatal ontogeny for facial orientation and skull morphology in humans and chimpanzees. *J Hum Evol* **47**, 359–381.

Bastir M, Rosas A (2016) Cranial base topology and basic trends in the facial evolution of Homo. *J Hum Evol* **91**, 26–35.

Bastir M, Rosas A, Lieberman DE, et al. (2008) Middle cranial fossa anatomy and the origin of modern humans. *Anat Rec (Hoboken)* **291**, 130–140.

Björk A, Skieller V (1976) Postnatal growth and development of the maxillary complex. *In*: Factors Affecting the Growth of the Midface. *Craniofacial Growth Series* **6**, 61–99. Ann Arbor: *University of Michigan.*

Bookstein FL (1991) *Morphometric Tools for Landmark Data: Geometry and Biology*. New York: Cambridge University Press.

Bookstein FL (1994) Partial least squares: a dose-response model for Measurement in the behavioral and brain sciences. *Psycoloquy* **5**.

Boyde A (1972) Scanning electron microscope studies of bone. In: *The Biochemistry and Physiology of Bone* (ed. Bourne GH). New York: Academic Press.

Boyde A, Hobdell MH (1969a) Scanning electron microscopy of lamellar bone. *Z. Zellforsch* **93**, 213–231.

Boyde A, Hobdell MH (1969b) Scanning electron microscopy of primary membrane bone. *Z. Zellforsch*, **99**, 98–108.

Boyde A, Jones S (1996) Scanning electron microscopy of bone: instrument, specimen, and issues. *Microsc Res Tech* **32**, 92–120.

Brachetta-Aporta N, Martinez-Maza C, Gonzalez PN, et al. (2014) Bone modeling patterns and morphometric craniofacial variation in individuals from two prehistoric human populations from Argentina. *Anat Rec* **297**, 1829–1838.

Brachetta-Aporta N, Gonzalez PN, Bernal V (2018) A quantitative approach for analyzing bone modelling patterns from craniofacial surfaces in hominins. *J Anat* **232**, 3–14.

Bromage TG (1984) Interpretation of scanning electron microscopic images of abraded forming bone surfaces. *Am J Phys Anthropol* **64**, 161–178.

Bromage TG (1985) Systematic inquiry of in tests of negative/ positive replica combinations for SEM. *J Microsc* **137**, 209–216.

Bromage TG (1989) Ontogeny of the early hominin face. *J Hum Evol* **18**, 751–773.

Bulygina E, Mitteroecker P, Aiello L (2006) Ontogeny of facial dimorphism and patterns of individual development within one human population. *Am J Phys Anthropol* **131**, 432–443.

Butaric LN, Maddux SD (2016) Morphological covariation between the maxillary sinus and midfacial skeleton among sub-Saharan and circumpolar modern humans. *Am J Phys Anthropol* **160**,483–497.

Duterloo HS, Enlow DH (1970) A comparative study of cranial growth in *Homo* and *Macaca*. *Am J Anat* **127**, 357–367.

Enlow DH (1962) A study of the post-natal growth and remodeling of bone. *Am J Anat* **110**, 79–101.

Enlow DH (1963) *Principles of Bone Remodeling: An Account of Post-natal Growth and Remodeling Processes in Long Bones and the Mandible*. Springfield: Charles C Thomas.

Enlow DH (1966a) A comparative study of facial growth in *Homo* and *Macaca*. Am J Phys Anthropol 24, 293–307.

Enlow DH (1966b) A morphogenetic analysis of facial growth. *Am J Orthod* **52**, 283–299.

Enlow DH, Bang DDS (1965) Growth and remodeling of the human maxilla. *Am J Orthod* **51**, 446–464.

Enlow DH, Hans MG (2008) *Essentials of facial growth*. Ann Arbor, Mich, MI: Needham Press.

Evteev A, Anikin A, Satanin L (2018) Midfacial growth patterns in males from newborn to 5 years old based on computed tomography. *Am J Hum Biol* **30**, e23132.

Freidline SE, Gunz P, Harvati K, et al. (2012) Middle Pleistocene human facial morphology in an evolutionary and developmental context. *J Hum Evol* **63**, 723–740.

Freidline SE, Gunz P, Hublin JJ (2015) Ontogenetic and static allometry in the human face: contrasting Khoisan and Inuit. *Am J Phys Anthropol* **158**, 116–131.

Freidline SE, Martinez-Maza C, Gunz P, et al. (2017) Exploring Modern Human Facial Growth at the Micro- and Macroscopic Levels. In: *Building bones*. Cambridge: Cambridge University Press.

Frost HM (1987) Bone 'mass' and the 'mechanostat': a proposal. *Anat Rec* **219**, 1–9.

Goergen MJ, Holton NE, Grunheid T (2017) Morphological interaction between the nasal septim and nasofacial skeleton during human ontogeny. *J Anat* **230**, 689-700.

Gunz P, Mitteroecker P (2013) Semilandmarks: a method for quantifying curves and surfaces. *Ital J Mammal* **24**, 103-109.

Gunz P, Neubauer S, Maureille B, et al. (2010) Brain development after birth differs between Neanderthals and modern humans. *Curr Biol* **20**, R921-R922.

Gunz P, Neubauer S, Golovanova L, et al. (2012) A uniquely modern human pattern of endocranial development. Insights

from a new cranial reconstruction of the Neandertal newborn from Mezmaiskaya. *J Hum Evol* **62**, 300–313.

Hallgrímsson B, Willmore K, Hall BK (2002) Canalization, developmental stability, and morphological integration in primate limbs. *Am J Phys Anthropol Suppl* **35**, 131–158.

Harvati K, Hublin J-J, Gunz P (2010) Evolution of middle-late Pleistocene human cranio-facial form: a 3-D approach. *J Hum Evol* **59**, 445–464.

Herring SW, Ochareon P (2016) The periosteum of the zygomatic arch: vascularization and growth. *Anat Rec* **299**, 1661–1670.

Holton NE, Alsamawi A, Yokley TR, et al. (2016) The ontogeny of nasal shape: an analysis of sexual dimorphism in a longitudinal sample. *Am J Phys Anthropol* **160**, 52–61.

Humphrey LT (1998) Growth patterns in the modern human skeleton. *Am J Phys Anthropol* **105**, 57–72.

Johnson PA, Atkinson PJ, Moore WJ (1976) The development and structure of the chimpanzee mandible. *JAnat* **122**,467–477.

Kranioti EF, Rosas A, Garcia-Vargas S, et al. (2009) Remodeling patterns of occipital growth: a preliminary report. *Anat Rec* **292**, 1764–1770.

Kurihara S, Enlow DH, Rangel RD (1980) Remodeling reversals in anterior parts of the human mandible and maxilla. *Angle Orthod* **50**, 98–106.

Lacruz RS, de Castro JM, Martinon-Torres M, et al. (2013) Facial morphogenesis of the earliest Europeans. *PLoS ONE* **8**, e65199.

Lacruz R.S., Bromage T.G., O'Higgins P., et al. (2015) Distinct growth of the nasomaxillary complex in *Au. sediba*. *Sci Rep* 5,15175.

Le Minor J.-M., Billmann F., Sick H., et al. (2009). *Anatomies et Pathologies, les collections morphologiques de la Faculté de médecine de Strasbourg*. Bernardswille: I.D. l'Edition.

Maddux S. D. (2011). *A quantitative assessment of infraorbital morphology in Homo: testing for character independence and evolutionary significance in the human midface.* Ph.D. Dissertation, University of Iowa, Iowa.

Maddux SD, Franciscus RG (2009) Allometric scaling of infraorbital surface topography in *Homo*. *J Hum Evol* **56**, 161–174.

Martinez-Maza C, Rosas A, Nieto-Diaz M (2010) Brief communication: identification of bone formation and resorption surfaces by reflected light microscopy. *Am JPhysAnthropol* **143**,313–320.

Martinez-Maza C, Rosas A, Garcia-Vargas S, et al. (2011) Bone remodelling in Neanderthal mandibles from the El Sidron site (Asturias, Spain). *Biol Lett* **7**, 593–596.

Martinez-Maza C, Rosas A, Nieto-Diaz M (2013) Postnatal changes in the growth dynamics of the human face revealed from bone modelling patterns. *J Anat* **223**, 228–241.

Martinez-Maza C, Freidline SE, Strauss A, et al. (2015) Bone growth dynamics of the facial skeleton and mandible in *Gorilla gorilla* and *w*

Mayer C, Metscher BD, Müller Gb, et al. (2014) Studying developmental variation with geometric morphometric image analysis (GMIA). *Plos ONE* **9**, e115076.

McCollum MA (1999) The robust australopithecine face: a morphogenetic perspective. *Science* **248**, 301-305.

McCollum MA (2008) Nasomaxillary remodeling and facial form in robust *Australopithecus*: a reassessment. *J Hum Evol* **54**, 2-14.

Mitteroecker P, Gunz P (2009) Advances in geometric morphometrics. *Evol Biol* **36**, 235-247.

Mitteroecker P, Gunz P, Bernhard M, et al. (2004) Comparison of cranial ontogenetic trajectories among great apes and humans. *J Hum Evol* **46**, 679-697.

Mitteroecker P, Gunz P, Neubauer S, et al. (2012) How to explore morphological integration in human evolution and development? *Evol Biol* **39**, 536-553.

Moss ML, Young RW (1960) A functional approach to craniology. Am *J Phys Anthropol* **18**, 281–292.

Mowbray K (2005) Surface bone histology of the occipital bone in humans and chimpanzees. *Anat Rec B New Anat* **283**, 14–22.

Nicholas CL (2016) Fetal and neonatal maxillary ontogeny in extant humans and the utility of prenatal maxillary morphology in predicting ancestral affiliation. *Am J Phys Anthropol* **161**, 448–455.

O'Higgins P (2000) The study of morphological variation in the hominid fossil record: biology, landmarks and geometry. *J Anat* **197**, 103–120.

O'Higgins P, Chadfield P, Jones N (2001) Facial growth and the ontogeny of morphological variation within and between the primates *Cebus apella* and *Cercocebus torquatus*. *J of Zoology* **254**, 337–357.

O'Higgins P, Jones N (1998) Facial growth in *Cercocebus torquatus*: an application of three-dimensional geometric morphometric techniques to the study of morphological variation. *J Anat* **193**, 251–272.

O'Higgins P, Bromage TG, Johnson DR, et al. (1991) A study of facial growth in the Sooty Mangabey *Cercocebus atys*. *Folia Primatol* **56**, 86–94.

O'Higgins P, Bastir M, Kupczik K (2006) Shaping the human face. *Int Congr Ser* **1296**, 55–73.

Popowics TE, Herring SW (2007) Load transmission in the nasofrontal suture of the pig, *Sus scrofa*. *J Biomech* **40**, 837–844.

Rak Y (1986) The Neanderthal: a new look at an old face. *J Hum Evol* **15**, 151–164.

Rampont M. (1994). *Les squelettes, os et dents de foetus, nouveaux-nés et enfants du musée anatomique de Strasbourg. Aspects historiques et catalogues.* Strasbourg: Université Louis Pasteur.

Rohlf FJ, Corti M (2000) Use of two-block partial least-squares to study covariation in shape. *Syst Biol* **49**, 740–753.

Rohlf FJ, Slice D (1990) Extensions of the Procrustes method for the optimal superimposition of landmarks. *Syst Zool* **39**, 40–59.

Rosas A, Martinez-Maza C (2010) Bone remodeling of the *Homo heidelbergensis* mandible; the Atapuerca-SH sample. J Hum Evol 58, 127–137.

Schneider CA, Rasband WS, Eliceiri KW (2012) NIH Image to ImageJ: 25 years of Image Analysis. *Nat Methods* **9**, 671–675.

Smith TD, Rossie JB, Cooper GM, et al. (2005) Secondary pneumatization of the maxillary sinus in callitrichid primates: insights from immunohistochemistry and bone cell distribution. *Anat Rec A Discov Mol Cell Evol Biol* **285A**, 677–689.

Smith TD, Kentzel ES, Cunningham JM, et al. (2014) Mapping bone cell distributions to assess ontogenetic origin of primate midfacial form. *Am J Phys Anthropol* **154**, 424–435.

Vidarsdóttir UE, O'Higgins P, Stringer C (2002) A geometric morphometric study of regional differences in the ontogeny of the modern human facial skeleton. *J Anat* **201**, 211–229.

Waddington CH (1942) Canalization of development and the inheritance of acquired characters. *Nature* **150**, 563.

Zelditch ML, Swiderski DL, Sheets HD (2012) *Geometric Morphometrics for Biologists.* New York: Academic Press.

Supporting Information

Additional Supporting Information may be found in the online version of this article:

Fig. S1 Percentages of bone resorption for males (M) and females (F) plotted against age (in years)

Chapter 2

Intraspecific variability in human maxillary bone modeling patterns during ontogeny

Received: 4 November 2019 | Revised: 12 August 2020 | Accepted: 15 September 2020
DOI: 10.1002/ajpa.24153

RESEARCH ARTICLE

American Journal of Physical Anthropology | WILEY

Intraspecific variability in human maxillary bone modeling patterns during ontogeny

Alexandra Schuh[1] | Philipp Gunz[1] | Chiara Villa[2] | Kornelius Kupczik[1,3] | Jean-Jacques Hublin[1] | Sarah E. Freidline[1]

[1]Department of Human Evolution, Max Planck Institute for Evolutionary Anthropology, Leipzig, Germany
[2]Laboratory of Advanced Imaging and 3D modelling, Section of Forensic Pathology, Department of Forensic Medicine, University of Copenhagen, Copenhagen, Denmark
[3]Max Planck Weizmann Center for Integrative Archaeology and Anthropology, Max Planck Institute for Evolutionary Anthropology, Leipzig, Germany

Correspondence
Alexandra Schuh, Department of Human Evolution, Max Planck Institute for Evolutionary Anthropology, Deutscher Platz 6, 04103, Leipzig, Germany.
Email: alexandra_schuh@eva.mpg.de

Abstract

Objectives: This study compares the ontogenetic bone modeling patterns of the maxilla to the related morphological changes in three human populations to better understand how morphological variability within a species is established during ontogeny at both micro- and macroscopic levels.

Materials and methods: The maxillary bones of an ontogenetic sample of 145 subadult and adult individuals from Greenland (Inuit), Western Europe (France, Germany, and Portugal), and South Africa (Khoekhoe and San) were analyzed. Bone formation and resorption were quantified using histological methods to visualize the bone modeling patterns. In parallel, semilandmark geometric morphometric techniques were used on 3D models of the same individuals to capture the morphological changes. Multivariate statistics were applied and shape differences between age groups were visualized through heat maps.

Results: The three populations show differences in the degree of shape change acquired during ontogeny, leading to divergences in the developmental trajectories. Only subtle population differences in the bone modeling patterns were found, which were maintained throughout ontogeny. Bone resorption in adults mirrors the pattern found in subadults, but is expressed at lower intensities.

Discussion: Our data demonstrate that maxillary morphological differences observed in three geographically distinct human populations are also reflected at the microscopic scale. However, we suggest that these differences are mostly driven by changes in rates and timings of the cellular activities, as only slight discrepancies in the location of bone resorption could be observed. The shared general bone modeling pattern is likely characteristic of all *Homo sapiens*, and can be observed throughout ontogeny.

KEYWORDS
bone formation, bone resorption, facial ontogeny, semilandmark geometric morphometrics

1 | INTRODUCTION

Among present day humans, geographic variation in adult facial morphology has been reported as reflecting population affinities (Hanihara, 1996, 2000; Hennessy & Stringer, 2002; Howells, 1973, 1989; Lynch, Wood, & Luboga, 1996). In addition to population history, environmental factors such as climate and subsistence strategies contribute to cranial shape variation among human populations.

Adaptation to climate has been observed in facial features (Butaric & Maddux, 2016; Cui & Leclercq, 2017; Evteev, Cardini, Morozova, & O'Higgins, 2013; Harvati & Weaver, 2006; Hubbe, Hanihara, & Harvati, 2009; Nicholson & Harvati, 2006; Roseman & Weaver, 2004), particularly in the shape of the nasal region (Churchill, Shackelford, Georgi, & Black, 2004; Franciscus & Long, 1991; Holton & Franciscus, 2008; Maddux, Yokley, Svoma, & Franciscus, 2016; Yokley, 2009). Noback, Harvati, and Spoor (2011), as well as Maddux, Butaric, Yokley, and Franciscus (2017), found correlations between cold-dry and hot-wet environments and the shape of the bony nose (particularly the nasal fossa), suggesting that aspects of the nasorespiratory system may be adaptations to particular environments. Moreover, according to several studies changes in diet across time as observed between hunter-gatherer and agricultural populations have been linked to the gracilization of the masticatory apparatus (Deter, 2009; Gonzalez-Jose et al., 2005; Noback & Harvati, 2015; Stynder, Ackermann & Sealy, 2007; von Cramon-Taubadel, 2011). Stansfield, Evteev, and O'Higgins (2018) suggested that a reduction of loadings during ontog- eny explains morphological differences in the mandible between prehis- toric and modern humans. Thus, in comparison to the rest of the skull, facial components may be more plastic being subjected to diverse sources of variation (Smith, 2009; von Cramon-Taubadel, 2014).

One way to understand how morphological variability is established within a species is by investigating its ontogenetic pro- cesses. Freidline, Gunz, and Hublin (2015) compared the ontogenetic and static allometry (i.e., the covariation between shape and size) of several geographically diverse human populations using geometric morphometric techniques. Their results support previous studies by showing that population differences in facial morphology are already present early in ontogeny, possibly prenatally (e.g., Bastir & Rosas, 2004; Lieberman, McBratney, & Krovitz, 2002; Mooney & Siegel, 1986; Nicholas, 2016; Ponce de Leon & Zollikofer, 2001). They also demonstrated subtle differences between populations in the patterns of absolute and relative growth and development. Therefore, changes in the patterns of ontogenetic allometry generate differences in facial morphology between human populations (Bulygina, Mitteroecker, & Aiello, 2006; Rosas & Bastir, 2002; Sardi & Ramirez- Rozzi, 2012; Vidarsdóttir, O'Higgins, & Stringer, 2002).

At the cellular level, both the rate of activity as well as the location on bone surfaces of the osteoblasts and osteoclasts, the cells responsible for bone formation (or apposition; Enlow & Bang, 1965, Enlow, 1966) and resorption, cause bone to change in size and shape during ontogeny. This process, visible on dry bone, is called bone modeling (Enlow, 1962; Enlow & Bang, 1965; Frost, 1987). It is of par- ticular interest for ontogenetic studies as it can help us better under- stand the development of morphological features (Bromage, 1989; McCollum, 1999; McCollum, 2008). A majority of the ontogenetic studies published in the past 20years employed geometric morphometric techniques as a methodological approach, as it is a powerful tool for the quantification and visualization of morphological changes (Gunz & Mitteroecker, 2013; Mitteroecker & Gunz, 2009; Mitteroecker, Gunz, Windhager, & Schaefer, 2013). However, few studies have focused on the relationship between bone modeling patterns and morphological changes during ontogeny. This was first assessed by O'Higgins and Jones (1998) in the Red-capped mangabey *Cercocebus torquatus*. The authors found that the bone modeling pat- terns reflect allometric patterns in the face of this species. Several recent studies combined surface histology and semilandmark geometric morphometric techniques to study facial ontogeny in great apes and humans (Freidline, Martinez-Maza, Gunz, & Hublin, 2016; Martinez-Maza, Freidline, Strauss, & Nieto-Diaz, 2015; Schuh, Kupczik, Gunz, Hublin, & Freidline, 2019). Such as O'Higgins and Jones (1998), these studies showed a correspondence between the morphological changes and the bone modeling patterns. Furthermore, these methods have shown to be complementary: while surface histology is informative about the microscopic processes underlying bone growth, geometric morphometric techniques help to quantify and visualize the morphological changes and displacements that cannot be observed through bone modeling alone.

Recently, Schuh et al. (2019) applied both methods on an ontogenetic sample of 48 maxillae from French individuals. In line with previous studies (Martinez-Maza et al., 2015; O'Higgins & Jones, 1998), the authors observed that maxillary bone modeling patterns in humans are rather constant through time from early stages on (i.e., the location of bone resorption on the surface is similar between age groups). This implies that the resorptive process is highly controlled (as discussed by Schulte et al., 2013), and that morphological differences within a group are likely driven by changes in bone formation and resorption rates rather than major differences in the bone modeling patterns. Regions of the maxilla showing less morphological variation, such as the maxillary arcade, are associated mainly to resorptive areas, suggesting that regions of high mechanical demands are more constrained and less variable. However, these inferences are based on a single population and may not reflect the variability within a species. McCollum (2008) proposed that the differences in the expression of bone resorption observed in her sample may reflect population history; however, like most bone modeling studies the limited sample size, as well as the lack of quantitative data, make this interpretation difficult.

In the present study, we quantify the bone modeling patterns in an ontogenetic series of three geographically distinct human populations: Western European, Greenlandic Inuit, and South African Khoekhoe and San descent. We investigate if differences observed at the macroscopic (or morphological) scale relate to those at the microscopic level. The Inuit facial morphology has long been the focus of many studies (Cruwys, 1988; Hawkes, 1916; Hrdlička, 1910; Hylander, 1977; Lynnerup, Homøe, & Skovgaard, 1999; Oschinsky, 1962), and different hypotheses have been proposed to explain their characteristic facial features, such as adaptation to a cold environment (Coon, Garn, & Birdsell, 1950; Wolpoff, 1968) and a hard diet (Hrdlička, 1910; Hylander, 1977). They are characterized by an elongated, narrow nasal aperture, vertical zygomatic processes, reduced nasal bones, and maxillary frontal process width, as well as a generally flat infra orbital area (Hylander,1977). South African populations such as Khoekhoe and San possess small faces with short and wide nasal apertures, anteriorly projecting zygomatic processes, wide orbits, and large maxillary frontal processes (Freidline et al., 2015). Europeans have been described as

showing long noses and retracted zygomatic bones (Hennessy & Stringer, 2002). Thus, we expect discrepancies in the expression and/or location of bone resorption between these populations where shape differences are the most pronounced, for example in the nasal area for which population differences have been described (Hennessy & Stringer, 2002; Maddux et al., 2017; Noback et al., 2011; Sardi & Ramirez-Rozzi, 2012). Moreover, a more pronounced canine fossa should be associated with more bone resorption, as discussed by Enlow and Bang (1965) and Schuh et al. (2019).

2 | MATERIALS AND METHODS

2.1 | Sample

The cross-sectional ontogenetic sample comprises 145 individuals from three different geographic areas (refer to Table 1 for the sample composition): Western Europe (Anatomical Institute of Strasbourg, France; Anatomical Institute of the University of Leipzig, Germany; Anthropological collection of the University of Coimbra, Portugal), Greenland (Inuit; Laboratory of Biological Anthropology, University of Copenhagen, Denmark) and South Africa (Khoekhoe and San; Iziko South African Museum, Cape Town; Anthropological collection of the Department of Human Biology, University of Cape Town; McGregor Museum, Kimberley, South Africa). Sex and calendar ages are known for some Western European individuals only, and were already previously investigated (Schuh et al., 2019). Thus, they were not considered in this study. We divided our sample into four age groups based on dental development, following AlQahtani, Hector, and Liversidge (2010): AG 1, developing deciduous dentition; AG 2, first permanent molar (M1) in occlusion; AG3, second permanent molar (M2) in occlusion; AG4, third permanent molar (M3) erupted, or adults. For the latter, variability in the bone modeling patterns is still largely unknown; however, as adult maxillae are larger than those of subadults, data collection is more time- consuming. Therefore, we were only able to include a limited number of individuals for this group. Finally, individuals with extensive tooth loss or surface alterations were avoided.

Negative molds of the maxillary surface (delimited by the surrounding sutures) were made using a low-viscosity silicone (President Plus light body, Coltène/Whaledent AG, Switzerland) following Bromage (1989). A positive replica of each negative mold was generated using an epoxy resin (5 Minute Epoxy Epoxidharz 2 K-Kleber transparent, Devcon). Only the better-preserved side of the maxilla was kept for the analysis (i.e., either left or right). Out of the 145 individuals, seven did not yield any data, which reduced the sample size

TABLE 2 Landmarks and semilandmarks numbers and definition (total:249)

Landmarks	Label	
Fixed landmarks		
Superolateral nasion	sln	
Dacryon	d	
Zygoorbitale	zyo	
Inferolateral rhinion	ilr	
Anterior nasal spine	ans	
Alveolare (infradentale superius)	ids	
Zygomaxillare	zm	
Malar root origin	mro	
Maxillo-palatine suture	mps	
Curve semilandmarks		***Number—definition***
Fronto-maxillary suture	FMS	2—Superolateral nasion to dacryon
Naso-maxillary suture	NMS	6—Superolateral nasion to inferolateral rhinion
Inferior orbital margin	IOM	6—Dacryon to zygoorbitale
Nasal aperture outline	NA	6—Inferolateral rhinion to Anterior nasal spine
Subnasal outline	SO	3—Nasal spine to alveolar
Zygomatico-maxillary suture	ZMS	5—Zygoorbitale to zygomaxillare
Maxillarycontour	MC	4—Zygomaxillare to malar root origin
Alveolar outline	AO	8—Alveolare to maxillo-palatine suture
Surface semilandmarks		200—Covering the whole surface of the bone

TABLE 1 Number of individuals for each population and age group

Age group	Greenlandic Inuit[a]	South African[b]	Western European[c]	Total
1	13	11	24	48
2	15	8	27	50
3	15	8	3	19
4	5	10	6	21
Total	48	37	60	145

[a]Laboratory of Biological Anthropology, University of Copenhagen, Denmark.
[b]Iziko Museum of Cape Town; University of Cape Town; McGregor Museum of Kimberley, South Africa.
[c]Strasbourg Anatomical Collection (Le Minor, Billmann, Sick, Vetter, & Ludes, 2009; Rampont, 1994), France; Leipzig University of medicine, Germany; Anthropological Collection of the University of Coimbra, Portugal.

to 138 individuals for the surface histology analysis. Those individuals were however kept for the morphological analysis. We used computed tomography (CT) scans of all individuals acquired at a resolution of 0.2 to 0.4mm (BIR ACTIS 225/300) and 0.6mm for the Western European/South African individuals and Greenlandic Inuit, respectively. For the South African sample, some of the scans were acquired using a portable Artec Space Spider (Artec3D, Luxembourg) surface scanner. The surface models were generated using the software packages Avizo (Thermo Fisher Scientific) and Artec Studio.

2.2 | Analyses

2.2.1 | Analysis of developmental changes

To quantify the morphological changes of the maxilla bone during ontogeny, we used a template of 249 landmarks and semilandmarks (Table 2) created in Viewbox (dHAL software) from the right maxilla (Figure 1a). Fixed landmarks (n = 9) and curve semilandmarks (n = 40) were placed manually, and surface semilandmarks (n = 200) were automatically projected onto each individual's surface using a thin- plate spline (TPS) interpolation function. Estimation of missing data was performed in RStudio (RStudio Team, 2020) by deforming the weighted estimate configurations that are the most similar to the defective configuration using a TPS interpolation (package Morpho; Schlager, 2017). Landmarks taken on left maxillae were mirrored to obtain a sample composed of only right configurations. To assure geometric homology between the landmark configurations, the curve and surface semilandmarks were allowed to slide along their respective tangent axis and plane, by minimizing the bending energy of the deformation between the sample mean and each configuration (Bookstein,1997; Gunz, Mitteroecker, & Bookstein, 2005).

The coordinates were then superimposed using a Generalized Procrustes Analysis (GPA; Rohlf & Slice, 1990). To first investigate the morphological variation in the ontogenetic patterns, developmental trajectories between populations were explored by using a Principal Component Analysis (PCA) in shape space. Shape differences between populations were visualized by computing and superimposing the mean shapes of each population. Differences and/or similarities in the devel- opmental trajectories were assessed with the use of developmental simulations. In a given population, the youngest individuals (from AG1) were simulated along the trajectory of another population by adding the mean developmental trajectory of the latter (computed as the vectors of the mean shape differences) to their Procrustes coordinates (Gunz, Neubauer, Maureille, & Hublin, 2010; Neubauer, Gunz, & Hublin, 2010; Scott, Neubauer, Hublin, & Gunz, 2014). As developmental trajectories are nonlinear, and as the number of variables largely exceeds the number of individuals in this study, performing linear statistical tests is not appropriate. By accounting for the nonlinearity of the trajectories, this method thus allows the analysis of ontogenetic

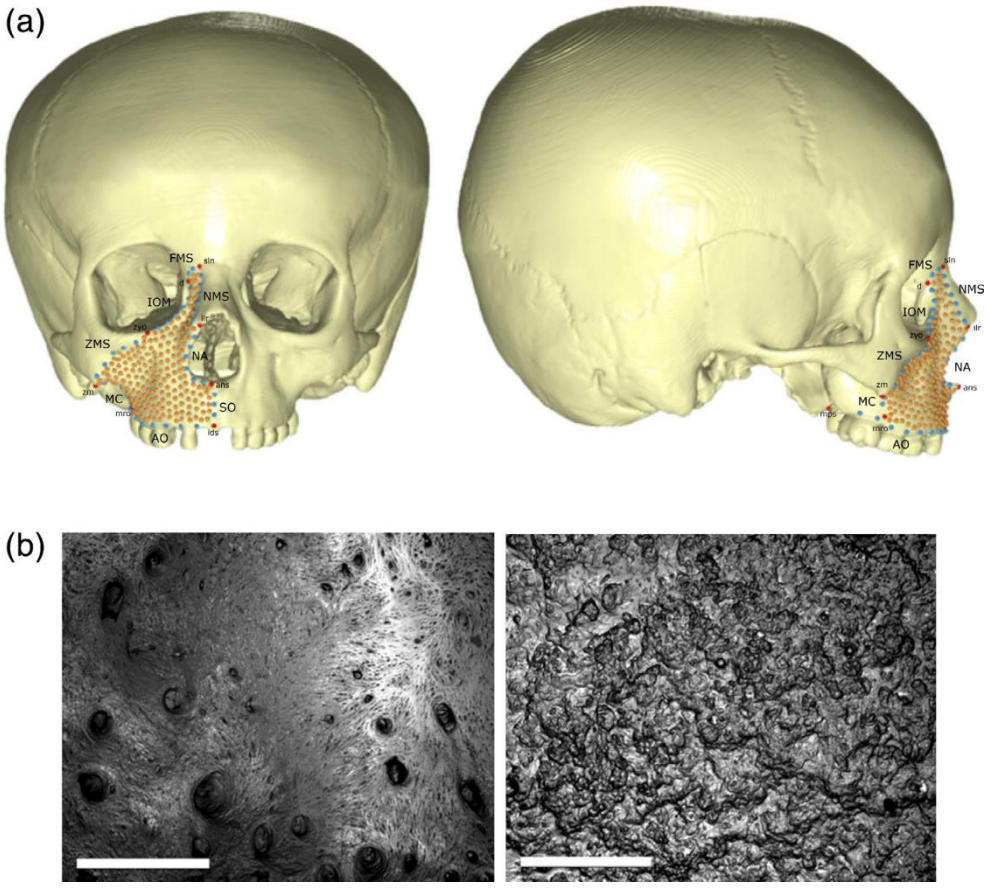

FIGURE 1 (a) Template of the right maxilla showing 249 landmarks (red dots)and semilandmarks (curve: blue dots; surface: orange dots).Names and definitions of fixed landmarks and curves semilandmarks are given in Table2. (b) Examples of bone formation (left) and bone resorption (right). Formation is characterized by collagen fibers that are mineralized and visible on dry bones as elongated structures. Scale bar: 1 mm. Bone resorption is detectable by the presence of small depressions, called Howship's lacunae. Scale bar: 500 µm

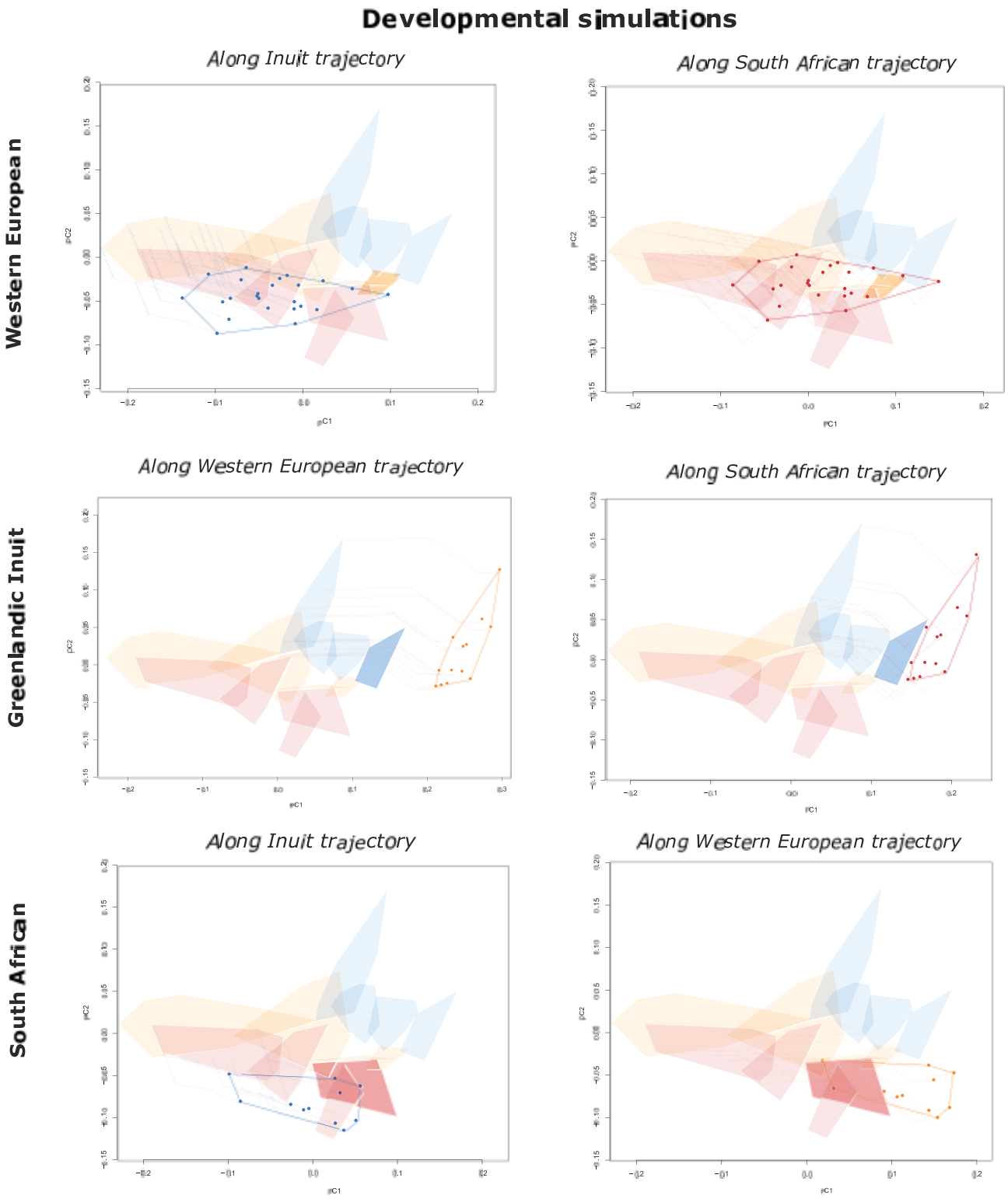

FIGURE 2 Developmental simulations. Top: Western European AG 1 individuals simulated along the Greenlandic Inuit (left) and South African (right) trajectories; Middle: Greenlandic Inuit AG 1 individuals simulated along the Western European (left) and South African (right) trajectories; Bottom: South African AG 1 individuals simulated along the Greenlandic Inuit (left) and Western European (right) trajectories. Each individual's trajectory is represented as a dotted line. Simulated individuals are shown as dots in a lined convex hull. Both lines and dots are shown in the color of the population for which the trajectory was used (e.g., Western Europeans and South Africans simulated along the Greenlandic Inuit trajectory are shown in blue). Each age group is represented by a filled convex hull in the color of the population (orange: Western European, blue: Greenlandic Inuit, red: South African). Non-simulated adults are shown in a dark shade convex hull

trajectories in a multivariate context. The simulated individuals were compared in a PCA to the non-simulated adults, first within one population (the Western European, as it is the most well-represented of the sample) to test the method, then between populations. If the simulated adults plot close to the non-simulated ones of their own population, then the trajectories are interchangeable. In the opposite case, the trajectories differ between populations (Neubauer et al., 2010).

Intra-population developmental differences across age groups were then visualized with the use of heat maps (Schlager, Profico, Di Vincenzo, & Manzi, 2018). First, independent GPAs were performed on each population to ensure that population differences do not influence the results. The mean shape of each age group was computed using the Procrustes coordinates. A mesh was then warped onto each mean shape using a TPS interpolation. Euclidean distances between two meshes of subsequent age group means (AG 1 and 2 [AG 1–2]; AG2 and 3 [AG2–3]; AG3 and 4 [AG3–4]) was calculated using a k- dimensional tree search for closest triangles (Schlager, 2017) from the Older to the younger age group. The distances are shown on a map as a color scale of maximum and minimum distances between meshes (a range of 2 and −2, respectively). Positive distances (from 0 to 2) are shown in warm colors, and are interpreted as an anterior displacement of the bone. Similarly, negative distances (from −2 to 0) are shown in cold colors, and are interpreted as a posterior displacement.

2.2.2 | Quantification and visualization of the bone modeling patterns

For the surface histology analysis, a grid of 5 × 5 mm squares was drawn on each cast (Martinez-Maza, Rosas, & Nieto-Diaz, 2013). The observations were made using an automated digital microscope (SmartZoom 5, Carl Zeiss Microscopy, Jena, Germany) with a 1.6x PlanApo D objective (zoom: ×34). Bone formation results from the activity of the osteoblasts that produce collagen fibers, identifiable as elongated structures on the

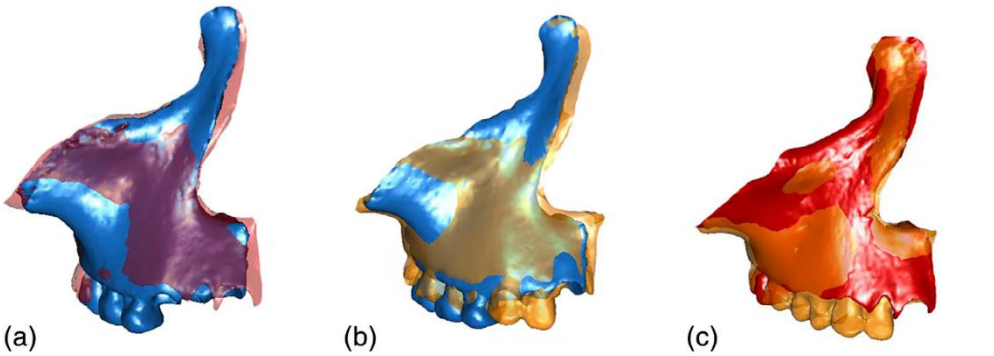

FIGURE 3 Shape differences between populations visualized by superimpositions of the mean shapes. A: Greenlandic Inuit (blue) and South African (red); Greenlandic Inuit (blue) and Western European (orange); C: Western European (orange) and South African (red)

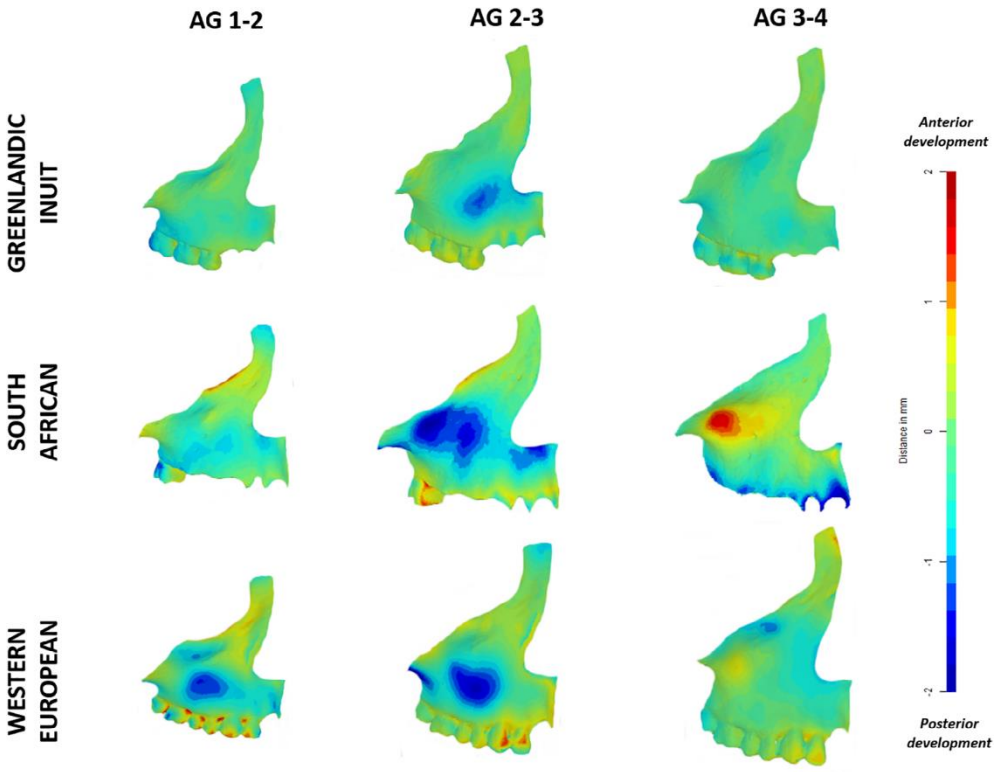

FIGURE 4 Heat maps showing morphological differences between AG1 and 2 (AG 1–2), AG 2 and 3 (AG 2–3), and AG 3 and 4 (AG3–4) for all populations. The differences are calculated as the closest distances between two meshes, which were first warped onto their corresponding mean configuration using a TPS interpolation (after independent GPA alignments for each population). Warm colors indicate positive distances, cold colors indicate negative distances. The color scale was set up on a range from −2 (minimum distance) to 2 (maximum distance). Informative data are only considered for the surface in relation to the template, which exclude the teeth

surface (Figure 1b, left). Bone resorption is defined by the digestion of the bone by the osteoclasts, and results in multiple cavities known as Howship's lacunae (Figure 1b, right; Boyde, 1972). We analyzed each square and recorded the presence of the two activities on handmade maps. When both activities were present, another 2.5 × 2.5 mm grid was drawn within the 5 × 5 mm squares so that pictures at a higher resolution (×101) could be taken with a PlanApo D ×5 objective.

Following Schuh et al. (2019), areas of bone resorption were manually selected in order to be quantified using the software ImageJ 1.46r (Schneider, Rasband, & Eliceiri, 2012). A percentage of bone resorption (%BR) for each square of the grid was calculated, as well as the amount of bone resorption per individual by dividing the total % BR by the total surface area of the bone. From these results, mean % BR and standard deviation were calculated for each age group. In order to compare and visualize the bone modeling patterns between populations, digital maps were computed for each individual in RStudio. The %BR at each square was associated with a color: low values of bone resorption were represented by warm colors, while high values were represented by cold colors. Areas with low amounts of bone resorption are represented by predominant amounts of bone formation; however, this analysis does not distinguish between highly active (as seen in young individuals) and quiescent (as seen in adults) bone formation. To make the comparison between the maps possible (as size differences exist between young and older individuals), scaling to a standardized grid of 8×8 squares was performed in R (see Schuh et al., 2019 for a detailed description of the method). We then computed mean bone modeling maps per age group by calculating the average %BR at each square, excluding missing values. In order to visualize both changes in shape together with the bone modeling patterns, each mean bone modeling map was warped onto the 3D surface of its corresponding mean shape in Geomagic® Studio (Research Triangle Park, NC). Population similarities in the bone modeling patterns were tested for the age groups that present a sufficient number of individuals (i.e., AG 1 and 2) using a PERMANOVA (1,000 iterations). Moreover, in order to test if population differences are found in different areas of the maxilla, we performed a MANOVA on each square of the grid, followed by a Bonferroni correction of the *p*-values.

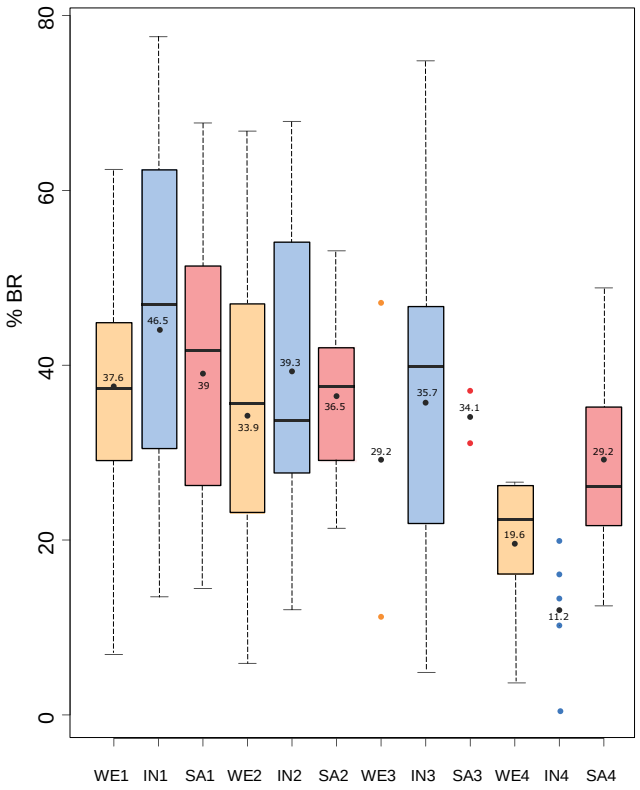

FIGURE 5 Boxplot representing the variation of the percentages of bone resorption (%BR) in each age group for all populations. Orange: Western European ("WE1"; "WE2"; "WE3"; "WE4"); blue: Greenlandic Inuit ("IN1", "IN2", "IN3", "IN4"); red: South African ("SA1"; "SA2"; "SA3"; "SA4"). Age groups' sizes equal to or less than five individuals were represented by dots in the corresponding population color. Each mean %BR is indicated as a black dot

2.2.3 | Joint analysis between bone modeling and morphological data

Although differences and/or similarities in the bone modeling patterns might explain the variation observed at the morphological scale, the covariation between maxillary morphology and bone modeling might differ between human populations. Thus, we carried out two-block Partial Least squares (PLS) analyses (Rohlf & Corti, 2000) on the bone modeling data and the Procrustes coordinates (see Mayer, Metscher, Müller, and Mitteroecker (2014) as well as Schuh et al.(2019) for more details on the method). The PLS analysis computes pairs of linear combinations (called singular warps, "SW"; Bookstein et al., 2003) that account for the maximum of covariance between two blocks using the covariance matrix. Different PLS analyses were performed on the pooled sample to investigate general trends of covariation, and for each

TABLE 3 Mean percentage and *SD* for each age group and population, associated to Figure 5

Age group	*Western European*		*Greenlandic Inuit*		*South African*	
	Mean	***SD***	**Mean**	***SD***	**Mean**	***SD***
1	37.6(24)	13.9	46.5(13)	19.9	39(11)	18
2	34.2(27)	16.1	39.3(15)	18.7	33.9(8)	10.6 **3**
	29.8(2)	25.4	35.7(15)	19.1	29.2(2)	4.2
4	19.6(6)	8.6	11.2(5)	7.4	19.6(10)	12.6

Note:The number of individuals is given in parenthesis after the mean.

population separately (to avoid the influence of a group on the others). Missing values were first estimated using a regularized iterative PCA algorithm of the missMDA package (Josse & Husson, 2016). After this step, only 32 squares (variables) were kept. To correct for the effect of size, we computed a multivariate linear regression of the shape coordinates on the natural logarithm of the centroid size and performed another two-block PLS analysis between the shape residuals and the bone modeling data including all populations. The significance of each singular value was assessed using a permutation test (1,000 iterations).

3 | RESULTS

3.1 | Developmental trajectories and patterns of shape changes

The developmental simulations are shown in Figure 2 (see also Supporting Information S1). Overall, all simulated individuals plot away from the non-simulated ones, implying different developmental trajectories for each population. In both cases, the simulated Inuit individuals from AG 1 result in an elongated trajectory along PC1 (shifted toward the positive values), although less elongated when following a South African trajectory. Similarly, South African individuals simulated along the Western European trajectory are shifted toward the positive values along PC 1, while Western Europeans simulated along the South African trajectory are shifted toward the negative values along PC 1, resulting in a shorter trajectory. Finally, both South Africans and Western Europeans, when simulated along the Inuit trajectory, are shifted toward the negative values (implying a shortened trajectory) as well as moved toward the negative values on PC2 (implying a change in direction). Shape differences between the three populations are shown in Figure 3. The Inuit maxilla is consistently shorter mediolaterally, both in the maxillary arcade and the frontal process that is more elongated superoinferiorly. South Africans are slightly more projected in the anterior maxilla, and Western Europeans show a more anteriorly developed anterior nasal spine (ANS).

Figure 4 shows the heat maps computed between age group means' Procrustes coordinates, thus showing the developmental (or shape) differences between two pairs of age group means (AG 1–2, 2–3, and 3–4). Overall, in all populations a posterior displacement (cold colors) is found in the inferior orbital ridge, the canine area, and in the anterior maxilla while a slight anterior dis- placement is found in the frontal process (warm colors). This suggests a shared general pattern of development between the three populations; however, slight differences can be observed. While in Inuit and South Africans the differences shown in AG 1–2 are small (the distance is close to 0 mm), Western Europeans show a marked

TABLE 4 Degree of freedom (df), coefficient of determination (R^2) and *p*-values of the PERMANOVA testing for population similarities in the bone modeling patterns at each age group, considered significant for $p \leq .05$

Age group	*df*	R^2	*p*-value
1	2	0.07	.06
2	2	0.07	.05

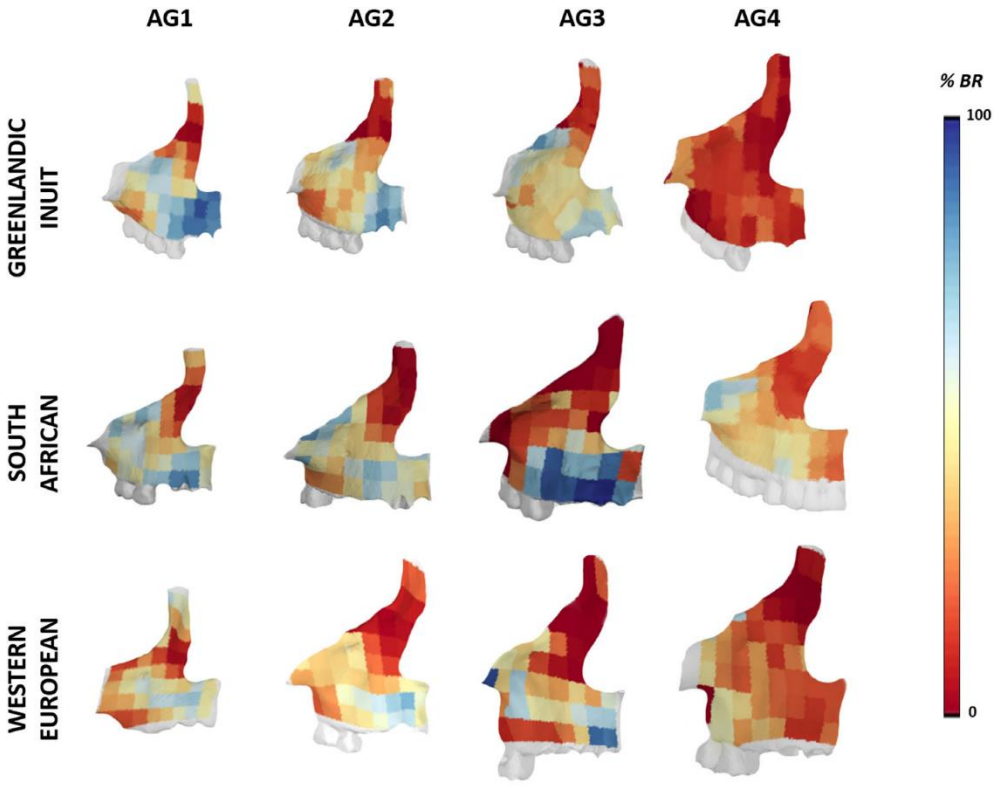

FIGURE 6 Maps showing the average bone modeling pattern at each age group and for each population. Cold colors (between 50 and 100%) indicate high amounts of bone resorption while warm colors (between 0 and 50%) indicate low amounts of bone resorption (i.e., predominant bone formation, whether it is in an active or quiescent state). Each map was projected onto the mean shape of the corresponding age group

posterior displacement in the canine fossa. Most evident shape differences are found in AG 2–3 in all populations, with a posterior displacement located in the canine fossa. Finally, developmental differences between AG 3 and 4 appear very slight in both Inuit and Western Europeans. South Africans show a marked anterior displacement in the infraorbital region.

3.2 | Patterns of bone modeling across human populations

A percentage of bone resorption was obtained for each individual, and average %BR were calculated for each age group. Results are represented as boxplots in Figure 5, and means and standard deviations are shown in Table 3. Overall, a similar pattern is observed in each population, showing a progressive decrease in the %BR, with the youngest age groups showing higher %BR on average than the adults (between 29.2 and 46.5% against 12 and 29.2%). Western Europeans show on average 10% less bone resorption than the two other populations, except in AG4. The average %BR in South African adults is higher than in the two other populations (29.2% against 19.6 and 12%). Standard deviations are generally higher in AG 1 and 2 (ranging from 13.9 to 18.7) compared with AG 4 (ranging from 7.4 to 12.6). The Western European and South African AG3 show the highest and lowest values (25.4 and 4.2 respectively; $n = 2$ in each population).

We computed the average bone modeling maps for each age group and projected them onto their corresponding mean shapes (Figure 6). We observed a general dichotomy of the bone, with the frontal process being mostly represented by bone formation (the %BR ranging from 0 to less than 50%), and the zygomatic process and maxillary arcade mostly resorptive (with percentages ranging from minimum 50 to 100%). Each population expresses differences in the location of bone resorption from early on. Western Europeans and South Africans show more resorption on the canine bulb and the canine fossa, with South Africans expressing also more resorption around the orbital ridge. The Inuit pattern expresses a maximum %BR in the ante- rior part of the maxillary arcade (on top of the incisors). Results from the PERMANOVA testing for population similarities in the bone modeling patterns are given in Table 4. Only AG 2 shows significantly different mean values in the %BR ($p \leq .05$). In each population, the bone modeling pattern expressed in AG 1 is repeated until at least AG 3. The decrease of %BR observed in Figure 5 in AG 4 is well represented by the adult bone modeling maps that express low amounts of bone resorption. However, compared with the two other populations adult South Africans seem to maintain the pattern found in the subadults by expressing more resorption in the maxillary arcade.

Figure7 shows the results of the MANOVA, testing for statistical differences in the bone modeling patterns at each square for each age group (see also Supporting Information S2). In AG 1, significant differences are located mostly at the bottom of the frontal process, along the zygomaticomaxillary suture and close to the inter-maxillary suture (in the anterior maxilla). In AG 2, the bone modeling pattern at the bottom and top (close to the frontomaxillary suture) of the frontal process were significantly different between populations, as well as along the zygomaticomaxillary suture.

3.3 | Comparison between the micro- and macroscopic changes

Figure 8 shows the PLS analysis between the Procrustes shape coordinates and the bone modeling data in all populations. The first pair of

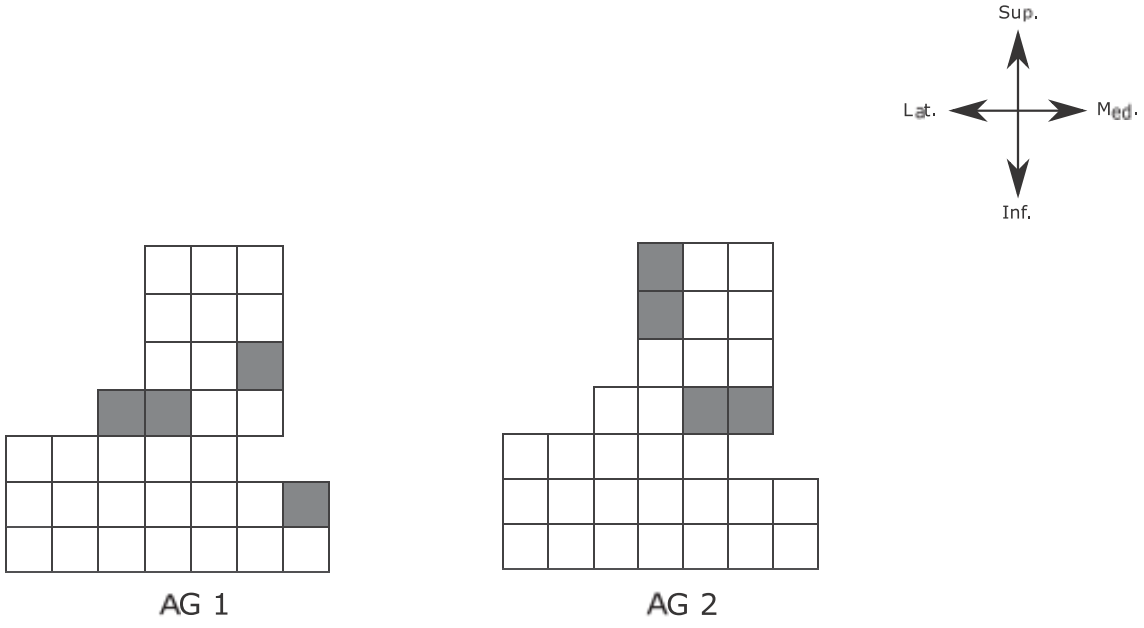

FIGURE 7 Maps showing the results of the MANOVA testing for significant differences between populations at each square of the grid. Gray squares show where the results are significant (for $p \leq .05$)

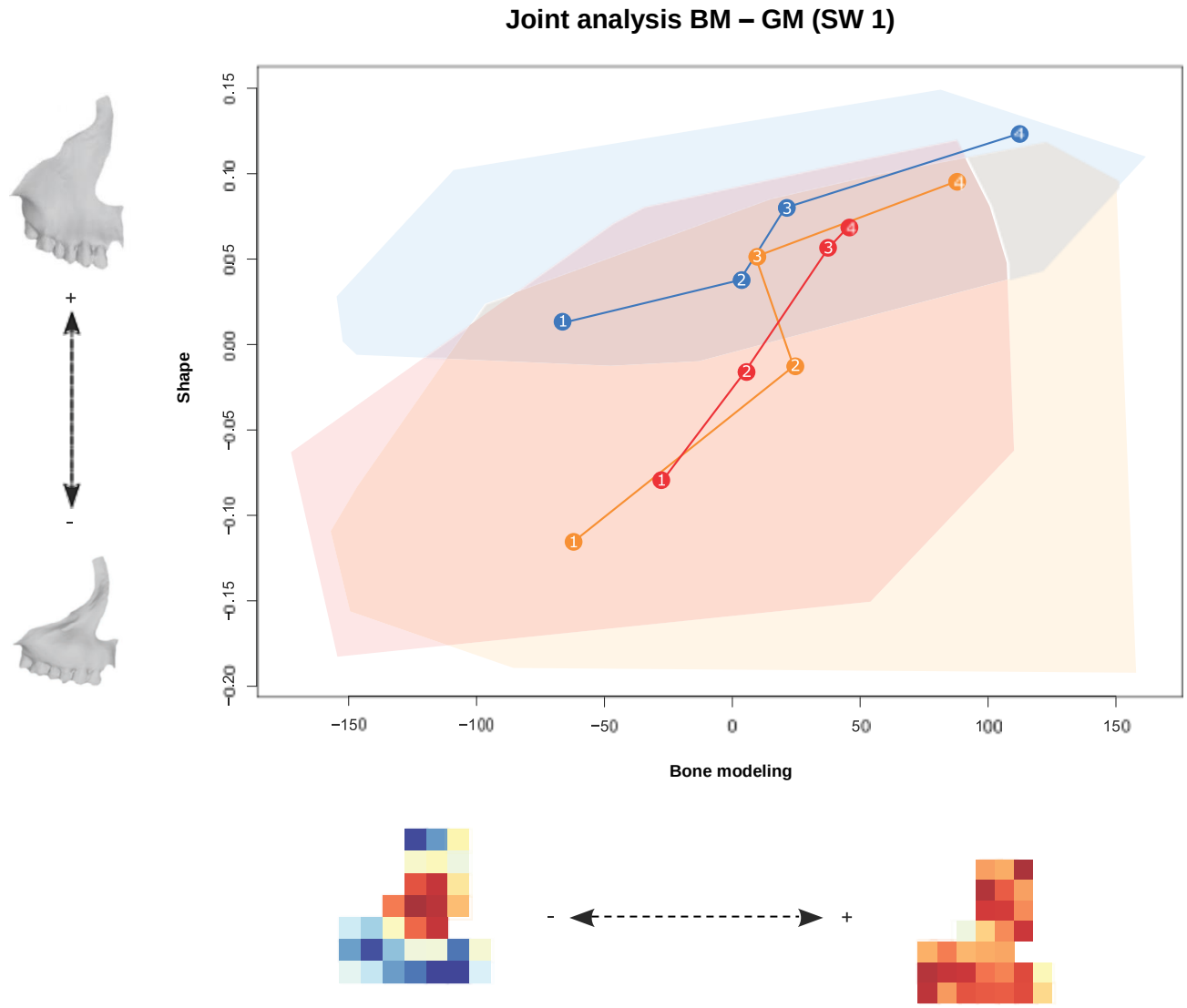

FIGURE 8 Two-block partial least square (PLS) analysis between the bone modeling and morphological (shape) data (SW1). X-axis: bone modeling data; y-axis: morphological data, represented by the Procrustes shape coordinates. Each population is represented by a convex hull (blue: Greenlandic Inuit; red: South African; orange: Western European). Age group means are represented by dots and corresponding numbers. Solid lines connect the subsequent means

TABLE 5 Percentages of total covariance, correlation coefficient and *p*-value, computed for the first singular warp (SW1) of the PLS analysis between Procrustes shape coordinates and the corresponding bone modeling patterns on all populations

	%Total covariance	Correlation coefficient (R)	*p*-value
SW1	73	0.42	.001

singular warps (SW 1) explains 75.6% of the total covariance between the two blocks (correlation coefficient: 0.42; Table 5). The x-axis separates the younger and older individuals (although more variation is seen in Western Europeans in the youngest age groups). On the y-axis, a shape change of the orbital ridge is observed. Although a high overlap is observed, the Inuit AG 1 individuals plot toward the positive values while the other two populations AG 1 plot toward the negative values. Changes on both axes toward positive values respectively correspond to a decrease in the bone resorption associated with an increase in height and width of the bone, particularly in the frontal process. Overall, the trajectories show a similar pattern of covariation between shape and bone modeling from AG 2 (corresponding to the completion of the M1) to AG 4 (adulthood), although the Inuit (in blue) show the most different trajectory (more constant, implying less shape change). They also show less overlap with the other two populations and less overall variability.

To avoid the influence of each population on the others, separate PLS analyses were performed (Figure 9; Table 6). As before, a similar pattern is observed in all populations, with the highest variability observed in the youngest individuals (AG 1) and the lowest in the adults (AG 4). This corresponds to a general decrease in bone resorption in all populations, and an increase in height and width of the maxilla. The distribution of bone resorption, although overall very similar,

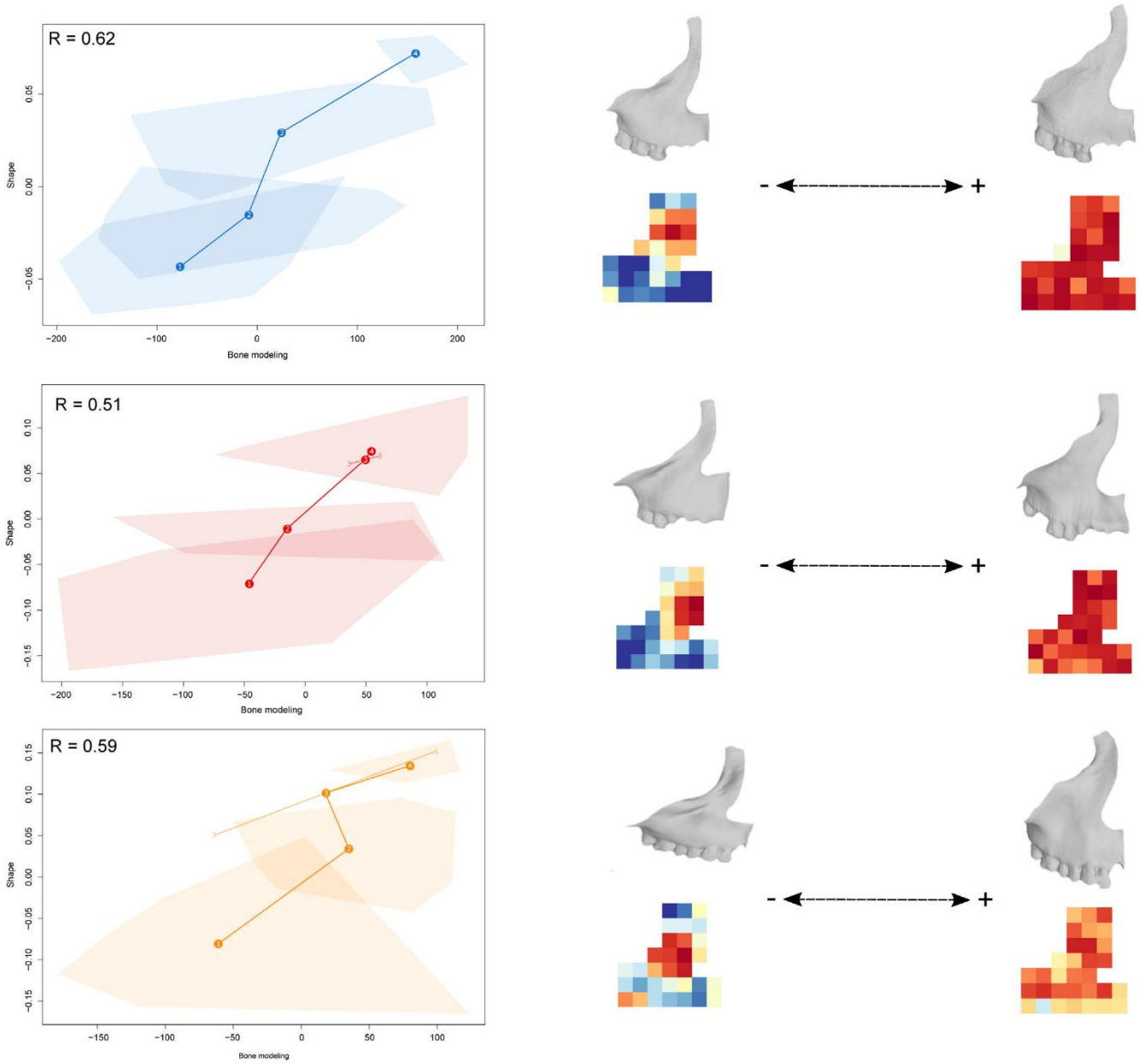

FIGURE 9 Two-block partial least square (PLS) analyses between the bone modeling and morphological (shape) data for each population (SW1). Left: plots for each population; (a) Greenlandic Inuit, (b) South African, (c) Western European. Age groups are delimited by convex hulls within each plot. Age group means are represented by dots and corresponding numbers. Solid lines connect the subsequent means. The Western European and South African AG 3 are only represented by two individuals, connected by a solid line and shown in the graph as numbers. Right: visualizations of the shape and bone modeling changes corresponding to SW1 positive and negative extremes

TABLE 6 Percentages of total covariance, correlation coefficients and *p*-values, computed for the first singular warp (SW1) of the PLS analyses between Procrustes shape coordinates and the corresponding bone modeling data for all age groups in each population, separately

	%Total covariance	Correlation coefficient (R)	p-value
Greenlandic Inuit	73	0.62	.001
Western European	85.2	0.59	.001
South African	74.2	0.51	.06

shows slight differences in each population that are linked to shape differences, mostly in the frontal process and the projection of the anterior maxilla.

4 | DISCUSSION

We investigated the intraspecific variability of the bone modeling patterns in the maxillae of three human populations, and compared the expression of their microscopic patterns to the development of their macroscale features during ontogeny.

4.1 | Maxillary morphology and ontogenetic patterns

Previous studies have already shown that population differences in facial morphology develop early, possibly prenatally (Bastir, O'Higgins, & Rosas, 2007; Bulygina et al., 2006; Freidline et al., 2015; Sardi & Ramirez-Rozzi, 2012; Vidarsdóttir et al., 2002; Viðarsdottir & O'Higgins, 2003); however, the morphological variation in prenatal stages has only been investigated in few studies (Mooney & Siegel, 1986; Weinberg, 2005; Morimoto, Ogihara, Katayama, & Shiota, 2008; Nicholas, 2016). Using geometric morphometric techniques, Nicholas (2016) found shape differences in the fetal maxilla between African- and European-Americans as early as the second trimester. The results of our morphological analysis further support these findings, as shape differences between the three populations can be observed already around birth (Figure 2). The developmental simulations performed on each population showed that they are not interchangeable, as differences in the trajectory sizes, shapes, and magnitudes could be observed (Adams & Collyer, 2009). At a similar age group, the Inuit maxilla is always larger and more developmentally advanced, and the shorter length of their developmental trajectory suggests less postnatal shape changes than in the two other populations. When interchanged, the South African and Western European trajectories mostly result in a displacement of the simulated adults along PC1, suggesting differences in the amount of shape change along a largely similar developmental trajectory in comparison to the Inuit. All of this suggests differential pre-, as well as postnatal, rates and/or timings of development as already suggested by other studies (Sardi & Ramirez-Rozzi, 2012; Vidarsdóttir et al., 2002). Freidline et al. (2015) who analyzed the whole face and employed similar populations as in this study, demonstrated as well that facial morphological variability arises from differential developmental patterns, mostly driven by size differences.

The heat maps in Figure 4 were computed to compare patterns of shape differences between subsequent age groups in the three populations. These shape differences were interpreted as the general, main displacements of the bone between two subsequent age groups (as the bones are continuously growing in all directions; Enlow,1966). All populations show a similar general pattern of displacements between age groups, with a main anterior displacement in the frontal process and most of the posterior displacement observed in the canine fossa. This corresponds to areas that are predominantly forming and resorptive throughout ontogeny, respectively (although bone resorption is expressed on intermediate levels; see the mean bone modeling maps in Figure 6). Inuit show less posterior displacement in the canine fossa, which can explain their midfacial flatness (Hennessy & Stringer, 2002); however, they do not differ from the other populations in the anterior maxilla where we expected the most differences (see discussion below). Interestingly, the heat maps all indicate a rather late development of the canine fossa, except between the Western European AG 1 and 2 that already show a mar- ked posterior displacement compared with the two other populations. The higher number of very young individuals in this population AG 1 might explain this difference (such as in the South African AG 3–4 represented by only two individuals).

4.2 | Variability of the bone modeling patterns

The analysis of bone resorption showed comparable distributions and means in the %BR in all populations (Figure 5, Table 3), although Inuit possess slightly more resorption on average. We found a shared general bone modeling pattern in all three populations (Figure 6), with predominant bone formation in the frontal process and bone resorption in the maxillary arcade as shown in former studies (Brachetta-Aporta, Gonzalez, & Bernal, 2019a; Enlow & Bang, 1965; Kurihara, Enlow, & Rangel, 1980; Martinez-Maza et al., 2013; Schuh et al., 2019). However, we did find significant statistical differences in bone modeling between the three populations (Table 4). These differences have been highlighted in the location of bone resorption (Figures 6 and 7), particularly in the Inuit pattern that shows a more anterior area of bone resorption (on top of the incisors' roots); this observation can already be made from AG 1 as shown by the results of the MANOVA (Figure 7, Supporting Information S2). Both Inuit and Western Europeans possess taller and narrower nasal regions than South Africans, and our results seem to suggest that significant differences in bone modeling exist in this region that comprises the frontal process and the anterior maxilla (Figure 7; also shown at the morphological level in Figure 3); although this would have to be tested on more individuals. Moreover, we observed that population-specific bone modeling patterns are present since early stages, and maintained throughout ontogeny until at least adolescence (AG 3 in our sample); however, this could not be tested statistically. Yet with this observation, we can still conclude that the expression of bone resorption is likely a highly genetically controlled process, and its location on bone surfaces underlies the development of a specific form. The repetition of a bone modeling pattern within a group/species may be indicative of developmental canalization (Hallgrímsson, Willmore, & Hall, 2002; Waddington,1942).

The progressive decrease observed throughout ontogeny in the percentages of bone resorption (attaining lower values and less variation in adults) implies lowered osteoblastic and osteoclastic activities that follow a general decrease in the growth rate of the face in later ontogeny (Bastir, Rosas, & O'Higgins, 2006). McCollum (2008) described different types of bone resorption, such as “aggressive” and “skimming.” Skimming resorption affects the bone less, and according to our data, is more predominant in adults, which again suggests differences in cellular rates between the latter and the subadults. Bone resorption is also slightly less predictable, and when present as small-localized fields, may indicate areas of bone remodeling in response to biomechanical demands. Interestingly, adult South Africans in our sample show a higher %BR than the two other populations; this might be due to the composition of this age group (with younger adults), but demonstrates that bone modeling can stay as active as during childhood until at least early adulthood. In a study from 2013, Martinez- Maza and colleagues found differences in the bone modeling patterns

of subadult and adult Western Europeans. According to the authors, resorption in adults is restricted to the posterior canine region. They concluded that these differences result in a change of the general facial growth vector, from a mainly forward/downward vector found in subadults to a unique forward direction in adults. Although a similar finding is shown in our adult Western Europeans (n = 6; Figure 6), we generally observed that areas affected by bone resorption in adults are comparable to those observed in subadults, as discussed by Brachetta-Aporta, Gonzalez, and Bernal (2019b). It is thus difficult to conclude whether a significant change in the general direction of growth occurs between the two. Changes in facial size and shape during adulthood have been demonstrated by several studies (Behrents, 1985; Behrents, 2008; Guagliardo, 1982; Hellman, 1927; Israel, 1968, 1977; Williams & Slice, 2010). These changes can be found in both the soft tissues (Behrents, 2008; Windhager et al., 2019) and bones (Albert, Ricanek, & Patterson, 2007). Williams and Slice (2010) observed a decrease in facial height in the supero-inferior direction, as well as a lateral expansion associated with age. The authors observed shape changes in the orbital, zygomatic, and maxillary alveolar regions, with variations dependent of the sex and/or ethnic origin studied. Whether they relate to bone modeling changes in elderly individuals remains to be tested.

4.3 | Facial ontogenetic patterns at the micro- and macroscopic scale

Inuit possess distinct external and internal nasal shapes that have been linked to an adaptation to cold climates (Maddux et al., 2017), and different analyses in this study suggest that bone modeling patterns of this area slightly differ between populations(Figures6and7). Apart from the nasal region, morphological adaptation to climate has proved complex in human populations, as their association can only be highlighted in cases of extremely cold environments (Evteev et al., 2013; Harvati & Weaver, 2006). South Africans who possess rather short and broad frontal processes (Figure 3) express slightly more bone formation in this area, while Inuit and Western Europeans who possess more elongated frontal processes show resorption until at least AG 3. Moreover, the anterior nasal spine (ANS), a unique human morphological feature (Ashley-Montagu, 1935), is known to show population differences in its development (Mooney & Siegel, 1986). In this study, the ANS region is often resorptive in subadults, particularly in Inuit who consistently show a reduction in the size of the ANS compared to the other two populations (Figure 3). Thus, the forward development of the ANSmight depend on the ratio between bone formation and resorption to which it is subjected during ontogeny. This also shows the importance of considering different human groups in the analysis of intraspecific variation of the bone modeling patterns, as previous work with reduced sample sizes found mostly bone formation in this region (Enlow & Bang, 1965). Moreover, the location of the maximum %BR (in the anterior maxilla) is unique to the Inuit sample of this study (Figure 6). According to Hylander (1977), the Inuit face is well adapted to high load demands, as many of their facial features facilitate the dissipation of vertical occlusion forces such as a more anteriorly positioned postorbital bar, an anterior root of the zygomatic bone, and hypertrophied masseter muscles. Coon (1962) also noted an anterior displacement of the temporalis (that is on average larger than in other populations) and masseter. Toro-Ibacache, Zapata Muñoz, and O'Higgins (2016) observed lowered peak strains in more vertical faces, which could apply to the Inuit as their facial prognathism is reduced compared with other populations. Thus, a more anterior resorptive field (on the incisors) as well as a more lateral development of the facial components might be linked to their facial flatness, whereas a more lateral resorptive field (on the canine fossa) might create a more concave maxilla as seen in Western Europeans and South Africans. We thus propose that the location of bone resorption on the bone may be a response to larger-scale ontogenetic patterns (such as integration patterns within the skull), and result from compensatory mechanisms as proposed by other authors (Mitteroecker et al., 2020; O'Higgins, Bromage, Johnson, Moore, & McPhie, 1991). Finally, the analysis of covariation between the shape residuals and the bone modeling patterns again highlighted subtle population differences (Figure 8, Supporting Information S3 and S4), while overall, a similar general pattern is found (Figure 9). This suggests that only slight, but significant changes in the location of the bone modeling patterns participate in the shape differences observed in human populations.

5 | CONCLUSION

This study investigates for the first time the bone modeling patterns of several geographically distinct human populations, and shows the importance of considering a large, diverse sample to try to better represent the variation at the species level. We showed that although Homo sapiens express overall similar general maxillary ontogenetic bone modeling patterns and shape changes, population-specific differences can be found at both levels. These are expressed in the rates and timing of development that occur pre- and post-natally, in the complex integration of the face with other cranial components during ontogeny as well as in the location of bone resorption (particularly in the nasal region). The subtle discrepancies in the bone modeling patterns observed in this study suggest that shape differences are merely due to differences in rates and/or timings of development (at the cellular level) than differences in the location of bone resorption. Inuit are the most distinct at both levels, showing more advanced maxillary development and a more anteriorly resorptive field, which could explain the horizontal development of their midface. Moreover, this study shows that population-specific bone modeling patterns in *H.sapiens* are maintained throughout ontogeny; and this may apply as well to other hominin species. Although most of the features are established at birth, changes in the bone modeling and morphological patterns observed here highlight the role of later phases of postnatal ontogeny in shaping the human face. Adults show an important reduction in the total percentage of bone resorption, but resorbing areas are found at similar locations than subadults. These results bring new

insights into our knowledge of ontogenetic patterns that lead to morphological variability.

ACKNOWLEDGMENTS

We would like to thank the two anonymous reviewers for their constructive comments, as well as J.-L. Kahn (Anatomical Institute of the University of Strasbourg, France), H. Coqueugniot (UMR 5199 PACEA, University of Bordeaux, France), C. Feja (University of Leipzig, Germany), N. Lynnerup (Department of Forensic Medicine of the University of Copenhagen, Denmark), the Greenland National Museum (Greenland), W. Seconna (Iziko Museum of Cape Town, South Africa) and V. Gibbons (University of Cape Town, South Africa), D. Morris (McGregor Museum of Kimberley, South Africa), A. Santos (Department of Life Sciences, University of Coimbra, Portugal) and A. Rosas (Department of Paleobiology, MNCN, Madrid, Spain) for giving us access to the collections. We are also grateful to P. Mitteroecker (University of Vienna, Austria) and V. Toro-Ibacache (Faculty of Dentistry, University of Chile, Santiago) for fruitful discussions, and E. Schulz-Kornas (University of Leipzig, Germany) and Heiko Temming (Max Planck Institute for Evolutionary Anthropology, Leipzig, Germany) for technical assistance. This work was funded by the Max Planck Society, and approved by the South African San Council. Open access funding enabled and organized by Projekt DEAL.

AUTHOR CONTRIBUTIONS

Alexandra Schuh: Conceptualization; formal analysis; investigation; methodology; validation; visualization; writing-original draft; writing-review and editing. **Chiara Villa:** Data curation; resources. **Kornelius Kupczik:** Project administration; resources; supervision. **Philipp Gunz:** Formal analysis; supervision; writing-original draft. **Jean-Jacques Hublin:** Funding acquisition. **Sarah Freidline:** Conceptualization; methodology; project administration; supervision; validation; writing-original draft; writing-review and editing.

CONFLICT OF INTEREST

The authors declare no conflict of interest.

DATA AVAILABILITY STATEMENT

The data that support the findings of this study are partly available on request from the corresponding author. The data are not publicly available due to ethical restrictions.

ORCID

Alexandra Schuh https://orcid.org/0000-0003-1645-1220

REFERENCES

Adams, D.C., & Collyer, M.L. (2009). A general framework for the analysis of phenotypic trajectories in evolutionary studies. *Evolution: International Journal of Organic Evolution, 63*(5),1143–1154.

Albert, A. M., Ricanek, K., & Patterson, E. (2007). A review of the literature on the aging adult skull and face: Implications for forensic science research and applications. *Forensic Science International, 172*(1), 1–9.

AlQahtani, S. J., Hector, M. P., & Liversidge, H. M. (2010). Brief communication: The London atlas of human tooth development and eruption. *American Journal of Physical Anthropology, 142*(3), 481–490.

Ashley-Montagu, M. F. (1935). The premaxilla in the primates. *The Quarterly Review of Biology, 10*(1), 32–59.

Bastir, M., O'Higgins, P., & Rosas, A. (2007). Facial ontogeny in Neanderthals and modern humans. *Proceedings of the Biological Sciences, 274* (1614), 1125–1132.

Bastir, M., & Rosas, A. (2004). Comparative ontogeny in humans and chimpanzees: Similarities, differences and paradoxes in postnatal growth and development of the skull. *Annals of Anatomy - Anatomischer Anzeiger, 186*(5), 503–509.

Bastir, M., Rosas, A., & O'Higgins, P. (2006). Craniofacial levels and the morphological maturation of the human skull. *Journal of Anatomy, 209* (5), 637–654.

Behrents, R. G. (1985). *Growth in the aging craniofacial skeleton* (2nd ed. Vol. Monograph 17). Ann Arbor: University of Michigan.

Behrents, R. G. (2008). Adult craniofacial growth. In D. H. Enlow & M. G. Hans (Eds.), *Essentials of facial growth* (2nd ed.). USA. Ann Arbor: Needham Press.

Bookstein, F. L. (1997). Landmark methods for forms without landmarks: Morphometrics of group differences in outline shape. *Medical Image Analysis, 1*(3), 225–243.

Bookstein, F. L., Gunz, P., Mitteroecker, P., Prossinger, H., Schæfer, K., & Seidler, H. (2003). Cranial integration in *Homo*: Singular warps analysis of the midsagittal plane in ontogeny and evolution. *Journal of Human Evolution*, 44(2), 167–187.

Boyde, A. (1972). Scanning electron microscope studies of bone. In G. H. Bourne (Ed.), *The biochemistry and physiology of bone*. New York: Academic Press.

Brachetta-Aporta, N., Gonzalez, P. N., & Bernal, V. (2019a). Variation in facial bone growth remodeling in prehistoric populations from southern South America. *American Journal of Physical Anthropology, 169*(3), 422–434.

Brachetta-Aporta, N., Gonzalez, P. N., & Bernal, V. (2019b). Integrating data on bone modeling and morphological ontogenetic changes of the maxilla in modern humans. *Annals of Anatomy - Anatomischer Anzeiger, 222*, 12–20.

Bromage, T. G. (1989). Ontogeny of the early hominin face. *Journal of Human Evolution, 18*, 751–773.

Bulygina, E., Mitteroecker, P., & Aiello, L. (2006).Ontogeny of facial dimorphism and patterns of individual development within one human population. *American Journal of Physical Anthropology, 131*(3), 432–443.

Butaric, L.N., & Maddux, S.D. (2016). Morphological Covariation between the maxillary sinus and Midfacial skeleton among sub-Saharan and circumpolar modern humans. *American Journal of Physical Anthropology, 160*(3), 483–497.

Churchill, S.E., Shackelford, L.L., Georgi, J.N., & Black, M.T. (2004). Morphological variation and airflow dynamics in the human nose. *American Journal of Human Biology: The Official Journal of the Human Biology Association 16*(6), 625-638.

Coon, C. (1962). The origin of races. New York: Alfred A. Knopf.

Coon, C., Garn, S., & Birdsell, J. (1950). Races: A study of the problems of race formation in man, Springfield, Illinois: Charles C. Thomas.

Cruwys, E. (1988). Morphological variation and wear in teeth of Canadian and Greenland Inuit. *Polar Record, 24*(151), 293–298.

Cui, Y., & Leclercq, S. (2017). Environment-related variation in the human mid-face. *The Anatomical Record, 300*(1), 238–250.

Deter, C. A. (2009). Gradients of occlusal wear in hunter-gatherers and agriculturalists. *American Journal of Physical Anthropology, 138*(3), 247–254.

Enlow, D. H. (1962). A study of the post-natal growth and remodeling of bone. *American Journal of Anatomy, 110*(2), 79–101.

Enlow, D. H. (1966). A morphogenetic analysis of facial growth. American *Journal of Orthodontics, 52*(4), 283–299.

Enlow, D. H., & Bang, D. D. S. (1965). Growth and remodeling of the human maxilla. *American Journal of Orthodontics, 51*(6), 446–464.

Evteev, A., Cardini, A. L., Morozova, I., & O'Higgins, P. (2013). Extreme climate, rather than population history, explains mid-facial morphology of northern Asians. *American Journal of Physical Anthropology, 153*(3), 449–462.

Franciscus, R. G., & Long, J. C. (1991). Variation in human nasal height and breadth. *American Journal of Physical Anthropology, 85*(4), 419–427.

Freidline, S. E., Gunz, P., & Hublin, J. J. (2015). Ontogenetic and static allometry in the human face: Contrasting Khoisan and Inuit. *American Journal of Physical Anthropology, 158*(1), 116–131.

Freidline, S. E., Martinez-Maza, C., Gunz, P., & Hublin, J. J. (2017). Exploring modern human facial growth at the micro- and macroscopic levels. Christopher J. Percival & Joan T. Richtsmeier In *Buidling bones*. Cambridge: Cambridge University Press.

Frost, H. M. (1987). Bone "mass" and the "mechanostat": A proposal. *The Anatomical Record, 219*(1), 1–9.

Gonzalez-Jose, R., Ramirez-Rozzi, F., Sardi, M., Martinez-Abadias, N., Hernandez, M., & Pucciarelli, H.M. (2005). Functional-cranial approach to the influence of economic strategy on skull morphology. *American Journal of Physical Anthropology, 128*(4), 757–771.

Guagliardo, M. (1982*). Craniofacial structure, aging and dental function: Their relationships in adult human skeletal series*. (doctoral dissertation). University of Tennessee, Knoxville.

Gunz, P., & Mitteroecker, P. (2013). Semilandmarks: A method for quantifying curves and surfaces. *Hystrix, the Italian Journal of Mammalogy, 24* (1), 103–109.

Gunz, P., Mitteroecker, P., & Bookstein, F. (2005). Semilandmarks in three dimensions. In D.E. Slice (Ed.), *Modern Morphometrics in physical Anthroplogy*. New York: Kluwer Press.

Gunz, P., Neubauer, S., Maureille, B., & Hublin, J.-J. (2010). Brain development after birth differs between Neanderthals and modern humans. *Current Biology, 20*(21), R921–R922.

Hallgrímsson, B., Willmore, K., & Hall, B. K. (2002). Canalization, developmental stability, and morphological integration in primate limbs. *American Journal of Physical Anthropology, Suppl 35,* 131–158.

Hanihara, T. (1996). Comparison of craniofacial features of major human groups. *American Journal of Physical Anthropology, 99*(3), 389–412.

Hanihara, T. (2000). Frontal and facial flatness of major human populations. *American Journal of Physical Anthropology, 111*(1), 105–134.

Harvati, K., & Weaver, T.D. (2006). Human cranial anatomy and the differential preservation of population history and climate signatures. *The Anatomical Record. Part A, Discoveries in Molecular, Cellular, and Evolutionary Biology, 288*(12), 1225–1233.

Hawkes, E. W. (1916). Skeletal measurements and observations on the point Barrow Eskimos with comparisons from other Eskimo groups. *American Anthropologist, 18*, 203–234.

Hellman, M. (1927). Changes in the human face brought about by development. *International Journal of Orthodontia, Oral Surgery and Radiography, 13*(6), 475–516.

Hennessy, R.J., & Stringer, C.B. (2002). Geometric morphometric study of the regional variation of modern human craniofacial form. *American Journal of Physical Anthropology, 117*(1), 37–48.

Holton, N.E., & Franciscus, R.G. (2008). The paradox of a wide nasal aperture in cold-adapted Neandertals: A causal assessment. *Journal of Human Evolution, 55*(6), 942–951.

Howells, W. (1973). *Cranial variation in man: A study by multivariate analysis of patterns of difference among recent human populations*. Cambridge: MA: Harvard University Press.

Howells, W. (1989). *Skull shapes and the map: Craniometric analyses in the dispersion of modern homo.* Cambridge: MA: Harvard University Press.

Hrdlička, A. (1910). Contributions to the anthropology of central and Smith sound Eskimo. *Anthropological Papers of the American Museum of Natural History, 5*, 177–280.

Hubbe, M., Hanihara, T., & Harvati, K. (2009). Climate Signatures in the Morphological Differentiation of Worldwide Modern Human Populations. *The Anatomical Record: Advances in Integrative Anatomy and Evolutionary Biology, 292*(11), 1720–1733.

Hylander, W. L. (1977). The adaptive significance of Eskimo craniofacial morphology. In A. A. G. Dahlberg & M. Thomas (Eds.), *Orofacial growth and development* (pp.129–169).The Hague: De Gruyter.

Israel, H. (1968). Continuing growth in the human cranial skeleton. *Archives of Oral Biology, 13*(1), 133–IN141.

Israel, H. (1977). The dichotomous pattern of craniofacial expansion during aging. *American Journal of Physical Anthropology, 47*(1), 47–51.

Josse, J., & Husson, F. (2016). missMDA: A package for handling missing values in multivariate data analysis. *Journal of Statistical Software, 70*, 1–31.

Kurihara, S., Enlow, D. H., & Rangel, R. D. (1980). Remodeling reversals in anterior parts of the human mandible and maxilla. *The Angle Orthodontics, 50*(2), 98–106.

Le Minor, J.-M., Billmann, F., Sick, H., Vetter, J.-M., & Ludes, B. (2009). Anatomies et Pathologies, les collections morphologiques de la Faculté de médicine de Strasbourg: I.D. l'Edition.

Lieberman, D. E., McBratney, B. M., & Krovitz, G. (2002). The evolution and development of cranial form in *Homo sapiens*. *Proceedings of the National Academy of Sciences, 99*(3), 1134–1139.

Lynch, J. M., Wood, C. G., & Luboga, S. A. (1996). Geometric Morphometrics in primatology: Craniofacial variation in *Homo sapiens* and *Pan troglodytes. Folia Primatologica, 67*(1), 15–39.

Lynnerup, N., Homøe, P., & Skovgaard, L. T. (1999). The frontal sinus in ancient and modern Greenlandic Inuit. *International Journal of Anthropology, 14*(1), 47–54.

Maddux, S.D., Butaric, L.N., Yokley, T.R., & Franciscus, R.G. (2017). Ecogeographic variation across morphofunctional units of the human nose. *American Journal of Physical Anthropology, 162*(1), 103-119.

Maddux, S. D., Yokley, T. R., Svoma, B. M., & Franciscus, R. G. (2016). Absolute humidity and the human nose: A reanalysis of climate zones and their influence on nasal form and function. *American Journal of Physical Anthropology, 161*(2), 309–320.

Martinez-Maza, C., Freidline, S. E., Strauss, A., & Nieto-Diaz, M. (2015). Bone growth dynamics of the facial skeleton and mandible in *Gorilla gorilla* and *Pan troglodytes. EvolutionaryBiology, 43*(1), 60–80.

Martinez-Maza, C., Rosas, A., & Nieto-Diaz, M. (2013). Postnatal changes in the growth dynamics of the human face revealed from bone modelling patterns. *Journal of Anatomy, 223*(3), 228–241.

Mayer, C., Metscher, B. D., Müller, G. B., & Mitteroecker, P. (2014). Studying developmental variation with geometric morphometric image analysis (GMIA). *PLoSOne, 9*(12), e115076.

McCollum, M. A. (1999). The robust australopithecine face: A morphogenetic perspective. *Science, 284*(5412), 301–305.

McCollum, M. A. (2008). Nasomaxillary remodeling and facial form in robust *Australopithecus*: A reassessment. *Journal of Human Evolution, 54*(1), 2–14.

Mitteroecker, P., Bartsch, S., Erkinger, C., Grunstra, N. D., Le Maître, A., & Bookstein, F. L. (2020). Morphometric variation at different spatial scales: Coordination and compensation in the emergence of organismalform. *Systematic Biology, 69*(5), 913–926.

Mitteroecker, P., & Gunz, P. (2009). Advances in geometric morphometrics. *Evolutionary Biology, 36*(2), 235–247.

Mitteroecker, P., Gunz, P., Windhager, S., & Schaefer, K. (2013). A brief review of shape, form, and allometry in geometric morphometrics, with applications to human facial morphology. *Biological Theory, 24*(1), 59–66.

Mooney, M.P., & Siegel, M.I. (1986). Developmental relationship between premaxillary-maxillary suture patency and anterior nasal spine morphology. *The Cleft Palate Journal, 23*(2), 101–107.

Morimoto, N., Ogihara, N., Katayama, K., & Shiota, K. (2008). Three-dimensional ontogenetic shape changes in the human cranium during the fetal period. Journal of Anatomy, 212(5), 627–635.

Neubauer, S., Gunz, P., & Hublin, J.-J. (2010). Endocranial shape changes during growth in chimpanzees and humans: A morphometric analysis of

unique and shared aspects. *Journal of Human Evolution, 59*(5), 555–566.
Nicholas, C.L. (2016). Fetal and neonatal maxillary ontogeny in extant humans and the utility of prenatal maxillary morphology in predicting ancestral affiliation. *American Journal of Physical Anthropology, 161*(3), 448–455.
Nicholson, E., & Harvati, K. (2006). Quantitative analysis of human mandibular shape using three-dimensional geometric morphometrics. *American Journal of Physical Anthropology, 131*(3), 368–383.
Noback, M. L., & Harvati, K. (2015). The contribution of subsistence to global human cranial variation. *Journal of Human Evolution, 80*, 34–50.
Noback, M.L., Harvati, K., & Spoor, F. (2011). Climate-related variation of the human nasal cavity. *American Journal of Physical Anthropology, 145*(4), 599-614.
O'Higgins, P., Bromage, T. G., Johnson, D. R., Moore, W. J., & McPhie, P. (1991). A study of facial growth in the sooty Mangabey *Cercocebus atys. Folia Primatologica, 56*(2), 86–94.
O'Higgins, P., & Jones, N. (1998). Facial growth in *Cercocebus torquatus*: An application of three-dimensional geometric morphometric techniques to the study of morphological variation. *Journal of Anatomy, 193*(2), 251–272.
Oschinsky, L. (1962). Facial flatness and cheekbone morphology in arctic mongoloids: A case of morphological taxonomy. *Anthropological Papers of the American Museum of Natural History, 4*(2), 349–377.
Ponce de Leon, M. S., & Zollikofer, C. P. E. (2001). Neanderthal cranial ontogeny and its implications for late hominid diversity. *Nature, 412* (6846), 534–538.
Rampont, M. (1994). Les squelettes, os et dents de fœtus, nouveau-nés et enfants du musée anatomique de Strasbourg. Aspects historiques et catalogues. Strasbourg: Université Louis Pasteur.
Rohlf, F. J., & Corti, M. (2000). Use of two-block partial least-squares to study Covariation in shape. *Systematic Biology, 49*(4), 740–753.
Rohlf, F. J., & Slice, D. (1990). Extensions of the Procrustes method for the optimal superimposition of landmarks. *Systematic Zoology, 39*, 40.
Rosas, A., & Bastir, M. (2002). Thin-plate spline analysis of allometry and sexual dimorphism in the human craniofacial complex. *American Journal of Physical Anthropology, 117*(3), 236–245.
Roseman, C. C., & Weaver, T. D. (2004). Multivariate apportionment of global human craniometrics diversity. *American Journal of Physical Anthropology, 125*(3), 257–263.
RStudio Team. (2020). *RStudio: Integrated development environment for R*. Boston, MA: RStudio, PBC.
Sardi, M. L., & Ramirez-Rozzi, F. V. (2012). Different cranial ontogeny in Europeans and southern Africans. *PLoSOne, 7*(4), e35917.
Schlager, S. (2017). Morpho and Rvcg—Shape analysis in R: R-packages for geometric Morphometrics, shape analysis and surface manipulations. In L. S. Z. Guoyan & S. Gabor (Eds.), *Statistical shape and deformation analysis* (pp. 217–256). London, England: Academic Press.
Schlager, S., Profico, A., Di Vincenzo, F., & Manzi, G. (2018). Retrodeformation of fossil specimens based on 3D bilateral semi-landmarks: Implementation in the R package "Morpho". *PLoSOne, 13*(3), e0194073.
Schneider, C. A., Rasband, W. S., & Eliceiri, K. W. (2012). NIH image to ImageJ: 25 years of image analysis. *Nature Methods, 9*(7), 671–675.
Schuh, A., Kupczik, K., Gunz, P., Hublin, J.-J., & Freidline, S. E. (2019). Ontogeny of the human maxilla: A study of intra-population variability combining surface bone histology and geometric morphometrics. *Journal of Anatomy, 235*, 233–245.
Schulte, F. A., Zwahlen, A., Lambers, F. M., Kuhn, G., Ruffoni, D., Betts, D.,Müller, R. (2013). Strain-adaptive in silico modeling of bone adaptation – A computer simulation validated by in vivo micro-computed tomography data. *Bone, 52*(1), 485–492.
Scott, N., Neubauer, S., Hublin, J.-J., & Gunz, P. (2014). A shared pattern of postnatal endocranial development in extant hominoids. *Evolutionary Biology, 41*(4), 572–594.
Smith, H. F. (2009). Which cranial regions reflect molecular distances reliably in humans? Evidence from three-dimensional morphology. *American Journal of Human Biology, 21*(1), 36–47.
Stansfield, E., Evteev, A., & O'Higgins, P. (2018). Can diet be inferred from the biomechanical response to simulated biting in modern and prehistoric human mandibles? *Journal of Archaeological Science: Reports, 22*, 433–443.
Stynder, D. D., Ackermann, R. R., & Sealy, J. C. (2007). Craniofacial variation and population continuity during the South African Holocene. *American Journal of Physical Anthropology, 134*(4), 489–500.
Toro-Ibacache, V., Zapata Muñoz, V., & O'Higgins, P. (2016). The relationship between skull morphology, masticatory muscle force and cranial skeletal deformation during biting. *Annals of Anatomy - Anatomischer Anzeiger, 203*, 59–68.
Viðarsdottir, S., & O'Higgins, P. (2003). Developmental variation in the facial skeleton of anatomically modern *Homo sapiens*. In K. G. Thompson & A. Nelson (Eds.), *Patterns of growth and development in the genus Homo* (pp.114–143). Cambridge: Cambridge University Press.
Vidarsdóttir, U. E., O'Higgins, P., & Stringer, C. (2002). A geometric morphometric study of regional differences in the ontogeny of the modern human facial skeleton. *Journal of Anatomy, 201*, 211–229.
von Cramon-Taubadel, N. (2011). Global human mandibular variation reflects differences in agricultural and hunter-gatherer subsistence strategies. *Proceedings of the National Academy of Sciences, 108*(49), 19546–19551.
von Cramon-Taubadel, N. (2014). Evolutionary insights into global patterns of human cranial diversity: Population history, climatic and dietary effects. *Journal of Anthropological Sciences, 92*, 43–77.
Waddington, C.H. (1942). Canalization of the development and the inheritance of acquired characters. *Nature, 150*, 563–565.
Williams, S. E., & Slice, D. E. (2010). Regional shape change in adult facial bone curvature with age. *American Journal of Physical Anthropology, 143*(3), 437–447.
Windhager, S., Mitteroecker, P., Rupić, I., Lauc, T., Polašek, O., & Schaefer, K. (2019). Facial aging trajectories: A common shape pattern in male and female faces is disrupted after menopause. *American Journal of Physical Anthropology, 169*(4), 678–688.
Wolpoff, M. (1968). Climatic influence on the skeletal nasal aperture. *American Journal of Physical Anthropology, 29*, 405–424.
Yokley, T. R. (2009). Ecogeographic variation in human nasal passages. *American Journal of Physical Anthropology, 138*(1), 11–22.

SUPPORTING INFORMATION

Additional supporting information may be found online in the Supporting Information section at the end of this article.

How to cite this article: Schuh A, Gunz P, Villa C, Kupczik K, Hublin J-J, Freidline SE. Intraspecific variability in human maxillary bone modeling patterns during ontogeny. *Am J Phys Anthropol.* 2020; 1–16.https://doi.org/10.1002/ajpa.24153

Chapter 3

Quantifying maxillary development in chimpanzees and humans: an analysis of prognathism and orthognathism at the morphological and microscopic scales

Quantifying maxillary development in chimpanzees and humans: an analysis of prognathism and orthognathism at the morphological and microscopic scales

Alexandra Schuh[a,*], Philipp Gunz[a], Kornelius Kupczik[a,b], Jean-Jacques Hublin[a], Sarah E. Freidline[a]

a. *Department of Human Evolution, Max Planck Institute for Evolutionary Anthropology, Deutscher Platz 6, 04103, Leipzig, Germany*
b. *Max Planck Weizmann Center for Integrative Archaeology and Anthropology, Max Planck Institute for Evolutionary Anthropology, Deutscher Platz 6, 04103 Leipzig, Germany*

*****Corresponding author**:**

Alexandra Schuh

Deutscher Platz 6, 04103 Leipzig, Germany

alexandra_schuh@eva.mpg.de

Highlights

- Overall, chimpanzees and humans express different patterns of maxillary bone modeling
- Some similarities in the location of bone resorption suggest that some aspects of the ontogenetic patterns are shared between the two species
- Chimpanzees show lower amounts of bone resorption than humans, and express a different pattern of variation
- The development of the canine eminence in chimpanzees, and the corresponding changes in bone modeling associated to this feature, is a major factor driving the differences in maxillary development between the two species

Abstract

The study of bone modeling (the simultaneous activities of bone formation and resorption during ontogeny) can help determine whether similar features in different species develop via similar or distinct ontogenetic patterns. Facial orientation (projection and degree of prognathism) in hominins is highly variable, and little is known about the dynamics behind the expression of the bone modeling patterns that lead to this variation. In this study, quantitative methods were applied to a cross-sectional ontogenetic sample of 33 chimpanzees (*Pan troglodytes verus*) and 59 *Homo sapiens* in order to compare the development of maxillary prognathism to orthognathism at both micro- and macroscopic (or morphological) scales. We find that the two species possess different bone modeling patterns. Chimpanzees express on average lower amounts of bone resorption than humans throughout ontogeny, as well as less variation within age group. Using Partial Least Squares analyses, we show that the covariation between bone modeling and shape is low in both species. This suggests that bone modeling is a highly stable process, and that most morphological changes are obtained via changes in cellular rates and/or timing of development. Moreover, although both patterns differ, some similarities in the location of bone resorption suggest the preservation of shared ontogenetic patterns.

Key words: bone modeling; bone resorption; facial ontogeny; premaxilla

Introduction

A general trend in hominin evolution relates to changes in position of the face in relation to the neurocranium. These changes have occurred in a complex, mosaic fashion, thus showing a high variability within and between species (Bastir and Rosas, 2004a). Early hominins such as *Australopithecus* and *Paranthropus* possess anteriorly projected and prognathic faces while in *Homo*, the face is less projected (Lacruz et al., 2019). It has long been proposed that these adjustments in orientation were concomitant with increases in brain size and basicranial flexion due to the morphological integration of the craniofacial

elements (e.g., Gould, 1977; Ross and Ravosa, 1993; Enlow and Hans, 1996; Lieberman et al., 2000a; Mitteroecker and Bookstein, 2008; Neaux, 2013a, 2018;). Several studies have pointed to the role of basicranial flexion and its influence on the positioning of the face during ontogeny, and vice versa (Lieberman et al., 2000b; Bastir and Rosas, 2005, 2006, 2016; Bastir et al., 2004, 2010; Scott et al., 2018). Recent findings have refined this view, and showed the complexity of the relationship between the two modules when considered on a larger evolutionary time scale (Hublin et al., 2017; Neubauer et al., 2018). Moreover, modifications of the degree of maxillary prognathism as well as in the shape of the maxillary and mandibular arcades (from a "U" to a more parabolic shape) have also been observed (e.g., Ward et al., 1999; Asfaw et al., 1999; Clarke, 2012; Spoor et al., 2015; Neaux et al., 2013b; Stelzer et al., 2017). However, the mechanisms leading to the aforementioned changes are still largely unknown.

Complex processes orchestrate developmental changes in shape and orientation of the craniofacial elements. The shape of a bone is driven by multiple pleiotropic genes (Hallgrímsson et al., 2019; Katz et al., 2019). As bones enlarge through local signaling between sutures (Rice, 2008) they are subjected to new developmental constraints due to the physical limitation imposed by the surrounding bones and soft tissues (Moss and Young, 1960). Consequently, responses from the osteogenic and osteoclastic cellular activities will be triggered, and modify and/or readjust the shape of the bone accordingly. This process is called bone modeling (Enlow, 1962; Frost, 1990). It is represented by bone formation, the apposition of new collagen fibers at the surface of the bone, and bone resorption, the reverse mechanism that removes bone. Along with sutural growth, bone modeling is thus the process by which a bone acquires its adult form. Previous studies have shown that the unique, orthognathic face of *H. sapiens* results from the presence of a large resorptive field in the maxilla from early to late ontogenetic stages (Enlow and Bang, 1965; Kurihara et al., 1980; Martinez-Maza et al., 2013; Brachetta-Aporta et al., 2017; Schuh et al., 2019). Thus, the study of facial bone modeling patterns can refine our understanding of the cellular mechanisms that drive macroscopic (or morphological) changes during facial ontogeny.

Bromage (1989) and McCollum (2008) analyzed the facial bone modeling patterns of several *Australopithecus*, as well as *Paranthropus* specimens. Both authors showed that differences in the expression of bone resorption exist between the two genera, mostly located in the maxilla. While *Paranthropus* consistently show a resorptive field in the premaxilla from early stages, this area is predominantly forming in *Australopithecus*, which suggests important differences regarding the development of their midfacial prognathism. Bromage (1989) proposed that this resorptive pattern, together with an extreme rotation of the maxilla in *Paranthropus*, explain their unique, derived facial

orientation. However, recent studies have shown that *Australopithecus sediba* (Berger et al., 2010) as well as *Homo antecessor* (Bermudez de Castro et al., 1997) also express resorption in the premaxillary region (Lacruz et al., 2013, 2015). This might suggest that, as showed by Martinez-Maza et al. (2015) on chimpanzees and gorillas, some aspects of the bone modeling patterns can be shared between species although they express specific facial features and orientations (Bromage, 1992). Thus, questions remain about the relationship between bone modeling and shape within and between species presenting different degrees of maxillary prognathism, and which of those aspects relate to primitive or derived conditions.

A new way to investigate these questions is by investigating the patterns of morphological changes together with the study of bone modeling in an integrative approach. The quantification and visualization of shape changes can be addressed via the use of geometric morphometric techniques (e.g., Bookstein, 1997; Gunz et al., 2005; Mitteroecker and Gunz, 2009), while surface histology allows for the study of the microscopic processes at the surface of dry bones (e.g., Boyde, 1972; Bromage, 1985). Previous studies using both methods have shown their complementarity for the analysis of facial ontogenetic processes, as it allows for a more global approach of the ontogenetic processes at the macro- and microscopic levels (O'Higgins and Jones, 1998; Martinez-Maza et al., 2015; Freidline et al., 2017). Moreover, the recent development of new methods for the quantification and visualization of the bone modeling patterns has improved our knowledge of these microscopic processes (Brachetta-Aporta et al., 2017; Schuh et al., 2019, 2020). Schuh et al. (2019) have shown that in humans, bone resorption covers about a third of the total surface of the maxilla throughout ontogeny, with only a slight increase observed between birth and the first months of life. Similarly, the location of bone resorption, and the patterns of covariation between bone modeling and maxillary shape show little variation across several diverse human populations with distinct maxillary morphologies (Schuh et al., 2020). Altogether, this suggests that bone resorption in the maxilla is a highly controlled process at all stages of life.

While intra-specific variation in human facial bone modeling has been reasonably explored, this is not the case for non-human great apes. In particular, the chimpanzee facial bone modeling pattern has been investigated in only a few studies (Johnson et al., 1976: the mandible; Bromage, 1989: the midface; McCollum, 2008: the maxilla; Martinez-Maza et al., 2015: the entire face) with somewhat contradicting results. McCollum (2008) showed that in the maxilla, resorptive areas are mostly located near the fronto-maxillary and zygo-maxillary sutures, in the premaxilla and posterior to the canine, as well as in the posterior maxilla. However, Bromage (1989) and Martinez-Maza et al. (2015) found little resorption in the

premaxilla. This stresses the need to further investigate the bone modeling patterns of this species, as it can represent a proxy for other species with comparable degrees of maxillary prognathism.

The objectives of the present study are to (1) refine our knowledge of the chimpanzee maxillary bone modeling pattern by using a sample with maximal preservation of the bone surface. As so far, studies of the chimpanzee bone modeling pattern have remained qualitative, the variability of this process is still unknown for that species. Moreover, it is still unclear which aspects of the bone modeling patterns are specific to or shared between species. Martinez-Maza and colleagues (2015) found similarities in the location of variable and constant bone modeling patterns between chimpanzees, gorillas and humans, which could suggest that some aspects of the bone modeling patterns are shared between great apes. Schuh et al. (2019) showed that maxillary bone resorption slightly increases between birth and the first months of life, and then stabilizes to about a third of the total surface area until adolescence. We thus test whether this pattern is found as well in chimpanzees. In doing so, we (2) quantify for the first time bone resorption in the chimpanzee maxilla. We predict that, in addition to possessing a different bone modeling pattern (Bromage, 1989; McCollum, 2008; Martinez-Maza et al., 2015), prognathism of the chimpanzee maxilla arises from lower amounts of bone resorption than in humans who possess vertically oriented (orthognathic) maxillae and high amounts of bone resorption (Schuh et al., 2019, 2020). As the chimpanzee's premaxilla follows an upward rotation during post-natal ontogeny (McCollum, 1999; Martinez-Maza et al., 2015), this displacement should be associated with predominant bone formation following Enlow (1965). We also (3) investigate if changes in size and shape induce changes in the bone modeling patterns. Indeed, most shape changes during ontogeny are due to ontogenetic allometry, the covariation between shape and size (Cheverud, 1982), and changes in this covariation pattern generates variation in adult forms (Vidarsdóttir et al., 2002; Freidline et al., 2015). However, some changes might be linked to other factors than growth of the bone itself, such as the development of the teeth. Chimpanzees develop large upper canines that together with the lower third premolars form a honing complex that has progressively been lost during the course of hominin evolution (Delson et al., 1977; Manthi et al., 2012; Delezene, 2015). We predict that a key difference between the human and chimpanzee bone modeling pattern relates to the development of the canine eminence in the latter. Finally, we (4) examine the covariation between the morphological shape and bone modeling changes.

Materials and Methods

Sample

Our sample comprises 59 *H. sapiens* of Western European origin (Anatomical Institute of the University of Strasbourg, France; Anatomical Institute of the University of Leipzig, Germany; Coimbra Anthropological collection, Portugal), and 33 chimpanzees (*Pan troglodytes verus*) from the Taï National Park, Côte d'Ivoire (housed at the Max Planck Institute for Evolutionary Anthropology, Leipzig, Germany; Table 1). Calendar ages and sexes are known for most of the individuals (SI 1). They were classified into five age groups according to dental development (AlQahtani et al., 2010; Smith et al., 2010): no teeth erupted (AG 1); developing deciduous dentition, until completion (AG 2); first permanent molar (M1) fully erupted (AG 3); second permanent molar (M2) fully erupted (AG 4); third permanent molar (M3) fully erupted (or adult; AG 5). In order to obtain negative molds of the right and left maxillae, a low-viscosity silicone (President Plus light body, Coltene/Whaledent AG, Switzerland) was applied onto the bone surface following Bromage (1989). High-resolution positive replicas were then obtained by applying a transparent 5 Minute epoxy resin (Epoxidharz 2K-Kleber transparent, Devcon) on the molds. Only the best-preserved side (left or right maxilla) was kept for the analysis. Individuals with obvious pathologies or important surface alterations were avoided. Computed tomography (CT) scans were acquired for each individual at a resolution between 0.06 to 0.2 mm (BIR ACTIS 225/300), and surface models were generated using the software Avizo (Thermo Fisher Scientific).

Table 1 Sample composition.

	Age groups					**Sex**			
	1	**2**	**3**	**4**	**5**	**Females**	**Males**	**Unknown**	***Total***
H. sapiens	7	36	8	2	6	32	27	/	***59***
P. troglodytes	2	7	8	7	9	15	14	4	***33***

Analyses

Microscopic analysis: surface histology Following Schuh et al. (2019), the surface analysis was performed using a digital optical microscope (Smart Zoom 5, Zeiss, Jena, Germany) with a 5x PlanApo D objective (zoom: 101x). A 5 x 5 mm grid was drawn on each cast, and pictures of the surfaces of interest (where both formation and resorption were seen in one square; see Fig. 1) were taken with the same objective after dividing the 5x5 mm squares into four 2.5 x 2.5 mm squares. All pictures were loaded into the software ImageJ 1.46r (Schneider et al., 2012) to be analyzed. As bone formation represents the predominant process, only areas of bone resorption were manually selected on each picture and transformed into percentages (for each square of the 5 x 5 mm grid, and then per specimen) to be quantified. From the obtained percentages of bone resorption (%BR), digital bone modeling maps of each individual were generated in R Studio (R Studio Team , 2016; see Schuh et al. (2019) for the details on the method). To visualize general trends in the bone modeling patterns in each species, mean bone modeling maps were computed for each age group and projected onto their respective mean forms (see below) in Geomagic Studio®.

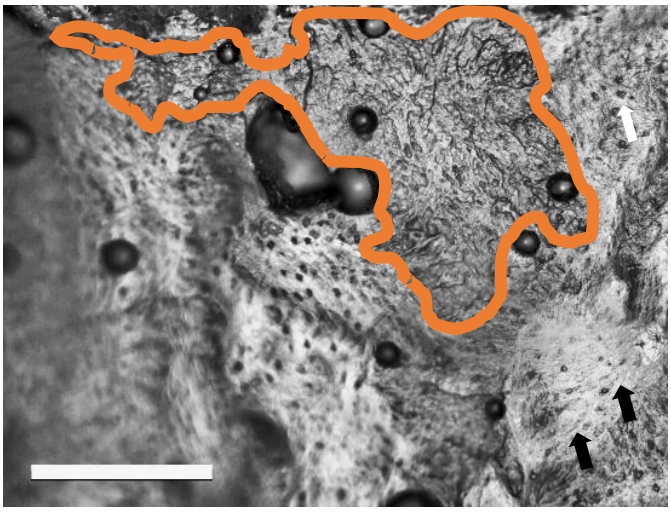

Fig. 1: Example of a subsquare showing both bone formation and resorption in *Pan troglodytes verus*. Bone formation is characterized by the presence of mineralized collagen fibers (black arrows), as well as small osteocytes lacunaes (white arrow). Bone resorption is identified by the presence of Howship's lacunaes that spread over the surface (delimited by the orange line). Scale bar: 1 mm.

Macroscopic analysis: geometric morphometrics A template of 249 semilandmarks (9 fixed landmarks, 40 curve semilandmarks and 200 surface semilandmarks) was applied on each individual (SI 2 and 3) in the software Viewbox (dHAL software). Missing data were estimated in R Studio (R Studio Team, 2016) using a TPS interpolation (package Morpho; Schlager, 2017). When applied on the left maxilla, the set of landmarks was mirrored to obtain only right configurations. In order to assure geometric homology, the curve and surface semilandmarks were allowed to slide along tangents to the curves, and planes to the surface, respectively. This step minimizes the bending energy of the TPS interpolation function between all configurations and the consensus (Gunz and Mitteroecker, 2013). Finally, a Generalized Procrustes Analysis (GPA) was performed (Rohlf and Slice, 1990; Bookstein, 1991) in order to standardize the position, orientation and scaling to a unit centroid size. Mean configurations were computed for each age group and species. As we were interested in visualizing both the changes in shape and size (i.e., form) together with bone modeling changes, the Procrustes shape coordinates were multiplied by their corresponding centroid size. A chimpanzee or human mesh was then warped onto each corresponding mean landmark configuration using a TPS interpolation. As described above, the corresponding mean bone modeling maps were then projected onto each mean form.

In order to investigate if changes in bone modeling relate to size increases and/or shape changes, the relative amounts of size and shape between birth and adulthood were calculated for each species. The mean centroid sizes and shapes were calculated for each age group, and differences between each subsequent age groups' means were computed. The adult means were considered as representing the total amount of changes (i.e., 100%) for both size and shape. Furthermore, the patterns of maxillary shape changes within each species were visualized. The shape differences were computed after calculating the Procrustes distances between AG 1 and 3, and AG 3 and 5 mean shapes only (so as to increase the differences for a better visualization). Prior to this step, independent GPAs were performed on each species to avoid any influence of the sample composition on the results. For the visualization, deformation grids were also computed using the thin plate spline method (Bookstein, 1998).

Joint analysis between morphological and bone modeling data To assess the covariation patterns between the morphological and microscopic changes in the two species, a two-block Partial Last square (PLS) analysis (Rohlf and Corti, 2000) between the Procrustes shape coordinates and the bone modeling data was performed on the pooled sample (see Mayer et al., 2014 as well as Schuh et al., 2019). To correct for species' differences in shape, the coordinates were mean-centered by removing each age group's mean

to all individuals in each species (Mitteroecker and Bookstein, 2008; Scott et al., 2018). Separate PLS analyses were performed as well on each species. Missing values in the bone modeling data were first estimated for each age group of each species in R Studio (R Studio Team) using a regularized iterative PCA algorithm of the missMDA package (Josse and Husson, 2016). Results were visualized by computing extreme shapes and bone modeling maps on each axis (+/- 2 standard deviations from the mean).

Results

Surface histology analysis

Visualization of the bone modeling patterns Figure 2 shows the mean bone modeling maps at each age group. In both species, the patterns are similar between all age groups, with the first age group differing the most from the others. In humans, the maximum %BR is found on the canine bulb and at the tip of the frontal process in AG 1. Similarly, AG 2 expresses a comparable pattern; however, resorption is distributed across the whole maxillary arcade and in higher percentages. The third and fourth age groups express similar patterns, with a reduction in %BR in the frontal process and comparable percentages in the maxillary arcade. In adults (AG 5), the maximum %BR is reduced and localized posteriorly in the canine fossa and zygomatic process.

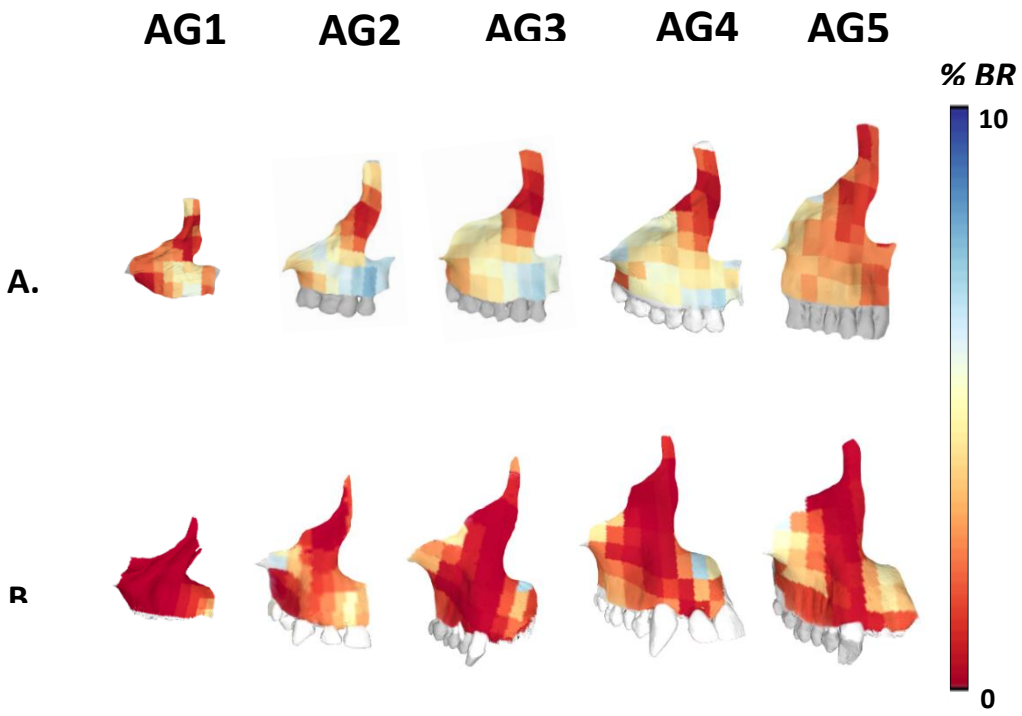

Fig. 2: Mean bone modeling maps for each age group and species. A: *H. sapiens*; B: *Pan troglodytes*. The color scale represents the percentages of bone resorption (blue tones: high %BR, red tones: low %BR). A low %BR indicate predominant bone formation.

In the chimpanzee AG 1, the highest %BR is found in the premaxilla while the rest of the bone is forming. In AG 2, the maximum %BR is found in the entire anterior maxilla, as well as in the zygomatic process. In the subsequent age groups, this pattern is repeated, although the canine eminence becomes predominantly forming in AG 3 and until adulthood, and resorption increases in the post canine region. Some resorption can be found as well near the fronto-maxillary suture and along the naso-maxillary suture up until AG 4.

Quantification of the bone modeling patterns The boxplot in Figure 3 shows the variation of the percentages of bone resorption in each age group in each species. Humans (in blue) already express high %BR in the first age group (mean: 23.5 %). This increases in AG 2 (mean: 37.7 %), and stabilizes in AG 3

(mean: 37 %). A progressive decrease is observed in the following age groups (mean AG 4: 29.2 %; mean AG 5: 19.6 %). The variation observed at each age group is high, mostly in AG 2 and 3.

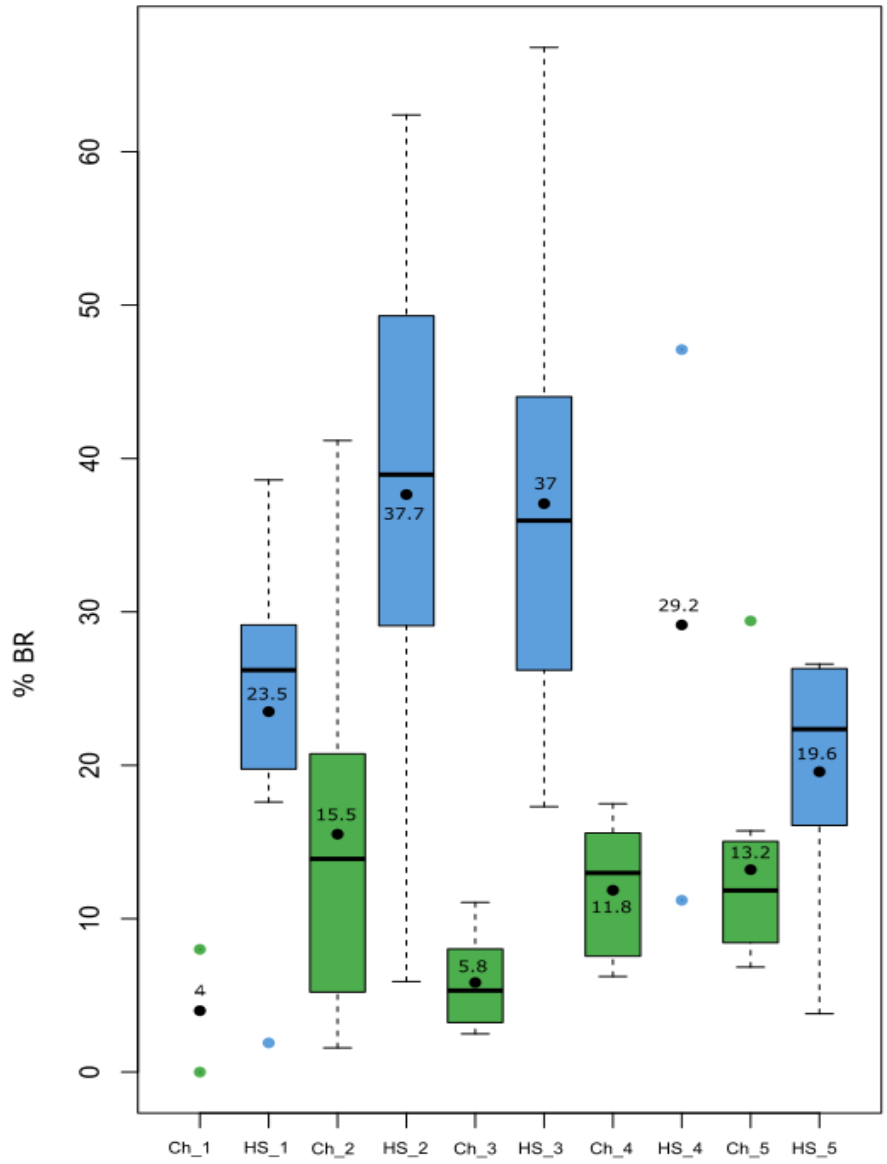

Fig. 3: Boxplots showing the variation of individual %BR, in *H. sapiens* (blue boxes) and *Pan troglodytes* (green boxes). Mean %BR values are indicated and represented as black dots. As the chimpanzee AG 1 and the human AG 4 are only represented by two individuals, they were only represented by dots.

Chimpanzees show a different pattern than humans, with on average lower values in each age group. An increase in resorption is found between AG 1 and 2 (from 4 to 15.5 %). A decrease is observed

at AG 3, showing an average value comparable to AG 1 (5.8 %). A slight increase is then found in AG 4 (mean: 11.9 %) and 5 (13.2 %). Compared to humans, the variability within each age group is lower, except in AG 2 that shows a comparably large distribution.

Morphological analysis

Relative amounts of growth and development Figure 4 shows the relative amounts of growth (inner circle) and development (outer circle) in each species and between age groups. In chimpanzees, a progressive decrease in growth is observed from AG 1 to 4 (from 31.7 to 19.2 %), followed by a slight increase between AG 4 and 5 (from 19.2 to 22.8 %). The largest amount of development in chimpanzees is found between the first two age groups (50.1%), which then progressively decreases (AG 2-3: 18.9%; AG 3-4: 17.1%; AG 4-5: 13.9%). In humans, most of the growth is acquired between AG 2 and 3 (41.7 %), after which it decreases to 8.5 %. An increase is then observed between AG 4 and 5 (19.4 %). The amounts of relative development between age groups is almost equally distributed (AG 1-2: 27%; AG 2-3: 25.9%; AG 3-4: 22.6%; AG 4-5: 24.5%).

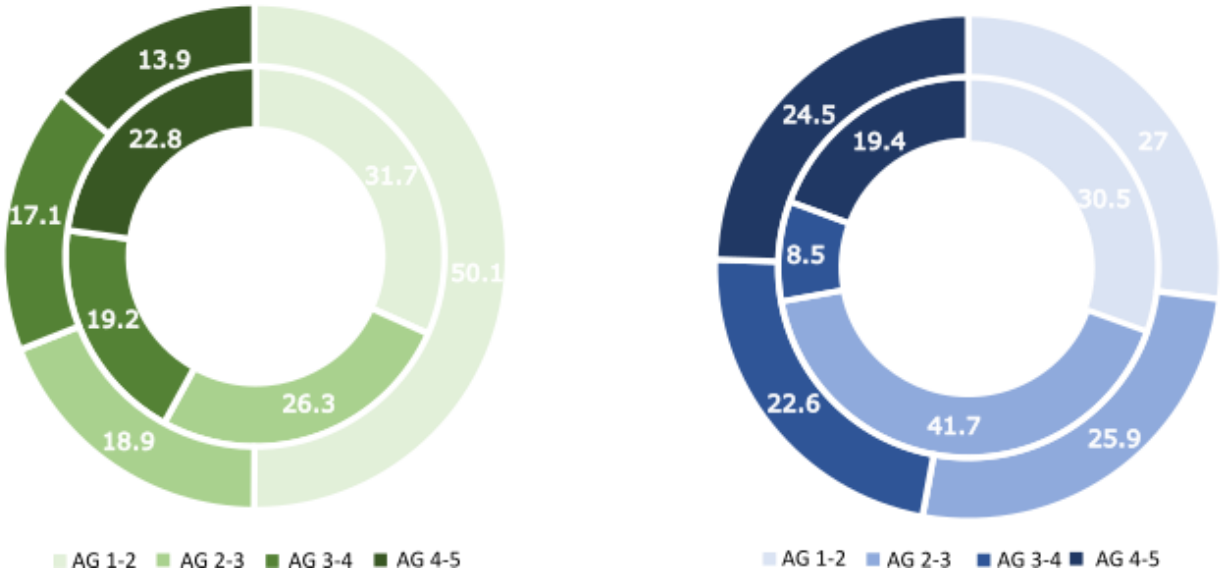

Fig. 4: Pie charts showing the relative amounts of growth (inner circles) and development (outer circles) in *Pan troglodytes verus* (left, green) and *Homo sapiens* (right, blue). Percentages indicate the amount of growth and developmental change between subsequent age groups.

Maxillary shape differences between age groups In order to visualize the patterns of shape changes in the two species, differences between age groups 1 and 3, and 3 and 5 are shown in Figure 5. In both species, differences between AG 1 and 3 are the largest, and highly similar. They are mostly present in the frontal and zygomatic process, as well as in the premaxilla. The slight difference between the two species lies in the area of the canine (see also the TPS grid, lateral view); arrows point to a more backward direction in the human compared to the more forward direction in the chimpanzee. In the comparison between AG 3 and 5, shape differences are also found in similar areas in both species, although more differences are found in the human AG 3-5. They are largely reduced compared to AG 1-3, and concern similar areas. The slight difference between the two species is found in the lower maxillary arcade in the human AG 3-5, which points to a more backward direction.

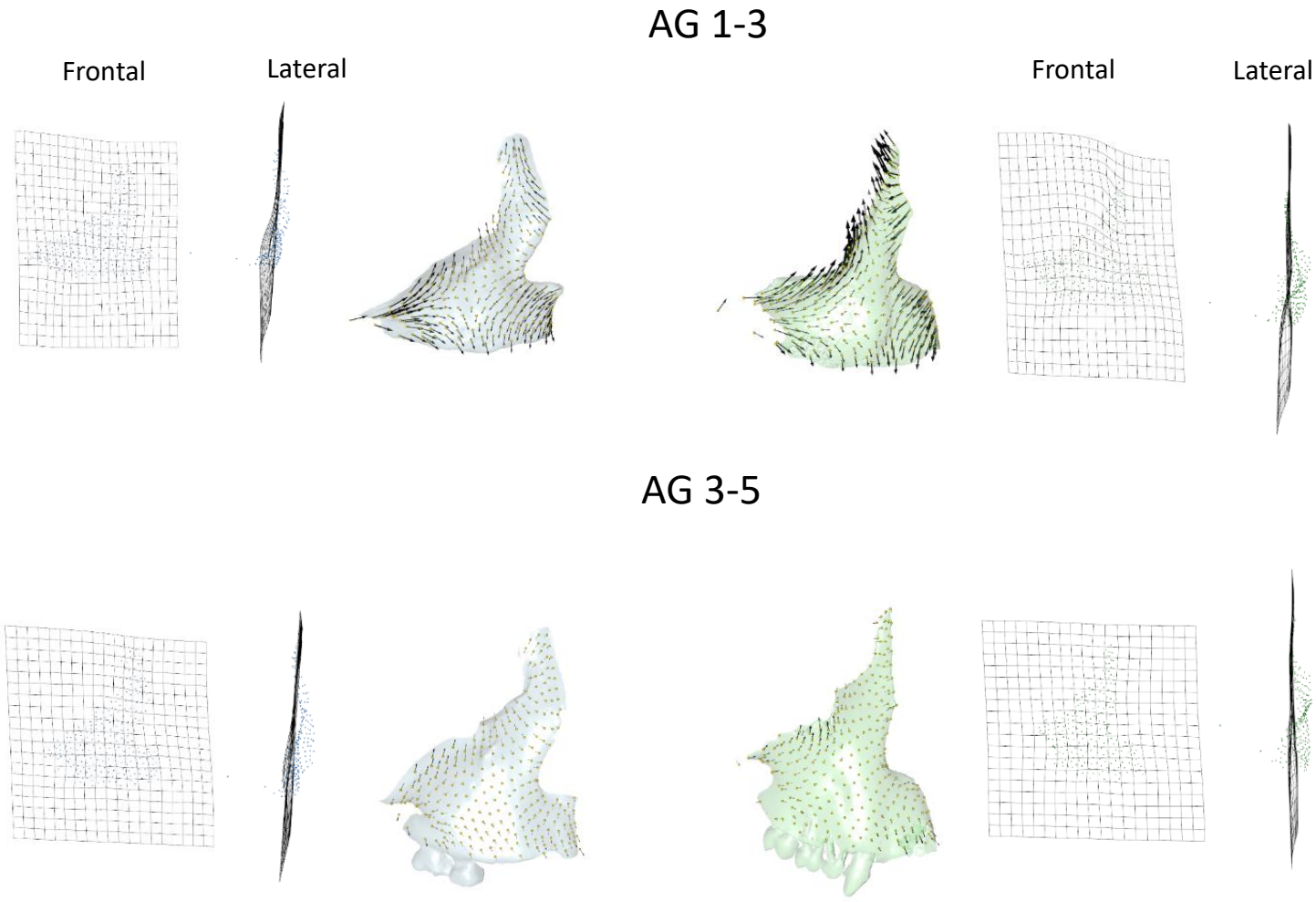

Fig. 5: Shape differences between the human (left, blue) and chimpanzee (right, green) age group means 1 and 3, and 3 and 5. Center: the largest differences are represented by longer arrows. On each side: TPS grids in the coronal plane are shown in frontal and lateral view, and represent shape differences between AG 1 and 3 (top) and AG 3 and 5 (bottom).

Covariation between maxillary bone modeling patterns and shape changes

A PLS analysis was computed between the bone modeling data and the Procrustes shape coordinates on the pooled sample. The first three singular warps represent 73.8 % of the total covariation (Table 2). The

first singular warp (SW1; Fig. 6) accounts for 36.2 % of the total covariance (R = 0.29). On the x-axis, humans (in blue) are slightly shifted towards higher values, especially in age groups 2, 3 and 4. The corresponding changes along this axis are associated to an increase in bone resorption in the maxillary arcade, and a slight decrease of the latter in the frontal process. The y-axis, represented by the shape data, separates the individuals along their ontogenetic sequence in both species. Changes are mostly associated with an increase in height of the maxilla. Overall, both species follow similar covariation patterns up until AG4, after which the direction of the covariation pattern changes. Human adults plot toward lower values, which corresponds to a general decrease in bone resorption while adult chimpanzees plot toward higher values which corresponds to an increase in bone resorption. The main differences observed between the two species are mostly due to the degrees of shape changes between age groups, as well as in the amounts of bone resorption. Humans are generally more variable in their bone modeling patterns than chimpanzees. In both species, only subtle changes in bone modeling are observed.

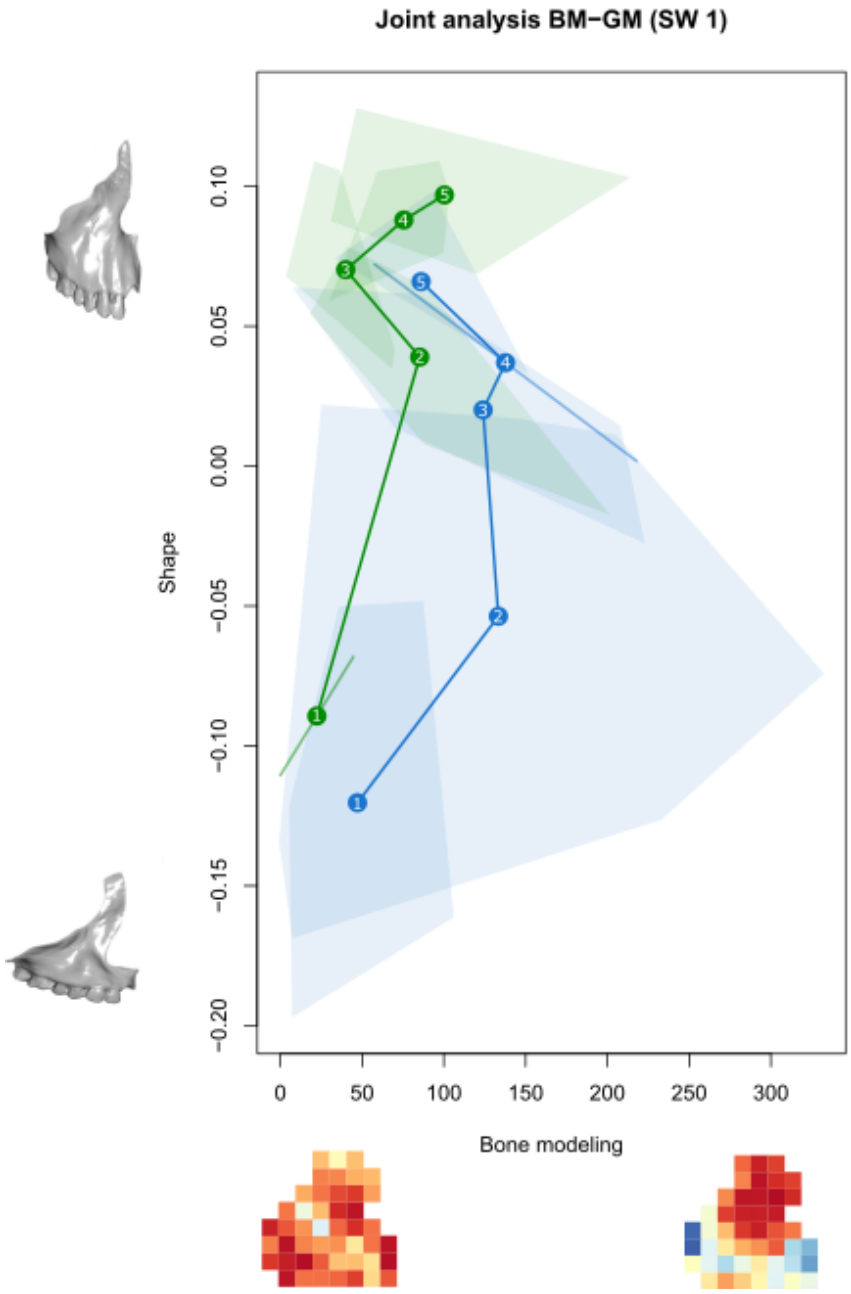

Fig. 6: Two-block partial least square (PLS) analysis between the bone modeling and morphological data (first singular warp; SW 1). X axis: bone modeling data. Y axis: Procrustes shape coordinates. Blue: *Homo sapiens*, green: *Pan troglodytes verus*. Convex hulls delimit each age group. The two individuals in the chimpanzee AG 1 and the human AG 4 are connected by a line. Age group means are represented by dots. Solid lines connect the subsequent means. Changes in bone modeling and shape along the axes are represented by bone modeling maps (x-axis) and warps (y-axis) with a standard deviation of +/- 2. In the bone modeling maps, cold colors indicate high percentages of bone resorption, and warm colors, low percentages of bone resorption.

Independent PLS analyses were performed on each species (Fig. 7 and 8). Figure 7 shows the results for the patterns of covariation between bone modeling data and shape changes in the chimpanzee (SW 1 and 2; Table 3). The first singular warp (SW 1) represents 59.3 % of the total covariance (R = 0.63). Both axes separate the young and the older individuals along the ontogenetic sequence. Changes along the x-axis (from negative to positive values) are associated to an increase in bone resorption in the zygomatic process and canine fossa, as well as along the inferior orbital margin and in the anterior maxilla. On the y-axis, an increase in height of the bone and an increase in width of the frontal process are observed. Moreover, the formation of a canine eminence and a deep canine fossa are found in positive values towards which older age groups plot. The second singular warp (SW 2) represents 19 % of the total covariance (R = 0.7). On the x-axis, AG 1 and 3 means are separated from AG 2, 4 and 5 (although a lot of overlap is found). This corresponds to an increase in bone resorption in the anterior part of the maxilla and in the zygomatic process, as well as a slight decrease in the frontal process. On the y-axis, AG 1, 2 and 3 means are separated from AG 4 and 5. Changes associated with this axis mostly concern the shape of the frontal process, which is enlarged at its base (from negative to positive values), as well as a slight decrease in prognathism.

Table 2 Percentages of total covariance, correlation coefficients and *p*-values, computed for the three first singular warps (SW 1, 2 and 3) of the PLS analysis between the Procrustes shape coordinates and the bone modeling patterns on the pooled sample.

	% Total covariance	**Correlation coefficient (R)**
SW1	36.2	0.29
SW2	27.1	0.28
SW3	10.5	0.44

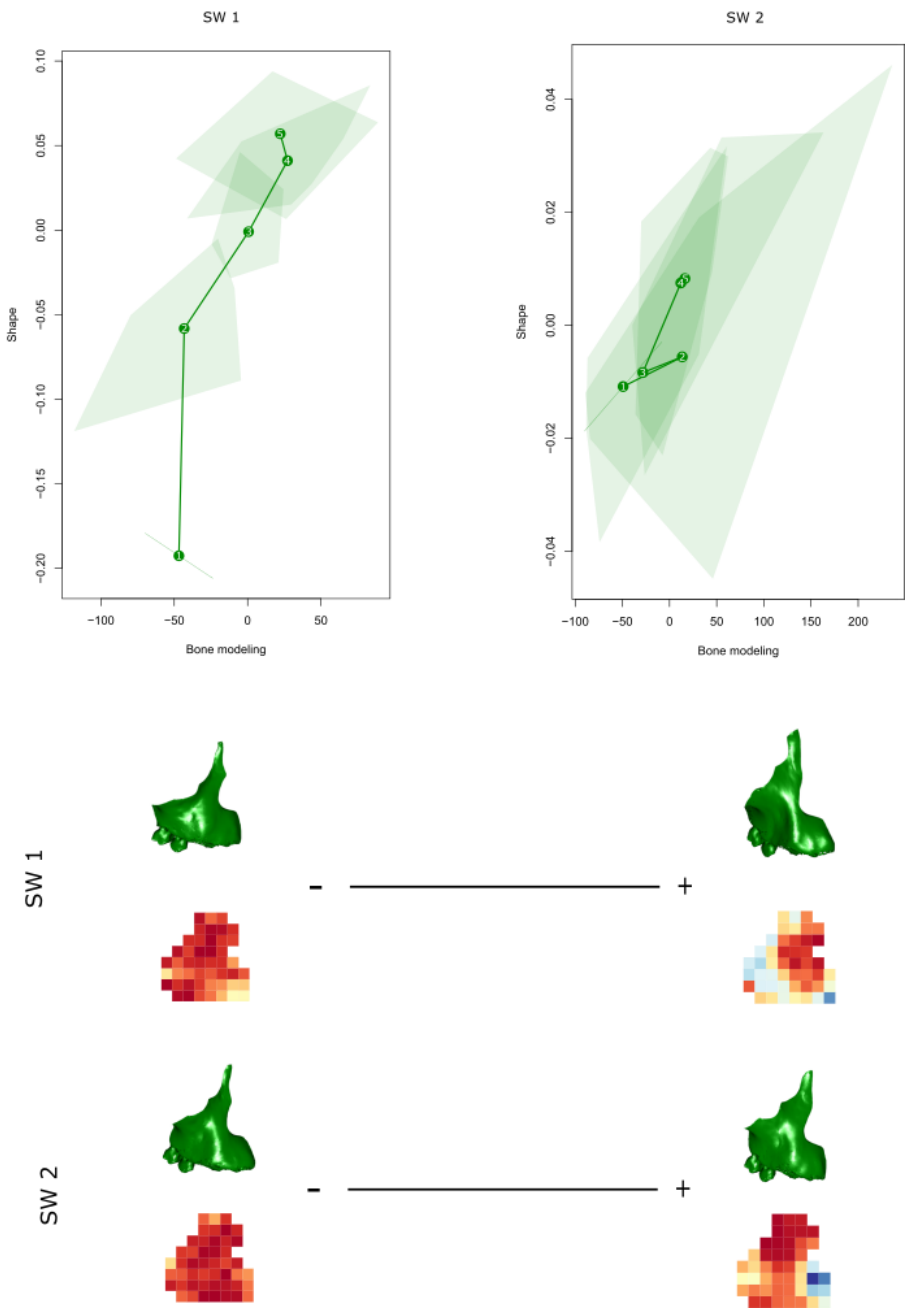

Fig. 7: Two-block partial least square (PLS) analysis between the chimpanzee bone modeling and morphological data on the first two singular warps (SW 1 and 2). Top: x axis: bone modeling data; y axis: Procrustes shape coordinates. Convex hulls delimit each age group. The two individuals in AG 1 are connected by a line. Means are represented by squares and connected by dark green solid lines. Similarly, males (triangles) and females (stars) means are connected by light green solid lines. The male's AG3 and AG5 means are connected by a dashed line as only one male is found in AG4. Bottom: bone modeling and shape changes associated to SW 1 and 2 (sd +/- 2). In the bone modeling maps, cold colors indicate high percentages of bone resorption, and warm colors, low percentages of bone resorption.

Figure 8 shows the results of the PLS analysis between bone modeling and shape data in humans (SW 1 and 2; Table 4). The first singular warp corresponds to 79.3 % of the total covariance (R = 0.56). Similar to the chimpanzees, both axes separate the individuals along the ontogenetic sequence. Changes along the x-axis from negative to positive values correspond to a decrease in bone resorption in the whole bone, which separates adults from subadults. Corresponding morphological shape changes are associated to an increase in height of the bone, as well as in width of the frontal process. In the latter, shape changes can also be observed. The second singular warp (SW 2) represents 11.2 % of the total covariance (R = 0.55). On the x-axis, AG 1 and 5 are separated from the other age groups that plot more towards negative values. This corresponds to a general decrease in bone resorption in the maxillary arcade and zygomatic process, as well as a slight increase at the tip of the frontal process. On the y-axis, AG 1 is separated from the other age groups. Associated shape changes (from negative to positive values) mostly correspond to a decrease in width of the frontal process.

Table 3 Percentages of total covariance, correlation coefficients and *p*-values, computed for the first two singular warps (SW 1 and 2) of the PLS analysis between the Procrustes shape coordinates and the bone modeling patterns in chimpanzees.

	% Total covariance	**Correlation coefficient (R)**
SW1	59.3	0.63
SW2	19	0.7

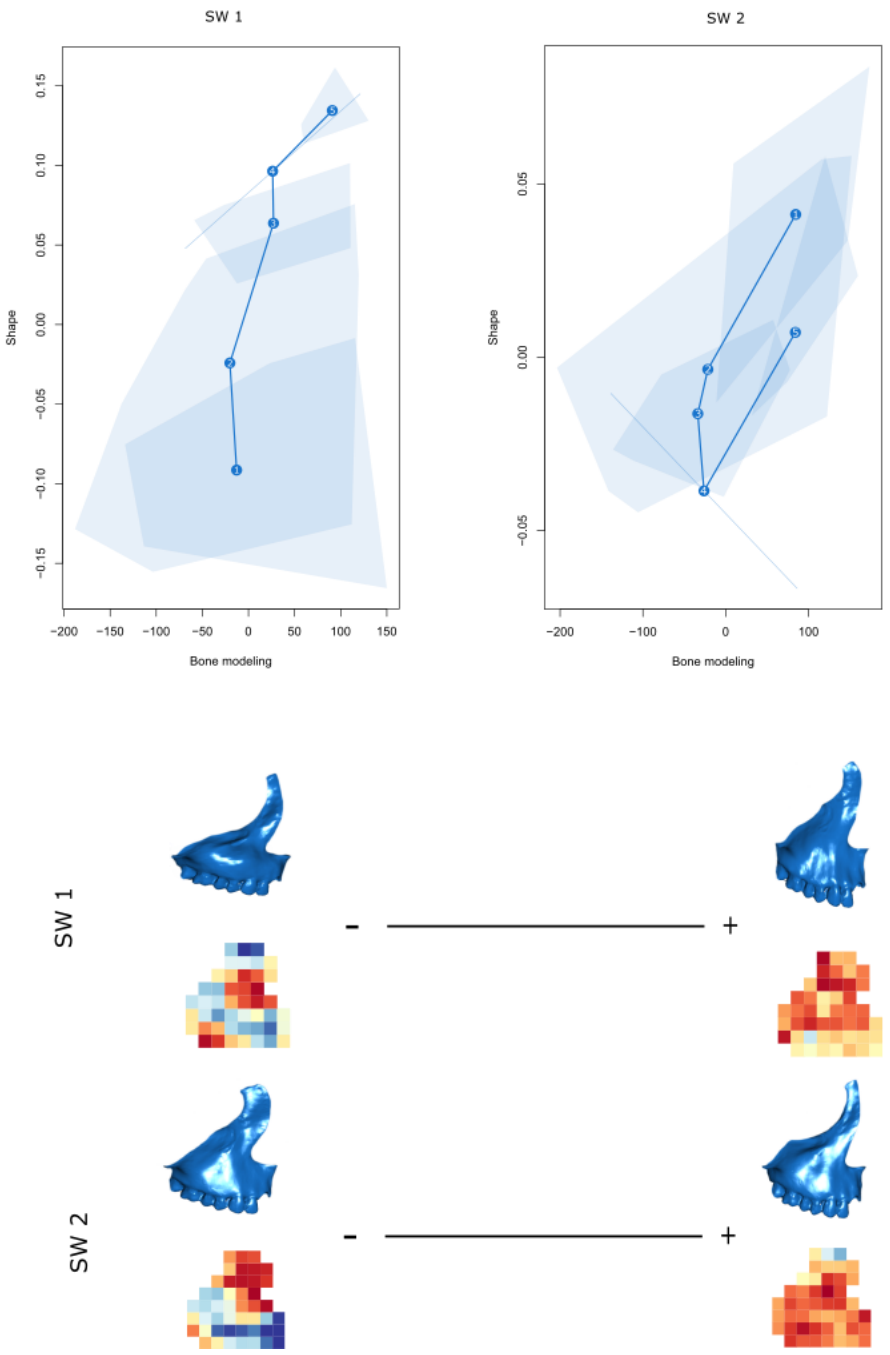

Fig. 8: Two-block partial least square (PLS) analysis between the human bone modeling and morphological data on the first two singular warps (SW 1 and 2). Top: x axis: bone modeling data; y axis: Procrustes shape coordinates. Convex hulls delimit each age group. The two individuals in AG 4 are connected by a line. Means are represented by squares and connected by dark green solid lines. Similarly, males (triangles) and females (stars) means are connected by light green solid lines. The male's AG3 and AG5 means are connected by a dashed line. Bottom: bone modeling and shape changes associated to SW 1 and 2 (sd +/- 2). In the bone modeling maps, cold colors indicate high percentages of bone resorption, and warm colors, low percentages of bone resorption.

Table 4 Percentages of total covariance, correlation coefficients and *p*-values, computed for the first two singular warps (SW 1 and 2) of the PLS analysis between the Procrustes shape coordinates and the bone modeling patterns in humans.

	% Total covariance	Correlation coefficient (R)
SW1	79.3	0.56
SW2	11.2	0.55

Discussion

This study sets out to quantify for the first time the bone modeling patterns of the chimpanzee maxilla during ontogeny in order to better understand how maxillary prognathism is established from a microscopic point of view in comparison to the orthognathic maxilla of *Homo sapiens*. The chimpanzee maxillary pattern was quantified, and investigated at both morphological and microscopic scales.

Prognathic or orthognathic: a microscopic point of view

As already showed in previous studies, the human and chimpanzee maxillary bone modeling patterns differ in the location of bone resorption (Fig. 2). While bone resorption is predominant in the human maxilla, chimpanzees possess low amounts of bone resorption, mostly restricted to the premaxilla and the zygomatic process. Thus, as expected prognathic faces are built via a majority of bone formation, which is seen in other primate species as well (Enlow, 1966; O'Higgins et al., 1991; Walters and O'Higgins, 1992; O'Higgins and Jones, 1998; Wealthall, 2002; Martinez-Maza et al., 2015). According to some of these aforementioned studies, cercopithecids seem to show less bone resorption on the maxilla than hominids, although this assumption is based on qualitative observations. Future studies applying quantitative

methods on a wider range of primate species will help refining which ontogenetic processes are specific to each family.

We also show for the first time that humans and chimpanzees possess different patterns of variation in their percentages of bone resorption (Fig. 3). Indeed, chimpanzees possess on average less bone resorption, and their expression of the osteoclastic activity during ontogeny differs. In humans, the mean %BR increases between AG 1 and 2 and then decreases, whereas in chimpanzees, changes are more variable (increasing between AG 1 and 2, then decreasing in AG 3, then slightly increasing again). In the chimpanzee AG 3, the variability within each age group is substantially reduced. Humans on the other hand, show a surprisingly high variability at each age group (as well as between individuals of similar ages; see Schuh et al., 2019). Interestingly, the chimpanzee AG 2 shows a similar distribution in the %BR than seen in humans, which corresponds to the highest amounts of bone resorption as well as the phase for which resorption is the most spread out in that species (Fig. 2). A high variability in the %BR indicates a rapid turnover between resorption and formation, which could be related to the maintenance of a stable cortical thickness. Indeed, the increased resorbing activity such as found in humans may have represented an evolutionary challenge, as the cortical thickness of the maxilla is almost constantly being resorbed; this must have been outweighed by compensatory mechanisms (such as a rapid replacement with bone formation) to prevent the bone from being destroyed.

Although we found that the human and chimpanzee bone modeling patterns differ, the results of the present study are in agreement with Martinez-Maza and Freidline (2015) who proposed that great apes share some aspects of their bone modelling pattern during ontogeny. In our data, both humans and chimpanzees are resorptive in the fronto-, zygomatico- and inter-maxillary sutures, although some differences exist in the expression of bone resorption at these sutures. This can be linked to a shared general pattern of facial integration, which has already been demonstrated by several studies (Ackermann, 2002; Bastir and Rosas, 2004; Mitteroecker and Bookstein, 2008; Singh, 2012; Neaux et al., 2018; Stelzer et al., 2017). Future studies should analyze the bone modeling patterns of other species to investigate which aspects of the bone modeling patterns are shared between all hominids. Another common aspect shared by both species is the similarity of the bone modeling patterns throughout ontogeny. Both humans and chimpanzees acquire their bone modeling pattern early (in the first year of life), and this pattern stays relatively constant until adulthood. This observation has already been made by several authors (O'Higgins et al., 1991; Martinez-Maza et al., 2015; Schuh et al., 2019, 2020), indicating that the maxilla is subjected to strong developmental constraints in both species. Moreover, the few

changes in location of bone resorption suggest that shape changes mostly stem from modifications of the rates and/or number of the cells (cellular differentiation) responsible for the two activities.

Our chimpanzee sample is unfortunately too unbalanced to further assess whether males and females differ in the expression of bone resorption. A preliminary investigation of males and females mean bone modeling patterns suggests no difference between sexes (SI 4; see also Schuh et al. (2019) for a similar discussion on humans), although differences in prognathism have been reported (Schultz, 1969; Mooney and Siegel, 1991). This will have to be tested on more individuals in the future. In the chimpanzee AG 3, which is mostly represented by males, the average %BR is particularly low. Although the sample size of this age group limits our interpretation, this could correspond to a growth phase of the canine, which is known as sexually dimorphic in chimpanzees (Leutenegger, 1982; Schwartz and Dean, 2001). The canine root completion occurs around 12 years of age, thus showing a rather late post-natal development (Kuykendall, 1996; Zihlman et al., 2007). Interestingly, McCollum (2008) also showed that individuals of a similar dental stage (M1 fully erupted) express overall less bone resorption, while Bromage (1989) only found forming areas in the premaxilla of specimens of a similar dental stage. It might thus be that the decrease in bone resorption highlighted by our study in AG 3 corresponds to a growth phase of the canine eminence rather than a sampling artefact. Moreover, it is likely that the reduction and progressive loss of the canine honing complex such as seen in hominins (Delezene, 2015) resulted as well in modifications of the corresponding bone modeling patterns.

Maxillary morphogenesis at the macroscopic scale

Due to their shorter life span, chimpanzees have faster post-natal ontogenetic rates than humans (Gavan, 1953; Hamada, 1996). When looking at the growth and development of the two species separately (Fig. 4), we can observe differences gained between each age group. Both species show the high amount of development between the first two age groups, which is linked to the highest amount of growth in chimpanzees. This is associated with a general increase in bone resorption in the whole bone in both species. However, in humans the amount of growth is largest between AG 2 and 3, which does not affect the total %BR of the bone. In this phase, resorption is replaced by formation in the frontal process, which implies potential changes in shape or a readjustment in position of this area. Similarly, the amount of shape (i.e., development) change between the human AG 3 and 4 is associated to a low amount of growth.

Although these results might be dependent on sample size, dissociations between shape and size suggest that not all shape changes are associated to size increases (i.e., allometry) as discussed by Bastir and Rosas (2004a). In chimpanzees, the amount of development decreases between each subsequent age group, while in humans this pattern remains rather constant, which could explain the maintenance of high percentages of bone resorption until late stages in the latter group (Fig. 4).

We found a similar overall patterns of shape change in the two species (Fig. 5). Both indicate a general forward/downward movement of the maxilla, which corresponds to the general growth vector of the whole face observed in great apes by different authors (Krogman, 1931 a,b,c; Todd, 1932; Enlow and Bang, 1965; Bromage, 1992; Bastir and Rosas, 2004a; Martinez-Maza et al., 2015). Moreover, we could observe each species' specific features such as a more backward displacement of the canine fossa in humans (Fig. 5, AG 1-3), and a more forward displacement of the anterior maxilla in chimpanzees (especially at later stages; see TPS grids and AG 3-5 in Fig. 5). In humans, this displacement is associated to high amounts of bone resorption in the canine fossa (Fig. 2), which, as mentioned above, has already been shown by several studies (Enlow and Bang, 1965; Kurihara, 1980; Martinez-Maza et al., 2013; Brachetta-Aporta et al., 2017; Schuh et al., 2019, 2020). Similarly, in chimpanzees the post canine region becomes progressively more concave, which is associated to an increase in bone resorption in this area in later age groups (Fig.2). In the meantime, the forward development of the canine eminence is associated to increased bone formation. Thus, bone modeling responds to both global as well as local factors.

The covariation patterns between bone modelling and morphology were assessed via the use of PLS analyses (Fig. 6, 7 and 8). We show that when considering the highest amount of covariance (SW 1), in both species changes in maxillary shape are mostly driven by ontogenetic allometry, and shows similar covariation patterns except between adolescent (AG 4) and adults (Fig. 7 and 8; see also SI 5). Overall, in both species this covariation is low, which implies few changes in the bone modeling patterns throughout ontogeny within each species, as already discussed above and showed by several authors (O'Higgins et al., 1998; Schuh et al., 2019, 2020). Again, this suggests that differences in shape are acquired through changes in rates and/or timing of the cellular activities during ontogeny. The second singular warp (SW 2) indicates divergent covariation patterns (Fig. 3 and 4); however, in both species the main change associated to SW 2 is found in the shape of the frontal process, which is likely associated to shape changes of the orbit (as described in Mitteroecker et al., 2004). This area is always predominantly associated to bone formation, which suggests that more plastic (i.e., variable) areas are found in regions of low bone resorption, as discussed by Schuh et al. (2019). As it seems that facial region that show high amounts of

bone resorption are more constrained during ontogeny, this might imply that these are also more informative on the phylogenetic level. In the present case, this corresponds to the shape of the maxillary arcade, often described as phylogenetically informative (Rak, 1983; McCollum, 1999; Spoor et al., 2015; Stelzer et al., 2018). Overall, these results suggest that the shape of the upper maxilla is highly dependent on the development of the surrounding bones (particularly in the upper part, or frontal process), which is due to its central position within the craniofacial complex. Finally, humans seem more variable in maxillary shape than chimpanzees, although this could be related to the small sample size of the latter. Including other subspecies of chimpanzees could increase the variation observed in this study on both micro- and macroscopic levels.

Premaxillary development in extant and extinct species

Bromage (1989) and McCollum (2008) both found that *Paranthropus* shows bone resorption in the premaxilla (or clivus) early in ontogeny (corresponding to AG 2 in our study). Bromage (1989) proposed that this resorptive represents a derived condition in comparison to the *Australopithecus* and chimpanzees used in the study, which consistently showed predominant bone formation in this area. Using a larger comparative sample of both humans and chimpanzees, McCollum (2008) refined this view by showing the presence of bone resorption in the chimpanzee premaxilla. However, the author could only observe resorption in late maxillary ontogenetic stages. In contrast, our results show that such as in *Homo sapiens*, resorption is already present around birth in chimpanzees, and covers the premaxilla during developing decidual dentition (Fig. 2). Moreover, other species such as *A. sediba* and *Homo antecessor* also express bone resorption in this area, as showed by Lacruz et al. (2013, 2015). Thus, it is still unclear whether bone resorption in the premaxilla represents a pattern shared by all hominins, or if the shape and orientation of this area resulted from multiple convergences.

As discussed by Villmoare et al. (2014), the hominin premaxilla is highly variable in morphology and orientation, which relates to its modularity. Such as in humans, an early closure of the premaxillary suture (connecting the maxilla to the premaxilla) occurs in *Paranthropus*, which, together with a reduction in size of the incisors, affected the orientation of the premaxilla (described as less prognathic; Wallace , 1978; Simpson et al., 1990; Braga , 1998; Maureille and Braga, 2002; Villmoare et al., 2014). In contrast, chimpanzees possess anteriorly projected premaxilla, large upper incisors and a long patency of the

premaxillary suture. On the individual scale, higher %BR are found closer to the nasal aperture in chimpanzees. This might be a continuation of the resorptive area found in the nasal cavity floor, which creates an upward rotation of the premaxilla found in all great apes (McCollum and Ward, 1997). Although we expected this displacement to be associated to predominant bone formation (H2), we propose that this rotation must be achieved via differential rates of the cellular activities between outer (periosteal) and inner (endosteal) surfaces. The resorptive activity on the periost might not be as active and/or rapid as the formation on the endost. Altogether, these results suggest that the premaxillary bone modeling pattern responds to more local rather general ontogenetic patterns as suggested by Martinez-Maza et al. (2013). Moreover, we show that similarities in the location of bone resorption such as seen in the premaxilla can result in various orientations of the concerned area. This implies that changes targeting the rates and modes of expression of the cellular activities are more easily accomplished in comparison to those implying their relocation on the bone surface. Moreover, premaxillary orientation seems highly dependent of the sutural activity and growth of inner elements (such as the vomer, hard palate, teeth and nasal septum; McCollum and Ward, 1997; Villmoare et al., 2014).

Conclusion

We have shown that in the growing human and chimpanzee maxilla, prognathism and orthognathism are established via different processes. These are found in the amounts of growth and development acquired throughout ontogeny between age groups in each species, which can be dissociated (i.e., not exclusively linked to allometric patterns). On the microscopic scale, differences in the amount of bone resorption can be found from birth on. Humans possess high amounts of bone resorption early and throughout ontogeny. Moreover, they express a tendency to more rapid turnovers between the two cellular activities, as seen by the high variation in the percentages of bone resorption. Our results also suggest that the development of the chimpanzee canine eminence, which implies an increase in bone formation on the periosteal surface, is a major factor driving the differences between the two species. It is likely that the mosaic evolution of the canine honing complex during hominin evolution was accompanied by changes in the bone modeling pattern of this area. However, some similarities in the location of bone resorption (such as found near the sutures) indicate that aspects of the ontogenetic patterns are shared between the two species. Moreover, resorption in the premaxilla is found in some species of *Australopithecus* and

Paranthropus. This suggests that similar patterns of bone modeling can result in different shapes and orientation. These results emphasize the need to investigate both macro- and microscopic scales together in an integrated approach.

Acknowledgements

We would like to acknowledge J.-L. Kahn (Anatomical Institute, University of Strasbourg, France), H. Coqueugniot (UMR 5199 PACEA, University of Bordeaux, France), C. Feja (Institute of Anatomy, University of Leipzig, Germany), A. Rosas (Department of Paleobiology, MNCN, Madrid, Sprain), A. L. Santos (Department of Life Sciences, University of Coimbra, Portugal), the Ivorian authorities, R. Wittig (Department of Primatology, Max Planck Institute for Evolutionary Anthropology, Leipzig, Germany) and U. Schwartz (Department of Human Evolution, Max Planck Institute for Evolutionary Anthropology, Leipzig, Germany) for providing access to the material. We would also like to thank J. Haesel and H. Temming for technical assistance in the preparation of the samples, as well as S. Neubauer and S. Natahi for helpful input. This work was funded by the Max Planck Society.

Bibliography

AlQahtani, S.J., Hector, M.P., & Liversidge, H.M. (2010). Brief communication: The London atlas of human tooth development and eruption. *Am J Phys Anthropol, 142*(3), 481-490.

Arsuaga, J.-L., Martínez, I., Lorenzo, C., Gracia, A., Mun, A., & Alonso, O. (1999). The human cranial remains from Gran Dolina lower Pleistocene site (Sierra de Atapuerca, Spain). *Journal of Human Evolution, 37*(3-4), 431-457.

Asfaw, B., White, T., Lovejoy, O., Latimer, B., Simpson, S., & Suwa, G. (1999). Australopithecus garhi: a new species of early hominid from Ethiopia. *Science, 284*(5414), 629-635.

Barak, M.M. (2019). Bone modeling or bone remodeling: That is the question. *American Journal of Physical Anthropology, 172*(2), 153-155.

Bastir, M., & Rosas, A. (2004). Facial heights: evolutionary relevance of postnatal ontogeny for facial orientation and skull morphology in humans and chimpanzees. *J Hum Evol, 47*(5), 359-381.

---. (2005). Hierarchical nature of morphological integration and modularity in the human posterior face. *Am J Phys Anthropol, 128*(1), 26-34.

---. (2006). Correlated variation between the lateral basicranium and the face: a geometric morphometric study in different human groups. *Arch Oral Biol, 51*(9), 814-824.

---. (2016). Cranial base topology and basic trends in the facial evolution of Homo. *J Hum Evol, 91*, 26-35.

Bastir, M., Rosas, A., & Kuroe, K. (2004). Petrosal orientation and mandibular ramus breadth: evidence for an integrated petroso-mandibular developmental unit. *Am J Phys Anthropol, 123*(4), 340-350.

Bastir, M., Rosas, A., Lieberman, D.E., & O'Higgins, P. (2008). Middle cranial fossa anatomy and the origin of modern humans. *Anat Rec (Hoboken), 291*(2), 130-140.

Bastir, M., Rosas, A., & O'Higgins, P. (2006). Craniofacial levels and the morphological maturation of the human skull. *J Anat, 209*(5), 637-654.

Bastir, M., Rosas, A., Stringer, C., Cuetara, J.M., Kruszynski, R., Weber, G.W., Ross, C.F., & Ravosa, M.J. (2010). Effects of brain and facial size on basicranial form in human and primate evolution. *J Hum Evol, 58*(5), 424-431.

Berger, L.R., De Ruiter, D.J., Churchill, S.E., Schmid, P., Carlson, K.J., Dirks, P.H., & Kibii, J.M. (2010). Australopithecus sediba: a new species of Homo-like australopith from South Africa. *Science, 328*(5975), 195-204.

Bermúdez de Castro, J.M., Arsuaga, J.L., Carbonell, E., Rosas, A., Martínez, I., & Mosquera, M. (1997). A Hominid from the Lower Pleistocene of Atapuerca, Spain: Possible Ancestor to Neandertals and Modern Humans. *276*(5317), 1392-1395.

Bookstein, F. (1991). *Morphometric Tools for Landmark Data: Geometry and Biology*. New York: Cambridge University Press.

Bookstein, F.L. (1997). Landmark methods for forms without landmarks: morphometrics of group differences in outline shape. *Medical Image Analysis, 1*(3), 225-243.

Boyde, A. (1972). Scanning electron microscope studies of bone. In G. H. Bourne (Ed.), *The Biochemistry and physiology of bone*. New York: Academic Press.

Boyde, A., & Hobdell, M.H. (1969a). Scanning electron microscopy of Lamellar bone. *Z. Zellforsch., 93*, 213-231.

---. (1969b). Scanning Electron Microscopy of Primary Membrane Bone. *Z.Zellfotsch., 99*, 98-108.

Boyde, A., & Jones, S. (1996). Scanning Electron Microscopy of Bone: Instrument, Specimen, and Issues. *Microscopy Research and Technique, 32*, 92-120.

Brachetta-Aporta, N., Gonzalez, P.N., & Bernal, V. (2017). A quantitative approach for analysing bone modelling patterns from craniofacial surfaces in hominins. *Journal of Anatomy*, n/a-n/a.

---. (2019a). Integrating data on bone modeling and morphological ontogenetic changes of the maxilla in modern humans. *Annals of Anatomy - Anatomischer Anzeiger, 222*, 12-20.

Brachetta-Aporta, N., Gonzalez, P.N., & Bernal, V. (2019b). Variation in facial bone growth remodeling in prehistoric populations from southern South America. *169*(3), 422-434.

Brachetta Aporta, N., Martinez-Maza, C., Gonzalez, P.N., & Bernal, V. (2014). Bone modeling patterns and morphometric craniofacial variation in individuals from two prehistoric human populations from Argentina. *Anat Rec (Hoboken), 297*(10), 1829-1838.

Braga, J. (1998). Chimpanzee variation facilitates the interpretation of the incisive suture closure in South African Plio-Pleistocene hominids. *American Journal of Physical Anthropology: The Official Publication of the American Association of Physical Anthropologists, 105*(2), 121-135.

Bromage, T.G. (1984). Interpretation of Scanning Electron Microscopic Images of Abraded Forming Bone Surfaces. *American Journal of Physical Anthropology, 64*, 161-178.

Bromage, T.G. (1985). Systematic inquiry of in tests of negative/positive replica combinations for SEM. *Journal of Microscopy, 137*(2), 209-216.

---. (1989). Ontogeny of the early hominin face. *Journal of Human Evolution, 18*, 751-773.

Bromage, T.G. (1992). The ontogeny of Pan troglodytes craniofacial architectural relationships and implications for early hominids. *Journal of Human Evolution, 23*(3), 235-251.

Bulygina, E., Mitteroecker, P., & Aiello, L. (2006). Ontogeny of facial dimorphism and patterns of individual development within one human population. *Am J Phys Anthropol, 131*(3), 432-443.

Butaric, L.N., & Maddux, S.D. (2016). Morphological Covariation between the Maxillary Sinus and Midfacial Skeleton among Sub-Saharan and Circumpolar Modern Humans. *American Journal of Physical Anthropology, 160*(3), 483-497.

Clarke, R.J. (2012). A Homo habilis maxilla and other newly-discovered hominid fossils from Olduvai Gorge, Tanzania. *Journal of Human Evolution, 63*(2), 418-428.

Cui, Y., & Leclercq, S. (2017). Environment-Related Variation in the Human Mid-Face. *The Anatomical Record, 300*(1), 238-250.

Day, M., & Stringer, C. (1982). L'Homo erectus et la place de l'homme de Tautavel permi les hominides fossiles. In: Centre National de la Recherche Scientifique, Nice, France.

Delezene, L.K. (2015). Modularity of the anthropoid dentition: Implications for the evolution of the hominin canine honing complex. *Journal of Human Evolution, 86*, 1-12.

Delmas, P.D. (1995). Biochemical markers of bone turnover. *Acta Orthopaedica Scandinavica, 66*(sup266), 176-182.

Delson, E., Eldredge, N., & Tattersall, I. (1977). Reconstruction of hominid phylogeny: a testable framework based on cladistic analysis. *Journal of Human Evolution, 6*(3), 263-278.

Duterloo, H.S., & Enlow, D.H. (1970). A comparative study of cranial growth in Homo and Macaca. *American Journal of Anatomy, 127*(4), 357-367.

Duval, M., Grün, R., Parés, J.M., Martín-Francés, L., Campaña, I., Rosell, J., Shao, Q., Arsuaga, J.L., Carbonell, E., & Bermúdez de Castro, J.M. (2018). The first direct ESR dating of a hominin tooth from Atapuerca Gran Dolina TD-6 (Spain) supports the antiquity of Homo antecessor. *Quaternary Geochronology, 47*, 120-137.

Enlow, D.H. (1962). A Study of the Post-Natal Growth and Remodeling of Bone. *American Journal of Anatomy, 110*(2), 79-101.

Enlow, D.H. (1966a). A comparative study of facial growth in Homo and Macaca. *American Journal of Physical Anthropology, 24*(3), 293-307.

---. (1966b). A morphogenetic analysis of facial growth. *American journal of orthodontics, 52*(4), 283-299.

Enlow, D.H., & Bang, D.D.S. (1965). Growth and remodeling of the human maxilla. *American journal of orthodontics, 51*(6), 446-464.

Enlow, D.H., & Hans, M.G. (1996). *Essentials of facial growth*: WB Saunders Company.

Evteev, A., Cardini, A.L., Morozova, I., & O'Higgins, P. (2013). Extreme climate, rather than population history, explains mid-facial morphology of northern asians. *American Journal of Physical Anthropology, 153*(3), 449-462.

Franciscus, R.G., & Trinkaus, E. (1995). Determinants of retromolar space presence in Pleistocene Homo mandibles. *Journal of Human Evolution, 28*(6), 577-595.

Freidline, S.E., Gunz, P., Harvati, K., & Hublin, J.-J. (2013). Evaluating developmental shape changes in Homo antecessor subadult facial morphology. *Journal of Human Evolution, 65*(4), 404-423.

Freidline, S.E., Gunz, P., Harvati, K., & Hublin, J.J. (2012). Middle Pleistocene human facial morphology in an evolutionary and developmental context. *J Hum Evol, 63*(5), 723-740.

Freidline, S.E., Gunz, P., & Hublin, J.J. (2015). Ontogenetic and static allometry in the human face: contrasting Khoisan and Inuit. *Am J Phys Anthropol, 158*(1), 116-131.

Freidline, S.E., Gunz, P., Jankovic, I., Harvati, K., & Hublin, J.J. (2012). A comprehensive morphometric analysis of the frontal and zygomatic bone of the Zuttiyeh fossil from Israel. *J Hum Evol, 62*(2), 225-241.

Freidline, S.E., Martinez-Maza, C., Gunz, P., & Hublin, J.J. (2017). Exploring Modern Human Facial Growth at the Micro- and Macroscopic Levels. In C. J. Percival & J. T. Richtsmeier (Eds.), *Buidling bones*. Cambridge: Cambridge University Press.

Frost, H.M. (1987). Bone "mass" and the "mechanostat": A proposal. *The Anatomical Record, 219*(1), 1-9.

Frost, H.M. (1990). Skeletal structural adaptations to mechanical usage (SATMU): 1. Redefining Wolff's law: the bone modeling problem. *The Anatomical Record, 226*(4), 403-413.

Frost, H.M. (2003). Bone's Mechanostat: A 2003 Update. *The Anatomical Record, 275*(A), 1081-1101.

Gavan, J.A. (1953). Growth and development of the chimpanzee; a longitudinal and comparative study. *Human biology, 25*(2), 93.

Gonzalez-Jose, R., Ramirez-Rozzi, F., Sardi, M., Martinez-Abadias, N., Hernandez, M., & Pucciarelli, H.M. (2005). Functional-cranial approach to the influence of economic strategy on skull morphology. *Am J Phys Anthropol, 128*(4), 757-771.

Gould, S.J. (1977). *Ontogeny and Phylogeny*. Cambridge: Harvard University Press.

Gunz, P., & Mitteroecker, P. (2013). Semilandmarks: a method for quantifying curves and surfaces. *Hystrix, the Italian Journal of Mammalogy, 24*(1), 103-109.

Gunz, P., Mitteroecker, P., & Bookstein, F. (2005). Semilandmarks in three dimensions. In D. E. Slice (Ed.), *Modern Morphometrics in Physical Anthroplogy*. New York: Kluwer Press.

Hadjidakis, D.J., & Androulakis, I.I. (2006). Bone remodeling. *Annals of the New York Academy of Sciences, 1092*(1), 385-396.

Hallgrimsson, B., Aponte, J.D., Katz, D.C., Bannister, J.J., Green, R.M., Young, N.M., Cheverud, J.M., Forkert, N.D., & Marcucio, R.S. (2019). Integration and the genetics of variation in facial shape. *The FASEB Journal, 33*(1_supplement), 330.332-330.332.

Hallgrímsson, B., Willmore, K., & Hall, B.K. (2002). Canalization, developmental stability, and morphological integration in primate limbs. *American Journal of Physical Anthropology, Suppl 35*, 131-158.

Hamada, Y., Udono, T., Teramoto, M., & Sugawara, T. (1996). The growth pattern of chimpanzees: Somatic growth and reproductive maturation inPan troglodytes. *Primates, 37*(3), 279-295.

Holton, N.E., Franciscus, R.G., Marshall, S.D., Southard, T.E., & Nieves, M.A. (2011). Nasal Septal and Premaxillary Developmental Integration: Implications for Facial Reduction in Homo. *The Anatomical Record, 294*(1), 68-78.

Holton, N.E., Franciscus, R.G., Nieves, M.A., Marshall, S.D., Reimer, S.B., Southard, T.E., Keller, J.C., & Maddux, S.D. (2010). Sutural growth restriction and modern human facial evolution: an experimental study in a pig model. *Journal of Anatomy, 216*(1), 48-61.

Holton, N.E., Yokley, T.R., & Figueroa, A. (2012). Nasal septal and craniofacial form in European- and African-derived populations. *Journal of Anatomy, 221*(3), 263-274.

Howells, W. (1973). *Cranial Variation in Man: A Study by Multivariate Analysis of Patterns of Difference among Recent Human Populations*. Cambridge: MA: Harvard University Press.

Hubbe, M., Hanihara, T., & Harvati, K. (2009). Climate Signatures in the Morphological Differentiation of Worldwide Modern Human Populations. *292*(11), 1720-1733.

Hublin, J.-J., Ben-Ncer, A., Bailey, S.E., Freidline, S.E., Neubauer, S., Skinner, M.M., Bergmann, I., Le Cabec, A., Benazzi, S., Harvati, K., & Gunz, P. (2017). New fossils from Jebel Irhoud, Morocco and the pan-African origin of Homo sapiens. *Nature, 546*, 289.

Huiskes, R., Ruimerman, R., Van Lenthe, G.H., & Janssen, J.D. (2000). Effects of mechanical forces on maintenance and adaptation of form in trabecular bone. *Nature, 405*(6787), 704-706.

Johnson, P.A., Atkinson, P.J., & Moore, W.J. (1976). The development and structure of the chimpanzee mandible. *Journal of Anatomy, 122*(2), 467-477.

Josse, J., & Husson, F. (2016). missMDA: A Package for Handling Missing Values in Multivariate Data Analysis. *Journal of Statistical Software; Vol 1, Issue 1 (2016)*.

Katz, D.C., Aponte, J.D., Liu, W., Green, R.M., Mayeux, J.M., Pollard, K.M., Pomp, D., Munger, S.C., Murray, S.A., Roseman, C.C., Percival, C.J., Cheverud, J., Marcucio, R.S., & Hallgrímsson, B. (2019). Facial shape and allometry quantitative trait locus intervals in the Diversity Outbred mouse are enriched for known skeletal and facial development genes. *bioRxiv*, 787291.

Kini, U., & Nandeesh, B.N. (2012). Physiology of Bone Formation, Remodeling, and Metabolism. 29-57.
Kranioti, E.F., Rosas, A., Garcia-Vargas, S., Estalrrich, A., Bastir, M., & Pena-Melian, A. (2009). Remodeling patterns of occipital growth: a preliminary report. *Anat Rec (Hoboken), 292*(11), 1764-1770.
Krogman, W.M. (1931a). Studies in growth changes in the skull and face of anthropoids. III. Growth changes in the skull and face of the gorilla. *American Journal of Anatomy, 47*(1), 89-115.
---. (1931b). Studies in growth changes in the skull and face of anthropoids. IV. Growth changes in the skull and face of the chimpanzee. *American Journal of Anatomy, 47*(2), 325-342.
---. (1931c). Studies in growth changes in the skull and face of anthropoids. V. Growth changes in the skull and face of the orang-utan. *American Journal of Anatomy, 47*(2), 343-365.
Kurihara, S., Enlow, D.H., & Rangel, R.D. (1980). Remodeling Reversals in Anterior Parts of the Human Mandible and Maxilla. *The Angle Orthodontics, 50*(2), 98-106.
Kuykendall, K.L. (1996). Dental development in chimpanzees (Pan troglodytes): the timing of tooth calcification stages. *American Journal of Physical Anthropology: The Official Publication of the American Association of Physical Anthropologists, 99*(1), 135-157.
Lacruz, R.S., Bromage, T.G., O'Higgins, P., Toro-Ibacache, V., Warshaw, J., & Berger, L.R. (2015). Distinct growth of the nasomaxillary complex in Au. sediba. *Sci Rep, 5*, 15175.
Lacruz, R.S., de Castro, J.M., Martinon-Torres, M., O'Higgins, P., Paine, M.L., Carbonell, E., Arsuaga, J.L., & Bromage, T.G. (2013). Facial morphogenesis of the earliest europeans. *PLOS ONE, 8*(6), e65199.
Lacruz, R.S., Stringer, C.B., Kimbel, W.H., Wood, B., Harvati, K., O'Higgins, P., Bromage, T.G., & Arsuaga, J.-L. (2019). The evolutionary history of the human face. *Nature Ecology & Evolution, 3*(5), 726-736.
Lahr, M.M. (1996). *The evolution of modern human diversity: a study of cranial variation* (Vol. 18): Cambridge University Press.
Leutenegger, W. (1982). Scaling of sexual dimorphism in body weight and canine size in primates. *Folia Primatologica, 37*(3-4), 163-176.
Lieberman, D.E., Pearson, O.M., & Mowbray, K.M. (2000). Basicranial influence on overall cranial shape. *J Hum Evol, 38*(2), 291-315.
Lieberman, D.E., Ross, C.F., & Ravosa, M.J. (2000). The primate cranial base: Ontogeny, function, and integration. *American Journal of Physical Anthropology, 113*(S31), 117-169.
Maddux, S.D., & Franciscus, R.G. (2009). Allometric scaling of infraorbital surface topography in Homo. *J Hum Evol, 56*(2), 161-174.
Manthi, F.K., Plavcan, J.M., & Ward, C.V. (2012). New hominin fossils from Kanapoi, Kenya, and the mosaic evolution of canine teeth in early hominins. *South African Journal of Science, 108*(3-4), 00-00.
Martinez-Maza, C., Freidline, S.E., Strauss, A., & Nieto-Diaz, M. (2015). Bone Growth Dynamics of the Facial Skeleton and Mandible in Gorilla gorilla and Pan troglodytes. *Evolutionary Biology, 43*(1), 60-80.
Martinez-Maza, C., Rosas, A., Garcia-Vargas, S., Estalrrich, A., & de la Rasilla, M. (2011). Bone remodelling in Neanderthal mandibles from the El Sidron site (Asturias, Spain). *Biol Lett, 7*(4), 593-596.
Martinez-Maza, C., Rosas, A., & Nieto-Diaz, M. (2013). Postnatal changes in the growth dynamics of the human face revealed from bone modelling patterns. *J Anat, 223*(3), 228-241.
Maureille, B. (1994). *La face chez Homo erectus et Homo sapiens: recherche sur la variabilité morphologique et métrique, Anthropologie.* Ph. D. Dissertation, Uni-versité de Bordeaux 1,
Maureille, B., & Braga, J. (2002). Between the Incisive Bone and Premaxilla From African Apes to Homo sapiens. *Human Evolution through Developmental Change*, 464.
Mayer, C., Metscher, B.D., Müller, G.B., & Mitteroecker, P. (2014). Studying Developmental Variation with Geometric Morphometric Image Analysis (GMIA). *PLOS ONE, 9*(12), e115076.
McCollum, M.A. (1999). The Robust Australopithecine Face: A Morphogenetic Perspective. *Science, 284*(5412), 301-305.
---. (2008). Nasomaxillary remodeling and facial form in robust Australopithecus: a reassessment. *J Hum Evol, 54*(1), 2-14.

McCollum, M.A., & Ward, S.C. (1997). Subnasoalveolar anatomy and hominoid phylogeny: Evidence from comparative ontogeny. *American Journal of Physical Anthropology, 102*(3), 377-405.

Mitteroecker, P., & Bookstein, F. (2008). The evolutionary role of modularity and integration in the hominoid cranium. *Evolution, 62*.

---. (2009). The ontogenetic trajectory of the phenotypic covariance matrix, with examples from craniofacial shape in rats and humans. *Evolution, 63*(3), 727-737.

Mitteroecker, P., & Gunz, P. (2009). Advances in Geometric Morphometrics. *Evolutionary Biology, 36*(2), 235-247.

Mitteroecker, P., Gunz, P., Bernhard, M., Schaefer, K., & Bookstein, F.L. (2004). Comparison of cranial ontogenetic trajectories among great apes and humans. *J Hum Evol, 46*(6), 679-697.

Mitteroecker, P., Gunz, P., & Bookstein, F.L. (2005). Heterochrony and geometric morphometrics: a comparison of cranial growth in Pan paniscus versus Pan troglodytes. *Evolution & Development, 7*(3), 244-258.

Mitteroecker, P., Gunz, P., Weber, G.W., & Bookstein, F.L. (2004). Regional dissociated heterochrony in multivariate analysis. *Annals of Anatomy - Anatomischer Anzeiger, 186*(5), 463-470.

Mooney, M.P., & Siegel, M.I. (1986). Developmental relationship between premaxillary-maxillary suture patency and anterior nasal spine morphology. *Cleft Palate J, 23*(2), 101-107.

Mooney, M.P., & Siegel, M.I. (1991). Premaxillary-maxillary suture fusion and anterior nasal tubercle morphology in the chimpanzee. *American Journal of Physical Anthropology, 85*(4), 451-456.

Moss, M.L., & Young, R.W. (1960). A Functional Approach to Craniology. *American Journal of Physical Anthropology, 18*(4), 281-292.

Mowbray, K. (2005). Surface bone histology of the occipital bone in humans and chimpanzees. *Anat Rec B New Anat, 283*(1), 14-22.

Neaux, D., Guy, F., Gilissen, E., Coudyzer, W., & Ducrocq, S. (2013). Covariation between midline cranial base, lateral basicranium, and face in modern humans and chimpanzees: a 3D geometric morphometric analysis. *Anat Rec (Hoboken), 296*(4), 568-579.

Neaux, D., Guy, F., Gilissen, E., Coudyzer, W., Vignaud, P., & Ducrocq, S. (2013). Facial orientation and facial shape in extant great apes: a geometric morphometric analysis of covariation. *PLOS ONE, 8*(2), e57026-e57026.

Neaux, D., Sansalone, G., Ledogar, J.A., Heins Ledogar, S., Luk, T.H.Y., & Wroe, S. (2018). Basicranium and face: Assessing the impact of morphological integration on primate evolution. *Journal of Human Evolution, 118*, 43-55.

Neubauer, S., Hublin, J.-J., & Gunz, P. (2018). The evolution of modern human brain shape. *Science advances, 4*(1), eaao5961.

Noback, M.L., & Harvati, K. (2015). The contribution of subsistence to global human cranial variation. *Journal of Human Evolution, 80*, 34-50.

O'Higgins, P., Bromage, T.G., Johnson, D.R., Moore, W.J., & McPhie, P. (1991). A Study of Facial Growth in the Sooty Mangabey *Cercocebus atys*. *Folia Primatologica, 56*(2), 86-94.

O'Higgins, P., Chadfield, P., & Jones, N. (2001). Facial growth and the ontogeny of morphological variation within and between the primates Cebus apella and Cercocebus torquatus. *Journal of Zoology, 254*, 337-357.

O'Higgins, P., & Dryden, I. (1992). Studies of craniofacial development and evolution. *Archaeology in Oceania, 27*(3), 105-112.

O'Higgins, P., & Jones, N. (1998). Facial growth in Cercocebus torquatus: an application of three-dimensional geometric morphometric techniques to the study of morphological variation. *Journal of Anatomy, 193*(2), 251-272.

O'Higgins, P., & Vidarsdóttir, U.E. (1999). New approaches to the quantitative analysis of craniofacial growth and variation. In C. U. Press (Ed.), *Human growth in the past: studies from bones and teeth* (pp. 128-160).

Parfitt, A. (1984). The cellular basis of bone remodeling: the quantum concept reexamined in light of recent advances in the cell biology of bone. *Calcified Tissue International, 36*(1), S37-S45.

Rak, Y. (1983). *The australopithecine face*. New-York: Academic Press.

Rice, D. (2008). *Craniofacial Sutures: Development, Disease, and Treatment.* (R. DP Ed. Vol. 12). Basel: Karger.

Rogers Ackermann, R., & Krovitz, G.E. (2002). Common patterns of facial ontogeny in the hominid lineage. *The Anatomical Record, 269*(3), 142-147.

Rohlf, F.J., & Corti, M. (2000). Use of Two-Block Partial Least-Squares to Study Covariation in Shape. *Systematic Biology, 49*(4), 740-753.

Rohlf, F.J., & Slice, D. (1990). Extensions of the Procrustes method for the optimal superimposition of landmarks. *Syst Zool, 39*.

Rosas, A., & Martinez-Maza, C. (2010). Bone remodeling of the Homo heidelbergensis mandible; the Atapuerca-SH sample. *J Hum Evol, 58*(2), 127-137.

Rosas, A., Martínez-Maza, C., Bastir, M., García-Tabernero, A., Lalueza-Fox, C., Huguet, R., Ortiz, J.E., Julià, R., Soler, V., de Torres, T., Martínez, E., Cañaveras, J.C., Sánchez-Moral, S., Cuezva, S., Lario, J., Santamaría, D., de la Rasilla, M., & Fortea, J. (2006). Paleobiology and comparative morphology of a late Neandertal sample from El Sidrón, Asturias, Spain. *Proceedings of the National Academy of Sciences, 103*(51), 19266-19271.

Ross, C.F., & Ravosa, M.J. (1993). Basicranial flexion, relative brain size, and facial kyphosis in nonhuman primates. *American Journal of Physical Anthropology, 91*(3), 305-324.

Schlager, S. (2017). Morpho and Rvcg–Shape Analysis in R: R-Packages for geometric morphometrics, shape analysis and surface manipulations. In *Statistical shape and deformation analysis* (pp. 217-256): Elsevier.

Schneider, C.A., Rasband, W.S., & Eliceiri, K.W. (2012). NIH Image to ImageJ: 25 years of Image Analysis. *Nature Methods, 9*(7), 671–675.

Schuh, A., Gunz, P., Villa, C., Kupczik, K., Hublin, J.J., & Freidline, S.E. (2020). Intraspecific variability in human maxillary bone modeling patterns during ontogeny. *American Journal of Physical Anthropology*.

Schuh, A., Kupczik, K., Gunz, P., Hublin, J.-J., & Freidline, S.E. (2019). Ontogeny of the human maxilla: a study of intra-population variability combining surface bone histology and geometric morphometrics. *Journal of Anatomy, 235*(2), 233-245.

Schulte, F.A., Ruffoni, D., Lambers, F.M., Christen, D., Webster, D.J., Kuhn, G., & Muller, R. (2013). Local mechanical stimuli regulate bone formation and resorption in mice at the tissue level. *PLOS ONE, 8*(4), e62172.

Schultz, A.H. (1969). The skeleton of the chimpanzee. *The chimpanzee, 1*, 50-103.

Schwartz, G.T., & Dean, C. (2001). Ontogeny of canine dimorphism in extant hominoids. *American Journal of Physical Anthropology: The Official Publication of the American Association of Physical Anthropologists, 115*(3), 269-283.

Scott, N.A., Strauss, A., Hublin, J.-J., Gunz, P., & Neubauer, S. (2018). Covariation of the endocranium and splanchnocranium during great ape ontogeny. *PLOS ONE, 13*(12), e0208999.

Simpson, S.W., Lovejoy, C.O., & Meindl, R.S. (1990). Hominoid dental maturation. *Journal of Human Evolution, 19*(3), 285-297.

Singh, N., Harvati, K., Hublin, J.J., & Klingenberg, C.P. (2012). Morphological evolution through integration: a quantitative study of cranial integration in Homo, Pan, Gorilla and Pongo. *J Hum Evol, 62*(1), 155-164.

Smith, T.M., Smith, B.H., Reid, D.J., Siedel, H., Vigilant, L., Hublin, J.-J., & Boesch, C. (2010). Dental development of the Taï Forest chimpanzees revisited. *Journal of Human Evolution, 58*(5), 363-373.

Spoor, F., Gunz, P., Neubauer, S., Stelzer, S., Scott, N., Kwekason, A., & Dean, M.C. (2015). Reconstructed Homo habilis type OH 7 suggests deep-rooted species diversity in early Homo. *Nature, 519*(7541), 83-86.

Stelzer, S., Gunz, P., Neubauer, S., & Spoor, F. (2017). Hominoid arcade shape: Pattern and magnitude of covariation. *Journal of Human Evolution, 107*, 71-85.

---. (2018). Using the covariation of extant hominoid upper and lower jaws to predict dental arcades of extinct hominins. *Journal of Human Evolution, 114*, 154-175.

Stynder, D.D., Ackermann, R.R., & Sealy, J.C. (2007). Craniofacial variation and population continuity during the South African Holocene. *134*(4), 489-500.

Team, R. (2020). RStudio: Integrated Development Environment for R. Boston, MA.

Todd, T.W. (1932). Prognathism: a Study in Development of the Face. *The Journal of the American Dental Association (1922), 19*(12), 2172-2184.

Vidarsdóttir, U.E., O'Higgins, P., & Stringer, C. (2002). A geometric morphometric study of regional differences in the ontogeny of the modern human facial skeleton. *Journal of Anatomy, 201*, 211-229.

Villmoare, B.A., Dunmore, C., Kilpatrick, S., Oertelt, N., Depew, M.J., & Fish, J.L. (2014). Craniofacial modularity, character analysis, and the evolution of the premaxilla in early African hominins. *Journal of Human Evolution, 77*, 143-154.

von Cramon-Taubadel, N. (2011). Global human mandibular variation reflects differences in agricultural and hunter-gatherer subsistence strategies. *Proceedings of the National Academy of Sciences, 108*(49), 19546-19551.

Waddington, C.H. (1942). Canalization of the development and the inheritance of acquired characters. *Nature, 150*, 563.

Wallace, J. (1978). Evolutionary trends in the early hominid dentition. In *Early hominids of Africa* (pp. 285-310): Duckworth London.

Walters, M., & O'Higgins, P. (1992). *Factors influencing craniofacial growth: a scanning electron microscope study of high resolution facial replicas.* Paper presented at the Proc Australas Soc Hum Biol.

Ward, C., Leakey, M., & Walker, A. (1999). The new hominid species Australopithecus anamensis. *Evolutionary Anthropology: Issues, News, and Reviews, 7*(6), 197-205.

Wealthall, R.J. (2002). Surface remodelling of the facial skeleton in juvenile Macaca mulatta: implications for sexual dimorphism. *Folia Primatologica, 73*(1), 49-53.

Zihlman, A.L., Bolter, D.R., & Boesch, C. (2007). Skeletal and dental growth and development in chimpanzees of the Taï National Park, Côte D'Ivoire. *Journal of Zoology, 273*(1), 63-73.

Conclusion

The primary aims of this thesis were to improve our understanding of ontogenetic variation in facial bone modeling patterns within and between extant species, and establish a solid framework for future bone modeling studies of fossil hominins via the development of objective methods for the quantification of facial bone modeling patterns. The *Homo sapiens* midface (in particular, the maxilla) exhibits unique features that are used to define us as a species and our phylogenetic relationships to other hominins. Among those features, the canine fossa is often cited as characterizing *H. sapiens*. However, its use in phylogenetic studies has been debated, as it might represent a secondary character acquired along with facial size reduction observed in *Homo* (Maddux & Franciscus, 2009; Freidline et al., 2013). Understanding the development of facial features is thus of crucial importance, as similar traits expressed in different species might follow distinct developmental pathways. This thesis investigated the variability of bone modeling patterns in three different chapters. Chapter 1 explored the ontogenetic maxillary bone modeling patterns in a single population of *H. sapiens* individuals in order to quantify their variability at the population level, and described the novel methodological approach. In Chapter 2, maxillary bone modeling patterns and shape changes during ontogeny were established in a larger ontogenetic sample of three geographically diverse human populations to infer intraspecific variability in maxillary bone modeling patterns. Finally, Chapter 3 compared the results obtained for *H. sapiens* in Chapters 1 and 2 to an ontogenetic sample of chimpanzees (*Pan troglodytes*) to evaluate maxillary bone modeling patterns in these two taxa with differing maxillary projections (orthognathic versus prognathic, respectively).

Previous studies of facial bone modeling patterns have mainly relied on qualitative instead of quantitative data, which has long represented a limitation to the interpretation of this ontogenetic process (although see Brachetta-Aporta et al., 2017). Moreover, visual representations of bone modeling patterns have so far been conducted using hand-drawn 2D maps, which could have hampered objective comparisons of the bone modeling patterns. To address these limitations, I developed a novel method that integrates bone modeling with morphological data (Chapter 1). Using optical microscopy and digital imaging (SmartZoom 5, Zeiss), I was able to collect data on an unprecedentedly large sample of individuals in a significantly lower amount of time. The quantification of bone resorption was directly performed on the images taken on the bone surface, and digital maps representing each individual's bone modeling pattern were created. These maps were projected onto 3D models of the growing maxilla, allowing for a dynamic vision of the changes in bone modeling throughout ontogeny. The analysis of bone modeling patterns included the observation and quantification of two critical parameters, which are discussed below: (1) the location of bone resorption on the bone surface, and (2) the amount of bone resorption calculated for each individual.

In Chapter 2, the variability of bone modeling and shape changes was assessed during growth in three human populations. The results demonstrated that there is actually a low intraspecific variation in the location of bone resorption throughout ontogeny, despite population differences in maxillary shape. It has been proposed that differences in diet found in human groups induce variation in facial morphology (González-José et al., 2005; Menéndez et al., 2014) and thus, in bone modeling (Brachetta-Aporta et al., 2017). To the contrary, the results of this thesis suggest a limited influence of such epigenetic factors on maxillary bone modeling patterns. Similarities in the location of bone resorption on the maxillary surface between human groups rather result from a process that is highly controlled throughout ontogeny. Moreover, a preliminary investigation of the variation in adult bone modeling patterns suggests a continuation of similar processes into at least early adulthood, although at reduced intensities (Chapter 2). Altogether, these results show that intraspecific variation in maxillary morphology among humans mostly stems from changes in rates and timings of bone formation and resorption instead of modifications of the location of these activities on the bone. Looking at the bone modeling patterns in a different primate (the sooty mangabey), O'Higgins and collaborators (1991) proposed a similar conclusion. Moreover, as these results were found as well in chimpanzees (Chapter 3), the stability in the location of bone resorption may apply to all primate species. Thus, bone modeling patterns can be inferred from a limited number of individuals, which will be beneficial to discuss the bone modeling patterns of extinct species for which sample sizes are generally low and subadult individuals are scarce.

Moreover, I show that the use of quantitative data, rather than previously qualitative methods, helped to refine which aspects of bone modeling are species-specific. Chimpanzees possess low amounts of bone resorption in the maxilla, which indicates that bone formation participates in the anterior projection of their face. In contrast, the human maxillary arcade shows high amounts of bone resorption. This constrains the forward direction of growth and results in a vertical face (see Chapters 1 and 3; Enlow , 1965, 1966a, b; Martínez-Maza et al., 2013). Another human specificity that is not found in chimpanzees, relates to the high variation in the amounts of bone resorption. It was found that individuals of similar ages can express drastically different amounts of bone resorption throughout ontogeny, varying up to 40 percent (Chapter 1). Such a high variation might indicate rapid turnover rates between bone formation and resorption. I propose that the frequent replacement of bone resorption by bone formation represents a protective mechanism, avoiding damage to the cortical bone, which is thin in human maxillae. Indeed, high amounts of bone resorption might be harmful for the maxillary arcade that contains the teeth. Altogether, these results demonstrate that changes in developmental factors affecting the regulation of osteoclasts and/or their precursor cells are likely to have occurred, to account for the specific maxillary morphology of *H. sapiens*.

Although humans and chimpanzees express different maxillary bone modeling patterns, some aspects of these patterns are shared between the two species. More generally, similarities in facial bone modeling patterns between species have already been highlighted in other studies. These mostly relate to the location of bone resorption, such as in the coronoid process of the

mandible (Johnson et al., 1976; Rosas & Martínez-Maza, 2010; Martínez-Maza et al., 2015). In Chapter 3, I showed that this applies to the maxilla as well, as bone resorption is present along all maxillary sutures in both chimpanzees and humans throughout ontogeny. Moreover, although the amount of bone resorption differs between humans and chimpanzees, in both taxa the region of highest bone resorption is expressed in the anterior maxilla (or premaxilla; the region that comprises the upper incisors) and the zygomatic process (along the zygomatico-maxillary suture). These results tentatively support previous studies showing that some aspects of growth and development are highly conserved within primates, and, more generally, within the mammalian skull (e.g., Krogman, 1931a,b,c; Todd, 1932; Hallgrímsson et al., 2007; Martínez-Abadías et al., 2012). Indeed, during embryonic development similar homeotic genes are found in a wide range of mammalian species (Martin et al., 1995; Xu et al., 2019). These genes are known to have pleiotropic effects (i.e., one gene is involved in the development of multiple phenotypic traits), which results in developmental covariation, or integration, of the craniofacial elements (Cheverud, 1996; Hallgrímsson et al., 2009). In the skull, patterns of developmental integration have been found to be shared among great apes (e.g., Ackermann, 2002; Bastir & Rosas, 2004; Mitteroecker & Bookstein, 2008; Coquerelle et al., 2013; Scott et al., 2018). Thus, the findings of this research demonstrate that similarities in bone modeling patterns are likely to result from conserved, shared patterns of growth and development in the hominid[1] skull.

Future directions

The findings of this thesis demonstrate the potential of bone modeling studies to investigate maxillary development, as well as other regions of the face and cranium. Additional future research avenues would improve our ability to understand the evolution of the face in humans as well as our extinct relatives. These include several research areas that are in their infancy, including the study of prenatal development, variability across primates, the relationship between genetics and morphology, as well as differences in the rates of development, such as in cellular activity and angiogenesis. These are discussed below.

The role of prenatal development in establishing species-specific features has been highlighted by numerous studies (e.g., Richtsmeier et al., 1993; Mooney & Siegel, 1986; Ponce de León & Zollikofer, 2001; Viðarsdóttir et al., 2002; Viðarsdóttir & O'Higgins, 2003; Weinberg, 2005; Bulygina et al., 2006; Bastir et al., 2007; Morimoto et al., 2008; Sardi & Ramirez-Rozzi, 2012; Freidline et al., 2015; Nicholas, 2016); however, prenatal bone modeling patterns remain poorly understood. A small number of preliminary investigations of the human fetal mandibular bone modeling patterns have been conducted (Enlow, 1975; Mauser et al., 1975; Radlanski et al., 2001, 2003), and remain to be performed on other facial bones and elements of the cranium. The analysis of young individuals (around birth) suggested that the human maxillary bone modeling pattern is already present in the first few months of life (Chapter 1). Investigating prenatal

[1] The family comprising the common ancestor of all hominins and great apes, and their descendants (Cartmill, 2018).

maxillary bone modeling patterns will establish at which stage of fetal development the conserved pattern of bone modeling can be found. Furthermore, as this thesis focused on the ontogenetic processes of the maxilla, postnatal bone modeling patterns of other facial bones remain to be examined. Some bones might show greater variation in bone modeling than the maxilla. For example, sex-specific craniofacial patterns of growth and development have been highlighted in humans, which relate to changes in rates and/or timings of development (Bulygina et al., 2006). Thus, sex-specific bone modeling patterns could be found in sexually dimorphic facial regions (such as the supraorbital margin, nasal and zygomatic bones), particularly around the growth peak occurring at puberty in humans (e.g., Björk & Skieller, 1976; Rosas & Bastir, 2002; Bulygina, 2006; Maddux, 2011). However, the preliminary results of this thesis could not find differences between male and female bone modeling patterns in both humans and chimpanzees, which might again indicate differences in cellular rates rather than in the location of the bone modeling patterns.

Investigating the latter point will thus be of major interest for future ontogenetic studies. In a study employing synchrotron X-ray imaging techniques on dry bones of fishes, Davesne and co-authors (2020) observed a relationship between large osteocytes lacunae and fast growing bone, suggesting that osteocytes might play a key role in bone formation rate. Future explorations of osteocytes lacunae in mammals could be facilitated by the use of non-destructive methods such as Nano-Computed tomography and synchrotron imaging (Sanchez et al., 2012), and bring new insights into the study of cellular rates. Furthermore, the analysis of angiogenesis (i.e., the development of new blood vessels) could act as a proxy for the rate and timing of bone development as proposed by some authors (Percival & Richtsmeier, 2013; Percival et al., 2017). In a preliminary examination of maxillary vascularization carried out during this thesis, I found a correlation between the number of vascular foramina and age (i.e., high number of foramina were associated to young individuals, while low number of foramina were associated to older individuals) in different parts of the bone (Schuh et al., 2017).

Moreover, bone modeling studies should be extended to a wider range of primate species. Indeed, non-human primates show various degrees of facial projections, from the highly anteriorly projected Papionin face to the more vertically oriented face of the squirrel monkey (S*aimiri sciureus*; Schultz, 1955; Corner & Richtsmeier, 1992; Neaux et al., 2018). The analysis of non-human primate bone modeling patterns will allow future studies to build stronger hypotheses on the relationship between bone modeling and facial orientation. Furthermore, it is still unclear if differences in bone modeling patterns can be found in closely related species, such as chimpanzees and bonobos. This will also help to refine which aspects of bone modeling are specific to hominins, and which are shared between all hominids. According to the results of Chapter 3, the chimpanzee bone modeling pattern displays some similarities with the reported maxillary pattern of the Pliocene hominin species *Paranthropus*, as they both express resorption in the premaxilla from early ontogenetic stages (Bromage, 1989; McCollum, 2008). Moreover, Lacruz et al. (2015a) found bone resorption in the premaxilla of *Australopithecus sediba*. This could suggest that resorption in the premaxilla is a plesiomorphic condition. However, contradicting results have been raised by Bromage (1989) and McCollum (2008) who only found bone formation in the

premaxilla of some specimens of *Australopithecus africanus* and *afarensis* (n = 13). Future work should seek to address bone modeling variability in other species of great apes, as well as on larger samples of early hominins. This will help to distinguish which facial traits are primitive versus derived in these taxa.

Similar questions apply to other hominins. Unlike humans, Neanderthals have an inflated maxilla (Rak, 1986; Arsuaga et al., 1997, 1999; Bermúdez de Castro et al., 1997; Rightmire , 1998; Maddux & Franciscus, 2009). Preliminary investigations of the midfacial and mandibular bone modeling patterns in Neanderthals and their ancestors found differences in bone modeling patterns compared to *H. sapiens* (Rosas & Martínez-Maza, 2010; Martínez-Maza et al., 2011; Lacruz et al., 2015b). This supports previous work showing that Neanderthals possess a different facial ontogenetic trajectory (Krovitz , 2003; Cobb & O'Higgins, 2004; Williams & Krovitz, 2004; Bastir et al., 2007). However, the relationship between the development of Neanderthal facial features and their respective bone modeling patterns remains largely unclear. Applying the methods of this thesis on a large sample of Neanderthal specimens (including newborn and young individuals for which data were collected during this thesis) will help clarify the ontogenetic process underlying Neanderthal facial morphology. Additionally, future studies focusing on older fossils (such as from the Early and Middle Pleistocene) will shed light on the origins of both the Neanderthal and *H. sapiens* face. Lacruz and co-authors (2013) analyzed the facial bone modeling patterns of the juvenile fossil *H. antecessor* (Bermudez de Castro et al., 1997). This specimen has been described as having a maxillary morphology similar to *H. sapiens*, and consequently, led some authors to place *H. antecessor* as a direct ancestor to the *H. sapiens* lineage (Bermudez de Castro et al., 1997; Arsuaga et al., 1999). The results of Lacruz and co-authors (2013) showed resorptive areas that are, according to the results of Chapter 3, more similar to the chimpanzee pattern (with bone resorption present in the premaxilla and posteriorly along the alveolar ridge). This could suggest that the *H. antecessor* maxillary bone modeling pattern is primitive in some aspects, and that a concave midface could have appeared multiple times during facial evolution through different ontogenetic patterns, as suggested by Freidline and co-authors (2013).

Lastly, a relatively novel approach in paleoanthropological studies concerns the analysis of the intricate relationship between genetic and phenotypic variation (e.g, Cheverud, 1982, 1988; Hallgrímsson et al., 2005; Szabo-Rogers et al., 2010; Mitteroecker et al., 2016; Percival et al., 2018; Gunz et al., 2019; Katz et al., 2020). To date, such research has been mostly carried in the case of syndromic facial development associated to genetic disorders, such as cleft lip and/or palate, Down, Apert and Hadju-Cheney syndromes (Boehringer et al., 2011; Heuzé et al., 2014; Canalis & Zanotti, 2016). More recently, genome-wide association studies (GWAS) allowed the discovery of new candidate genes involved in non-syndromic facial development and phenotypic variation (Adhikari et al., 2016; Liu et al., 2012; Young et al., 2010; Paternoster et al., 2012; Crouch et al., 2018; Richmond et al., 2018). Among the genes directly involved in osteoblasto- and osteoclastogenesis, NOTCH2 (Zanotti & Canalis, 2010) and RUNX2 (which has also been linked to variation in facial length and orientation in several species of mammals; Ritzman et al. 2017) might represent promising avenues to the study of facial development. This could be

addressed by applying geometric morphometric methods on mouse models who carry mutated versions of these genes, such as what has been recently conducted in collaboration with the Department of Evolutionary Genetics (MPI-EVA). More generally, future comparisons of DNA between present day humans and archaic species such as Neanderthals and Denisovans (Meyer et al., 2012; Green et al., 2010; Prüfer et al., 2014; Kuhlwilm & Boeckx, 2019), will greatly improve our understanding of the role of genetic factors in the evolutionary processes that led to the development of species-specific bony facial morphology. Aiming to adopt a holistic approach by linking large-scale changes in facial growth with microscopic changes will offer a new, dynamic vision to future facial ontogenetic studies.

Bibliography

Ackermann, R.R., & Krovitz, G.E. (2002). Common patterns of facial ontogeny in the hominid lineage. *The Anatomical Record, 269*(3), 142-147.

Adhikari, K., Fuentes-Guajardo, M., Quinto-Sánchez, M., Mendoza-Revilla, J., Camilo Chacón-Duque, J., Acuña-Alonzo, V., Jaramillo, C., Arias, W., Lozano, R.B., Pérez, G.M., Gómez-Valdés, J., Villamil-Ramírez, H., Hunemeier, T., Ramallo, V., Silva de Cerqueira, C.C., Hurtado, M., Villegas, V., Granja, V., Gallo, C., Poletti, G., Schuler-Faccini, L., Salzano, F.M., Bortolini, M.-C., Canizales-Quinteros, S., Cheeseman, M., Rosique, J., Bedoya, G., Rothhammer, F., Headon, D., González-José, R., Balding, D., & Ruiz-Linares, A. (2016). A genome-wide association scan implicates DCHS2, RUNX2, GLI3, PAX1 and EDAR in human facial variation. *Nature Communications, 7*(1), 11616.

Arsuaga, J.-L., Martínez, I., Lorenzo, C., Gracia, A., Mun, A., & Alonso, O. (1999). The human cranial remains from Gran Dolina lower Pleistocene site (Sierra de Atapuerca, Spain). *Journal of Human Evolution, 37*(3-4), 431-457.

Arsuaga, J.L., Martınez, I., Gracia, A., & Lorenzo, C. (1997). The Sima de los Huesos crania (Sierra de Atapuerca, Spain). A comparative study. *Journal of Human Evolution, 33*(2-3), 219-281.

Bastir, M., O'Higgins, P., & Rosas, A. (2007). Facial ontogeny in Neanderthals and modern humans. *Proc Biol Sci, 274*(1614), 1125-1132.

Bastir, M., & Rosas, A. (2004). Facial heights: evolutionary relevance of postnatal ontogeny for facial orientation and skull morphology in humans and chimpanzees. *J Hum Evol, 47*(5), 359-381.

Bermúdez de Castro, J.M., Arsuaga, J.L., Carbonell, E., Rosas, A., Martínez, I., & Mosquera, M. (1997). A Hominid from the Lower Pleistocene of Atapuerca, Spain: Possible Ancestor to Neandertals and Modern Humans. *276*(5317), 1392-1395.

Björk, A., & Skieller, V. (1976). Postnatal growth and developmemt of the maxillary complex. In F. A. McNamara (Ed.), *Factors Affecting the Growth of the Midface* (pp. 61-69). Ann Arbor, MI: University of Michigan Press.

Boehringer, S., van der Lijn, F., Liu, F., Günther, M., Sinigerova, S., Nowak, S., Ludwig, K.U., Herberz, R., Klein, S., Hofman, A., Uitterlinden, A.G., Niessen, W.J., Breteler, M.M.B.,

van der Lugt, A., Würtz, R.P., Nöthen, M.M., Horsthemke, B., Wieczorek, D., Mangold, E., & Kayser, M. (2011). Genetic determination of human facial morphology: links between cleft-lips and normal variation. *European Journal of Human Genetics, 19*(11), 1192-1197.

Brachetta-Aporta, N., Gonzalez, P.N., & Bernal, V. (2017). A quantitative approach for analysing bone modelling patterns from craniofacial surfaces in hominins. *Journal of Anatomy*, n/a-n/a.

Bromage, T.G. (1989). Ontogeny of the early hominin face. *Journal of Human Evolution, 18*, 751-773.

Bulygina, E., Mitteroecker, P., & Aiello, L. (2006). Ontogeny of facial dimorphism and patterns of individual development within one human population. *Am J Phys Anthropol, 131*(3), 432-443.

Canalis, E., & Zanotti, S. (2016). Hajdu-Cheney Syndrome, a Disease Associated with NOTCH2 Mutations. *Current Osteoporosis Reports, 14*(4), 126-131.

Cheverud, J.M. (1982). Phenotypic, genetic, and environmental morphological integration in the cranium. *Evolution*, 499-516.

Cheverud, J.M. (1988). A Comparison of Genetic and Phenotypic Correlations. *Evolution, 42*(5), 958-968.

---. (1996). Developmental Integration and the Evolution of Pleiotropy1. *American Zoologist, 36*(1), 44-50.

Cobb, S.N., & O'Higgins, P. (2004). Hominins do not share a common postnatal facial ontogenetic shape trajectory. *Journal of Experimental Zoology Part B: Molecular and Developmental Evolution, 302B*(3), 302-321.

Coquerelle, M., Prados-Frutos, J.C., Rojo, R., Mitteroecker, P., & Bastir, M. (2013). Short Faces, Big Tongues: Developmental Origin of the Human Chin. *PLOS ONE, 8*(11), e81287.

Corner, B.D., & Richtsmeier, J.T. (1992). Cranial growth in the squirrel monkey (Saimiri sciureus): A quantitative analysis using three dimensional coordinate data. *American Journal of Physical Anthropology, 87*(1), 67-81.

Crouch, D.J.M., Winney, B., Koppen, W.P., Christmas, W.J., Hutnik, K., Day, T., Meena, D., Boumertit, A., Hysi, P., Nessa, A., Spector, T.D., Kittler, J., & Bodmer, W.F. (2018). Genetics of the human face: Identification of large-effect single gene variants. *Proceedings of the National Academy of Sciences, 115*(4), E676-E685.

Davesne, D., Schmitt, A.D., Fernandez, V., Benson, R.B.J., & Sanchez, S. (2020). Three-dimensional characterization of osteocyte volumes at multiple scales, and its relationship with bone biology and genome evolution in ray-finned fishes. *Journal of Evolutionary Biology, 33*(6), 808-830.

Enlow, D. (1975). Handbook of Facial Growth. 423 pp. *W. B. Saunders Co*.

Enlow, D.H. (1966a). A comparative study of facial growth in Homo and Macaca. *American Journal of Physical Anthropology, 24*(3), 293-307.

---. (1966b). A morphogenetic analysis of facial growth. *American journal of orthodontics, 52*(4), 283-299.

Enlow, D.H., & Bang, D.D.S. (1965). Growth and remodeling of the human maxilla. *American journal of orthodontics, 51*(6), 446-464.

Freidline, S.E., Gunz, P., Harvati, K., & Hublin, J.-J. (2013). Evaluating developmental shape changes in Homo antecessor subadult facial morphology. *Journal of Human Evolution, 65*(4), 404-423.

Freidline, S.E., Gunz, P., & Hublin, J.J. (2015). Ontogenetic and static allometry in the human face: contrasting Khoisan and Inuit. *Am J Phys Anthropol, 158*(1), 116-131.

Gonzalez-Jose, R., Ramirez-Rozzi, F., Sardi, M., Martinez-Abadias, N., Hernandez, M., & Pucciarelli, H.M. (2005). Functional-cranial approach to the influence of economic strategy on skull morphology. *Am J Phys Anthropol, 128*(4), 757-771.

Green, R.E., Krause, J., Briggs, A.W., Maricic, T., Stenzel, U., Kircher, M., Patterson, N., Li, H., Zhai, W., & Fritz, M.H.-Y. (2010). A draft sequence of the Neandertal genome. *Science, 328*(5979), 710-722.

Gunz, P., Tilot, A.K., Wittfeld, K., Teumer, A., Shapland, C.Y., van Erp, T.G.M., Dannemann, M., Vernot, B., Neubauer, S., Guadalupe, T., Fernández, G., Brunner, H.G., Enard, W., Fallon, J., Hosten, N., Völker, U., Profico, A., Di Vincenzo, F., Manzi, G., Kelso, J., St. Pourcain, B., Hublin, J.-J., Franke, B., Pääbo, S., Macciardi, F., Grabe, H.J., & Fisher, S.E. (2019). Neandertal Introgression Sheds Light on Modern Human Endocranial Globularity. *Current Biology, 29*(1), 120-127.e125.

Hallgrímsson, B., Brown, J.J.Y., & Hall, B.K. (2005). The Study of Phenotypic Variability: An Emerging Research Agenda for Understanding the Developmental—Genetic Architecture Underlying Phenotypic Variation. In B. Hallgrímsson & B. K. Hall (Eds.), *Variation* (pp. 525-551). Burlington: Academic Press.

Hallgrimsson, B., Jamniczky, H., Young, N.M., Rolian, C., Parsons, T.E., Boughner, J.C., & Marcucio, R.S. (2009). Deciphering the Palimpsest: Studying the Relationship Between Morphological Integration and Phenotypic Covariation. *Evol Biol, 36*(4), 355-376.

Hallgrimsson, B., Lieberman, D.E., Liu, W., Ford-Hutchinson, A.F., & Jirik, F.R. (2007). Epigenetic interactions and the structure of phenotypic variation in the cranium. *Evol Dev, 9*(1), 76-91.

Heuzé, Y., Singh, N., Basilico, C., Jabs, E.W., Holmes, G., & Richtsmeier, J.T. (2014). Morphological comparison of the craniofacial phenotypes of mouse models expressing the Apert FGFR2 S252W mutation in neural crest- or mesoderm-derived tissues. *Bone, 63*, 101-109.

Johnson, P.A., Atkinson, P.J., & Moore, W.J. (1976). The development and structure of the chimpanzee mandible. *Journal of Anatomy, 122*(2), 467-477.

Katz, D.C., Aponte, J.D., Liu, W., Green, R.M., Mayeux, J.M., Pollard, K.M., Pomp, D., Munger, S.C., Murray, S.A., & Roseman, C.C. (2020). Facial shape and allometry quantitative trait locus intervals in the Diversity Outbred mouse are enriched for known skeletal and facial development genes. *PLOS ONE, 15*(6), e0233377.

Katz, D.C., Aponte, J.D., Liu, W., Green, R.M., Mayeux, J.M., Pollard, K.M., Pomp, D., Munger, S.C., Murray, S.A., Roseman, C.C., Percival, C.J., Cheverud, J., Marcucio, R.S., & Hallgrímsson, B. (2019). Facial shape and allometry quantitative trait locus intervals in the Diversity Outbred mouse are enriched for known skeletal and facial development genes. *bioRxiv*, 787291.

Krogman, W.M. (1931a). Studies in growth changes in the skull and face of anthropoids. III. Growth changes in the skull and face of the gorilla. *American Journal of Anatomy, 47*(1), 89-115.

---. (1931b). Studies in growth changes in the skull and face of anthropoids. IV. Growth changes in the skull and face of the chimpanzee. *American Journal of Anatomy, 47*(2), 325-342.

---. (1931c). Studies in growth changes in the skull and face of anthropoids. V. Growth changes in the skull and face of the orang-utan. *American Journal of Anatomy, 47*(2), 343-365.

Krovitz, G., Nelson, A., & Thompson, J. (2003). *Patterns of Growth and Development in the Genus Homo (Cambridge Studies in Biological and Evolutionary Anthropology; 37)*: Cambridge University Press.

Kuhlwilm, M., & Boeckx, C. (2019). A catalog of single nucleotide changes distinguishing modern humans from archaic hominins. *Scientific Reports (Nature Publisher Group), 9*(1).

Lacruz, R.S., Bromage, T.G., O'Higgins, P., Arsuaga, J.L., Stringer, C., Godinho, R.M., Warshaw, J., Martinez, I., Gracia-Tellez, A., de Castro, J.M., & Carbonell, E. (2015). Ontogeny of the maxilla in Neanderthals and their ancestors. *Nat Commun, 6*, 8996.

Lacruz, R.S., Bromage, T.G., O'Higgins, P., Toro-Ibacache, V., Warshaw, J., & Berger, L.R. (2015). Distinct growth of the nasomaxillary complex in Au. sediba. *Sci Rep, 5*, 15175.

Liu, F., Van Der Lijn, F., Schurmann, C., Zhu, G., Chakravarty, M.M., Hysi, P.G., Wollstein, A., Lao, O., De Bruijne, M., & Ikram, M.A. (2012). A genome-wide association study identifies five loci influencing facial morphology in Europeans. *PLoS Genet, 8*(9), e1002932.

Maddux, S.D. (2011). *A quantitative assessment of infraorbital morphology in Homo: testing for character independence and evolutionary significance in the human midface.* (Ph.D. Dissertation), Universisty of Iowa, Iowa.

Maddux, S.D., & Franciscus, R.G. (2009). Allometric scaling of infraorbital surface topography in Homo. *J Hum Evol, 56*(2), 161-174.

Martin, J.F., Bradley, A., & Olson, E.N. (1995). The paired-like homeo box gene MHox is required for early events of skeletogenesis in multiple lineages. *Genes & development, 9*(10), 1237-1249.

Martinez-Abadias, N., Mitteroecker, P., Parsons, T.E., Esparza, M., Sjovold, T., Rolian, C., Richtsmeier, J.T., & Hallgrimsson, B. (2012). The Developmental Basis of Quantitative Craniofacial Variation in Humans and Mice. *Evol Biol, 39*(4), 554-567.

Martinez-Maza, C., Freidline, S.E., Strauss, A., & Nieto-Diaz, M. (2015). Bone Growth Dynamics of the Facial Skeleton and Mandible in Gorilla gorilla and Pan troglodytes. *Evolutionary Biology, 43*(1), 60-80.

Martinez-Maza, C., Rosas, A., Garcia-Vargas, S., Estalrrich, A., & de la Rasilla, M. (2011). Bone remodelling in Neanderthal mandibles from the El Sidron site (Asturias, Spain). *Biol Lett, 7*(4), 593-596.

Martinez-Maza, C., Rosas, A., & Nieto-Diaz, M. (2013). Postnatal changes in the growth dynamics of the human face revealed from bone modelling patterns. *J Anat, 223*(3), 228-241.

Mauser, C., Enlow, D., Overman, D., & McCafferty, R. (1975). Growth and remodeling of the human fetal face and cranium. *Determinants of mandibular form and growth*, 243-275.

McCollum, M.A. (2008). Nasomaxillary remodeling and facial form in robust Australopithecus: a reassessment. *J Hum Evol, 54*(1), 2-14.

Menéndez, L., Bernal, V., Novellino, P., & Perez, S.I. (2014). Effect of bite force and diet composition on craniofacial diversification of Southern South American human populations. *American Journal of Physical Anthropology, 155*(1), 114-127.

Meyer, M., Kircher, M., Gansauge, M.-T., Li, H., Racimo, F., Mallick, S., Schraiber, J.G., Jay, F., Prüfer, K., & De Filippo, C. (2012). A high-coverage genome sequence from an archaic Denisovan individual. *Science, 338*(6104), 222-226.

Mitteroecker, P., & Bookstein, F. (2008). The evolutionary role of modularity and integration in the hominoid cranium. *Evolution, 62*.

Mitteroecker, P., Cheverud, J.M., & Pavlicev, M. (2016). Multivariate Analysis of Genotype–Phenotype Association. *Genetics, 202*(4), 1345-1363.

Mooney, M.P., & Siegel, M.I. (1986). Developmental relationship between premaxillary-maxillary suture patency and anterior nasal spine morphology. *Cleft Palate J, 23*(2), 101-107.

Morimoto, N., Ogihara, N., Katayama, K., & Shiota, K. (2008). Three-dimensional ontogenetic shape changes in the human cranium during the fetal period. *Journal of Anatomy, 212*(5), 627-635.

Neaux, D., Sansalone, G., Ledogar, J.A., Heins Ledogar, S., Luk, T.H.Y., & Wroe, S. (2018). Basicranium and face: Assessing the impact of morphological integration on primate evolution. *Journal of Human Evolution, 118*, 43-55.

Nicholas, C.L. (2016). Fetal and neonatal maxillary ontogeny in extant humans and the utility of prenatal maxillary morphology in predicting ancestral affiliation. *American Journal of Physical Anthropology, 161*(3), 448-455.

O'Higgins, P., Bromage, T.G., Johnson, D.R., Moore, W.J., & McPhie, P. (1991). A Study of Facial Growth in the Sooty Mangabey *Cercocebus atys*. *Folia Primatologica, 56*(2), 86-94.

Paternoster, L., Zhurov, A.I., Toma, A.M., Kemp, J.P., Pourcain, B.S., Timpson, N.J., McMahon, G., McArdle, W., Ring, S.M., & Smith, G.D. (2012). Genome-wide association study of three-dimensional facial morphology identifies a variant in PAX3 associated with nasion position. *The American Journal of Human Genetics, 90*(3), 478-485.

Percival, C.J., Green, R., Roseman, C.C., Gatti, D.M., Morgan, J.L., Murray, S.A., Donahue, L.R., Mayeux, J.M., Pollard, K.M., Hua, K., Pomp, D., Marcucio, R., & Hallgrímsson, B. (2018). Developmental constraint through negative pleiotropy in the zygomatic arch. *EvoDevo, 9*(1), 3.

Percival, C.J., Kawasaki, K., Huang, Y., Weiss, K., Jabs, E.W., Li, R., & Richtsmeier, J.T. (2017). The Contribution of Angiogenesis to Variation in Bone Development and Evolution. In C. J. Percival & J. T. Richtsmeier (Eds.), *Building Bones: Bone Formation and Development in Anthropology* (Vol. 77, pp. 26). Cambridge: Cambridge University Press.

Percival, C.J., & Richtsmeier, J.T. (2013). Angiogenesis and intramembranous osteogenesis. *Developmental Dynamics, 242*(8), 909-922.

Ponce de Leon, M.S., & Zollikofer, C.P.E. (2001). Neanderthal cranial ontogeny and its implications for late hominid diversity. *Nature, 412*(6846), 534-538.

Prufer, K., Racimo, F., Patterson, N., Jay, F., Sankararaman, S., Sawyer, S., Heinze, A., Renaud, G., Sudmant, P.H., de Filippo, C., Li, H., Mallick, S., Dannemann, M., Fu, Q., Kircher, M., Kuhlwilm, M., Lachmann, M., Meyer, M., Ongyerth, M., Siebauer, M., Theunert, C., Tandon, A., Moorjani, P., Pickrell, J., Mullikin, J.C., Vohr, S.H., Green, R.E., Hellmann, I., Johnson, P.L., Blanche, H., Cann, H., Kitzman, J.O., Shendure, J., Eichler, E.E., Lein, E.S., Bakken, T.E., Golovanova, L.V., Doronichev, V.B., Shunkov, M.V., Derevianko, A.P., Viola, B., Slatkin, M., Reich, D., Kelso, J., & Paabo, S. (2014). The complete genome sequence of a Neanderthal from the Altai Mountains. *Nature, 505*(7481), 43-49.

Radlanski, J.R., & Klarkowski, M.-C. (2001). Bone Remodeling of the Human Mandible during Prenatal Development. *Journal of Orofacial Orthopedics / Fortschritte der Kieferorthopädie, 62*(3), 191-201.

Radlanski, R.J., Renz, H., & Klarkowski, M.C. (2003). Prenatal development of the human mandible. 3D reconstructions, morphometry and bone remodelling pattern, sizes 12-117 mm CRL. *Anat Embryol (Berl), 207*(3), 221-232.

Rak, Y. (1986). The Neanderthal: a new look at an old face. *Journal of Human Evolution, 15*, 151-164.

Richmond, S., Howe, L.J., Lewis, S., Stergiakouli, E., & Zhurov, A. (2018). Facial Genetics: A Brief Overview. *Frontiers in Genetics, 9*(462).

Richtsmeier, J.T., Corner, B.D., Grausz, H.M., Cheverud, J.M., & Danahey, S.E. (1993). The Role of Postnatal Growth Pattern in the Production of Facial Morphology. *Systematic Biology, 42*(3), 307-330.

Rightmire, G.P. (1998). Evidence from facial morphology for similarity of Asian and African representatives of Homo erectus. *American Journal of Physical Anthropology: The Official Publication of the American Association of Physical Anthropologists, 106*(1), 61-85.

Ritzman, T.B., Banovich, N., Buss, K.P., Guida, J., Rubel, M.A., Pinney, J., Khang, B., Ravosa, M.J., & Stone, A.C. (2017). Facing the facts: The Runx2 gene is associated with variation in facial morphology in primates. *Journal of Human Evolution, 111*, 139-151.

Rosas, A., & Bastir, M. (2002). Thin-plate spline analysis of allometry and sexual dimorphism in the human craniofacial complex. *Am J Phys Anthropol, 117*(3), 236-245.

Rosas, A., & Martinez-Maza, C. (2010). Bone remodeling of the Homo heidelbergensis mandible; the Atapuerca-SH sample. *J Hum Evol, 58*(2), 127-137.

Sanchez, S., Ahlberg, P.E., Trinajstic, K.M., Mirone, A., & Tafforeau, P. (2012). Three-dimensional synchrotron virtual paleohistology: a new insight into the world of fossil bone microstructures. *Microsc Microanal, 18*(5), 1095-1105.

Sardi, M.L., & Ramirez-Rozzi, F.V. (2012). Different Cranial Ontogeny in Europeans and Southern Africans. *PLOS ONE, 7*(4), e35917.

Schultz, A.H. (1955). The position of the occipital condyles and of the face relative to the skull base in primates. *American Journal of Physical Anthropology, 13*(1), 97-120.

Schuh, A., Kupczik, K., Freidline, S.E. (2017) The relationship between maxillary bone growth and dental eruption in humans: a study using microscopy and geometric morphometric techniques. *International Symposium on Dental Morphology*, Poster.

Scott, N.A., Strauss, A., Hublin, J.-J., Gunz, P., & Neubauer, S. (2018). Covariation of the endocranium and splanchnocranium during great ape ontogeny. *PLOS ONE, 13*(12), e0208999.

Szabo-Rogers, H.L., Smithers, L.E., Yakob, W., & Liu, K.J. (2010). New directions in craniofacial morphogenesis. *Developmental biology, 341*(1), 84-94.

Todd, T.W. (1932). Prognathism: a Study in Development of the Face. *The Journal of the American Dental Association (1922), 19*(12), 2172-2184.

Viðarsdottir, S., & O'Higgins, P. (2003). Developmental variation in the facial skeleton ofanatomically modern *Homo sapiens*. In K. G. Thompson J, Nelson A (Ed.), *Patterns of growth and development in the genus Homo* (pp. 114-143). Cambridge: Cambridge University Press.

Vidarsdóttir, U.E., O'Higgins, P., & Stringer, C. (2002). A geometric morphometric study of regional differences in the ontogeny of the modern human facial skeleton. *Journal of Anatomy, 201*, 211-229.

Williams, F.L.E., & Krovitz, G.E. (2004). Ontogenetic migration of the mental foramen in Neandertals and modern humans. *Journal of Human Evolution, 47*(4), 199-219.

Xu, Q., Jamniczky, H., Hu, D., Green, R.M., Marcucio, R.S., Hallgrimsson, B., & Mio, W. (2015). Correlations Between the Morphology of Sonic Hedgehog Expression Domains and Embryonic Craniofacial Shape. *Evolutionary Biology, 42*(3), 379-386.

Young, N.M., Chong, H.J., Hu, D., Hallgrímsson, B., & Marcucio, R.S. (2010). Quantitative analyses link modulation of sonic hedgehog signaling to continuous variation in facial growth and shape. *Development, 137*(20), 3405-3409.

Zanotti, S., & Canalis, E. (2010). Notch and the skeleton. *Molecular and cellular biology, 30*(4), 886-896.

Appendix

Supplementary information

Chapter 1

S1 Percentages of bone resorption for males (M) and females (F) plotted against age (in years).

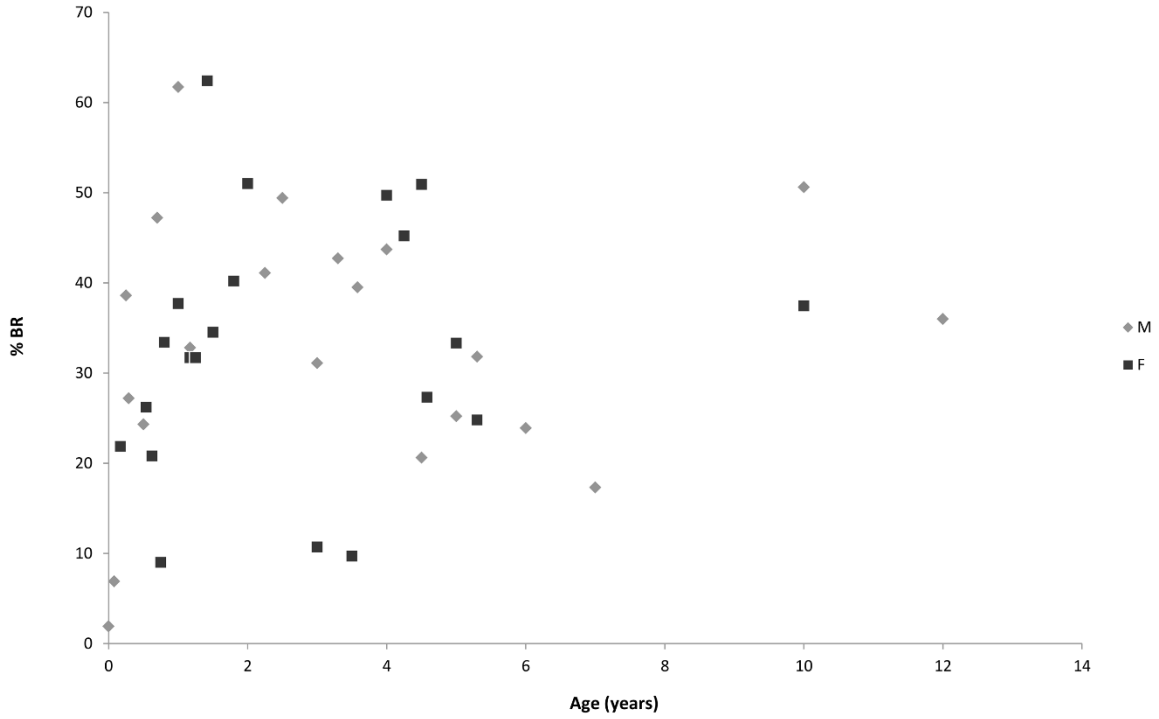

Supplementary information

Chapter 2

SI 1 Developmental simulations of ontogenetic shape trajectories. The method is tested on the Western Europeans following their own trajectory. Each simulated individual's trajectory is represented as a dotted line. Simulated individuals are shown as dots and delimited by a lined convex hull. Each age group is represented by a colored convex hull (blue: Greenlandic Inuit; orange: Western Europeans; red: South Africans). The Western European AG 4 (adults) convex hulls is shown in dark orange.

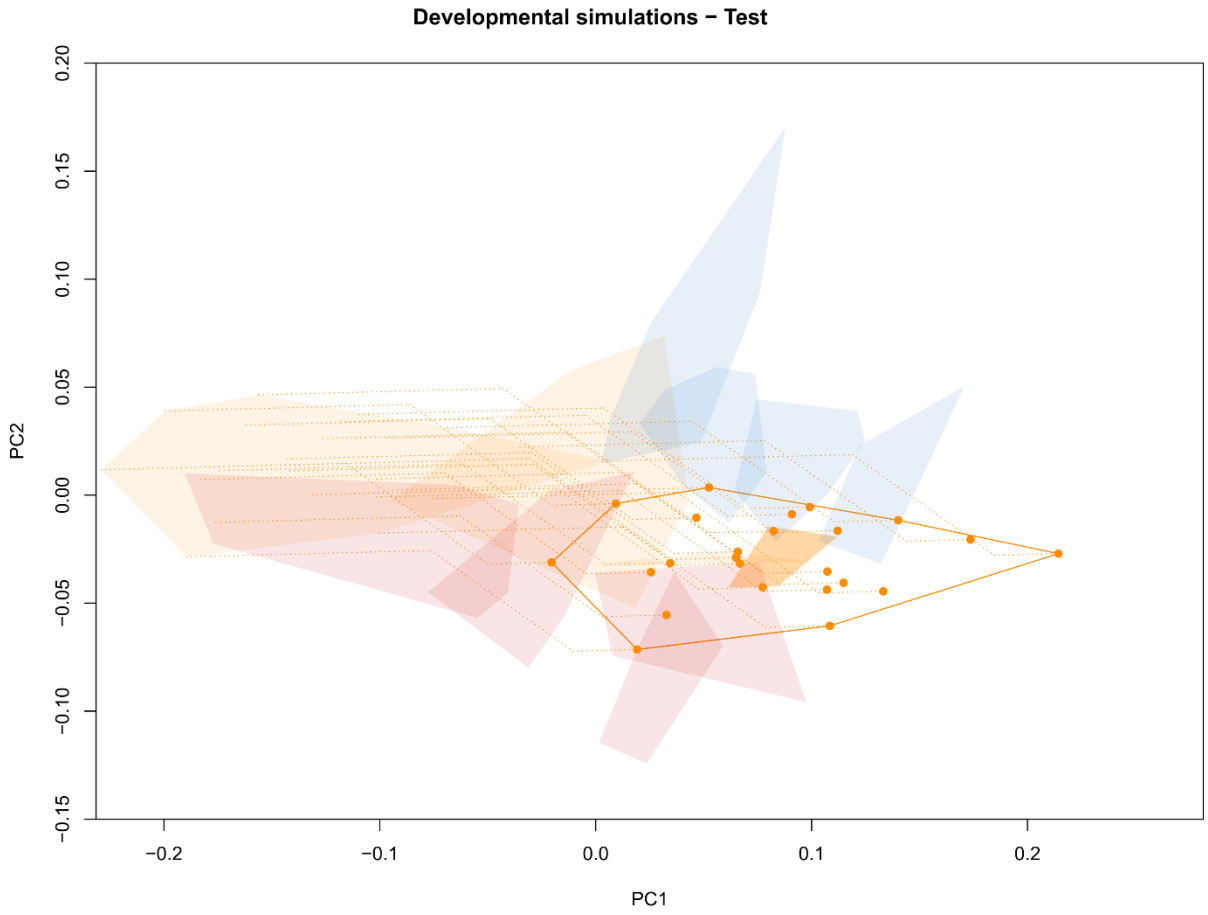

SI 2 Degree of freedom (Df), F statistics, p-values and corrected p-values (Bonferroni method) for each square of the grid after performing a MANOVA testing for population differences in the bone modeling patterns. Significant *p*-values are highlighted in bold.

	AG 1				AG 2			
Square	**Df**	**F value**	**p-value**	**Corrected**	**Df**	**F value**	**p-value**	**Corrected**
1	2	0.97	0.38	1.14	2	1.6	0.19	0.57
2	2	0.41	0.66	1.98	2	0.4	0.66	1.98
3	2	1.2	0.3	0.9	2	1.66	0.2	0.6
4	2	0.56	0.57	1.71	2	1.66	2	6
5	2	0.8	0.46	1.38	2	0.07	0.9	2.7
6	2	1.2	0.3	0.9	2	2.15	0.12	0.36
7	2	3.7	0.03	0.09	2	1.7	0.2	0.6
8	2	0.2	0.8	2.4	2	1.1	0.33	0.99
9	2	0.001	0.99	2.97	2	0.6	0.56	1.68
10	2	1.34	0.27	0.81	2	0.13	0.8	2.4
11	2	0.53	0.59	1.77	2	0.44	0.64	1.92
12	2	0.35	0.7	2.1	2	1.16	0.32	0.96
13	2	1.2	0.3	0.9	2	1.33	0.27	0.81
14	2	5.1	0.01	**0.03**	2	0.66	0.52	1.56
15	2	0.21	0.8	2.4	2	1.7	0.18	0.54
16	2	0.91	0.4	1.2	2	3.2	0.05	0.15
17	2	3.2	0.05	0.15	2	0.98	0.38	1.14
18	2	2.3	0.1	0.3	2	0.82	0.44	1.32
19	2	1.55	0.22	0.66	2	2.07	0.13	0.39
20	2	9.34	0.0004	**0.0012**	2	1.4	0.3	0.9
21	2	7.22	0.002	**0.006**	2	1.3	0.3	0.9
22	2	3.5	0.04	0.12	2	6.5	0.003	**0.009**
23	2	2.8	0.07	0.21	2	4.61	0.01	**0.03**
24	2	1.55	0.22	0.66	2	0.33	0.7	2.1
25	2	0.13	0.88	2.64	2	1.8	0.17	0.51
26	2	4.7	0.01	**0.03**	2	0.03	0.96	2.88
27	2	1.57	0.22	0.66	2	22.5	1.40E-07	**4.20E-07**
28	2	0.89	0.41	1.23	2	3.03	0.06	0.18
29	2	1.96	0.15	0.45	2	1.22	0.3	0.9
30	2	2.27	0.11	0.33	2	7.9	0.001	**0.003**
31	2	0.73	0.48	1.44	2	1.7	0.19	0.57
32	2	2.2	0.12	0.36	2	1.34	0.27	0.81

SI 3 Two-block partial least square (PLS) analysis between the bone modeling and the shape residuals (SW 1). X axis: bone modeling data. Y axis: shape residuals. Variability in each population is represented by convex hulls. Blue: Greenlandic Inuit, red: South African, orange: Western European. Age group means are represented at each age group by dots and numbers following the same color code. Solid lines connect the subsequent means.

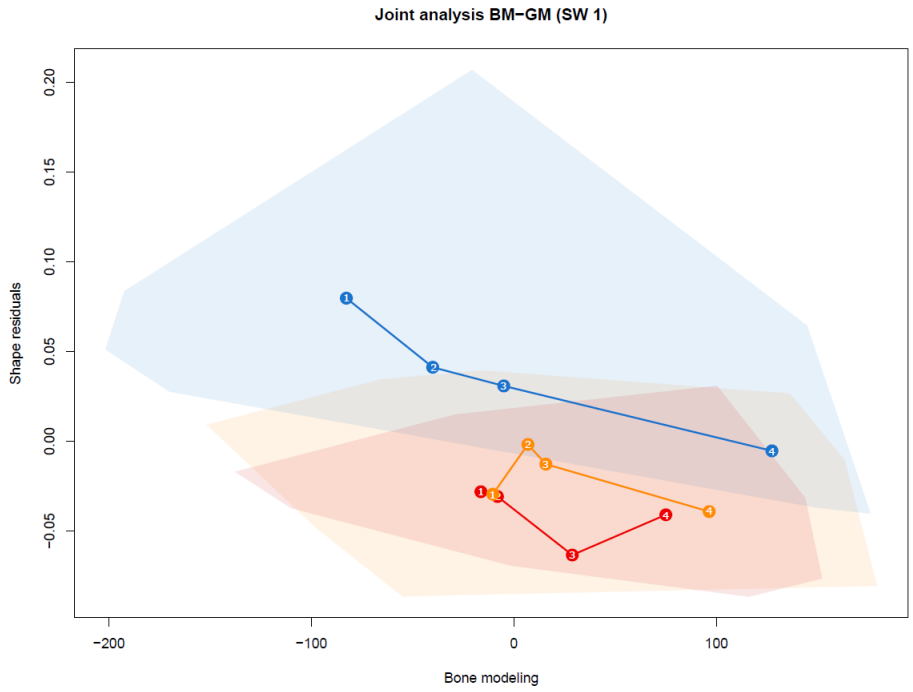

SI 4 Percentage of total covariance, correlation coefficient and p-value, computed for the first singular warp (SW 1) of the PLS analysis between the Procrustes shape residuals and the bone modeling data on all populations.

	% Total covariance	Correlation coefficient (R)	*p*-value
Shape residuals	56.1	0.37	**0.02**

Supplementary information

Chapter 3

SI 1 Reference numbers, age, sex (M: males; F: females; NA: unknown) and location of individuals used in the study.

	Reference number	Age (years)	Sex	Location
H. sapiens	100	7	M	a
	100A	11	M	a
	101	12	F	a
	126	8	M	a
	199	13	F	a
	201	12	M	a
	1879-73-121	5	F	b
	1886-87-99	6	M	b
	1890-91-21	10	M	b
	1891-92-49	6	M	b
	1892-93-285	10	F	b
	1892-93-286_180	0.83	F	b
	1892-93-307	0.5	M	b
	1892-93-308_199	1	F	b
	1892-93-320	3.58	M	b
	1892-93-321_202	3.5	F	b
	1893-94-5	5	M	b
	1893-94-8_210	4.5	F	b
	1893-94-9	3	F	b
	1893-94-10_212	5	F	b
	1893-94-11	2.5	M	b
	1893-94-52_222	1.42	F	b
	1893-94-58	0.29	M	b
	1893-94-74	6	M	b
	1893-94-86	4	M	b
	1893-94-113_248	1.17	F	b
	1894-95-25	2	F	b
	1894-95-142_277	0.5	M	b
	1894-95-159_281	1.83	F	b
	1895-96-127_308	0.17	F	b
	1896-97-6_314	1.17	M	b
	1896-97-15_319	4	F	b
	1896-97-16	4.58	F	b
	1896-97-17_321	0.67	M	b
	1896-97-77_325	0	M	b
	1896-97-78_328	1.5	F	b

	1897-98-164_388	1	M	b
	1898-99-156	4.25	F	b
	1898-99-231	2	F	b
	1898-99-232_476	0.83	F	b
	1899-288-512	4.5	M	b
	1899-299-513	0.58	F	b
	1900-109-542	0.25	F	b
	1900-123-544	0.67	M	b
	1900-156-551	4	F	b
	1901-51-562	2	F	b
	1902-03-46_574	5.33	F	b
	1902-03-53_577	1.25	F	b
	1902-144-594	12	M	b
	1903-20-599	3	F	b
	1904-89-616	2.25	M	b
	1906-07-37	7	M	b
	1919-14	4	M	b
	218	10	F	c
	284	17	F	c
	342	28	F	c
	46	38	M	c
	52	38	F	c
	92	27	M	c
P. troglodytes verus	11776	11	F	d
	11777	2	M	d
	11780	25	F	d
	11783	5	F	d
	11787	0.06	M	d
	11788	3.75	F	d
	11789	14	M	d
	11790	9	F	d
	11791	6.41	NA	d
	11792	12	F	d
	11796	NA	M	d
	11903	19	M	d
	12175	5	M	d
	13432	2	M	d
	13433	7.6	M	d
	13437	11.4	F	d
	13438	NA	M	d
	14991	8	F	d
	14992	NA	M	d

14993	NA	F	d
14994	NA	F	d
15000	NA	NA	d
15002	NA	F	d
15003	NA	NA	d
15005	6	M	d
15011	7	M	d
15013	NA	F	d
15015	0.17	NA	d
15019	14	M	d
15020	10	F	d
15030	0.67	M	d
15040	NA	F	d
15041	NA	F	d

a. Anatomical Institute, Leipzig (Germany); b. Anatomical Institute, Strasbourg (France); c. Anthropological collection of the University of Coimbra, Portugal; d. Max Planck Institute for Evolutionary Anthropology, Leipzig (Germany)

SI 2 Landmarks and semilandmarks numbers, labels and definitions (total: 249) used in the template (SI 3).

Landmarks	**Labels**
Fixed	
Superolateral nasion	1
Dacryon	2
Zygoorbitale	3
Inferolateral rhinion	4
Anterior nasal spine	5
Alveolare (infradentale superius)	6
Zygomaxillare	7
Malar root origin	8
Maxillo-palatine suture	9

Curve semilandmarks		***Number - definition***
Fronto-maxillary suture	Fms	2 – superolateral nasion to dacryon
Naso-maxillary suture	Nms	6 – superolateral nasion to inferolateral rhinion
Inferior orbital margin	Iom	6 – dacryon to zygoorbitale
Nasal aperture outline	Nao	6 – inferolateral rhinion to anterior nasal spine
Subnasal outline	So	3 – nasal spine to alveolar
Zygomatico-maxillary suture	Zms	5 – zygoorbitale to zygomaxillare
Maxillary contour	Mc	4 – zygomaxillare to malar root origin
Alveolar outline	Ao	8 – alveolare to maxillo-palatine suture
Surface semilandmarks		200 – covering the whole surface of the bone

SI 3 Template of the right maxilla (see SI 2 for the description of the labels).

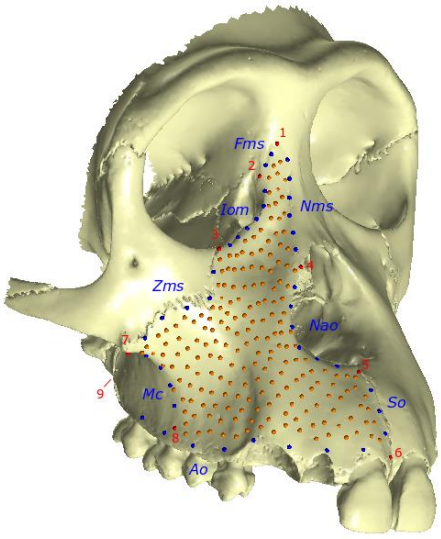

View 1

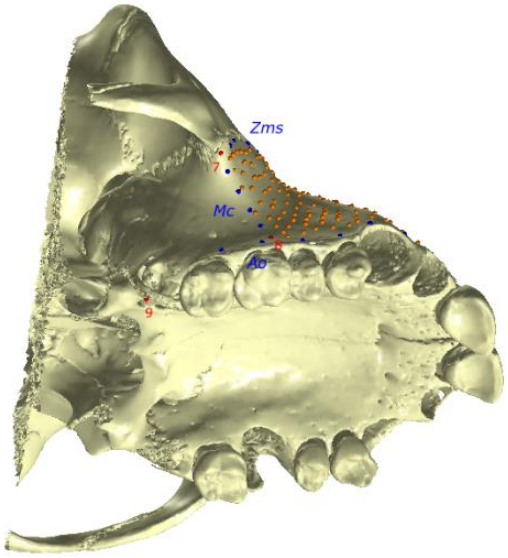

View 2

SI 4 Mean bone modeling maps at each age group for males and females chimpanzees.

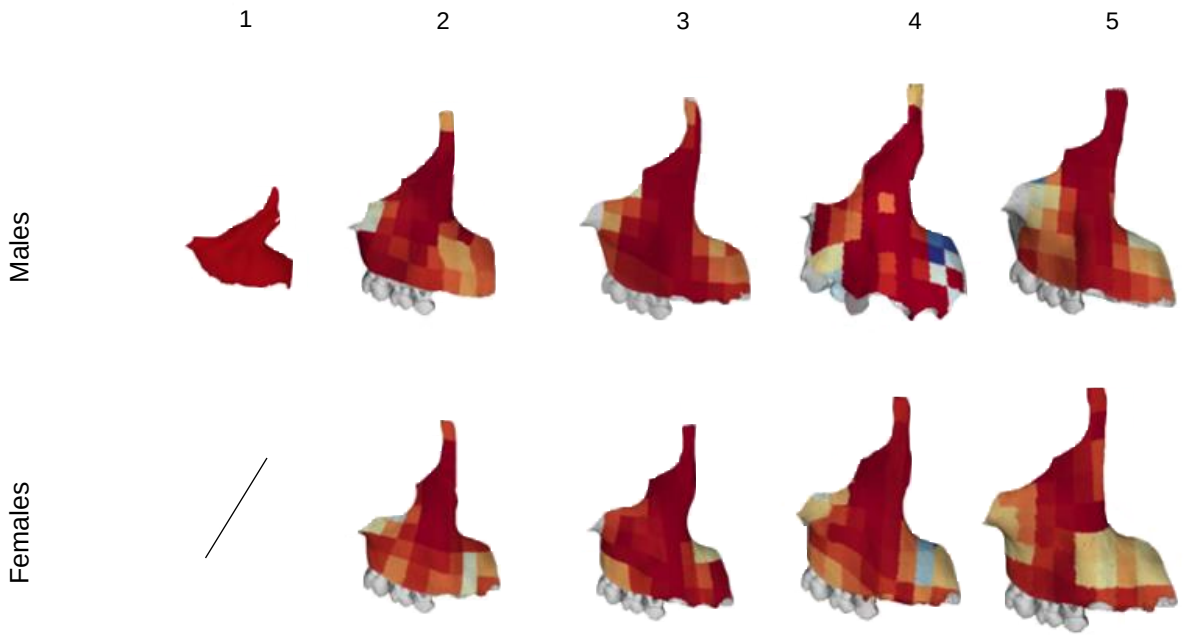

SI 5 Two-block partial least square (PLS) analysis between the bone modeling and morphological data (second and third singular warps; SW 2 and 3). X axis: bone modeling data. Y axis: Procrustes shape coordinates. Blue: *Homo sapiens*, green: *Pan troglodytes verus*. Convex hulls delimit each age group. Age group means are represented by dots. The two individuals in the chimpanzee AG 1 and the human AG 4 are connected by a line. Solid lines connect the subsequent means.

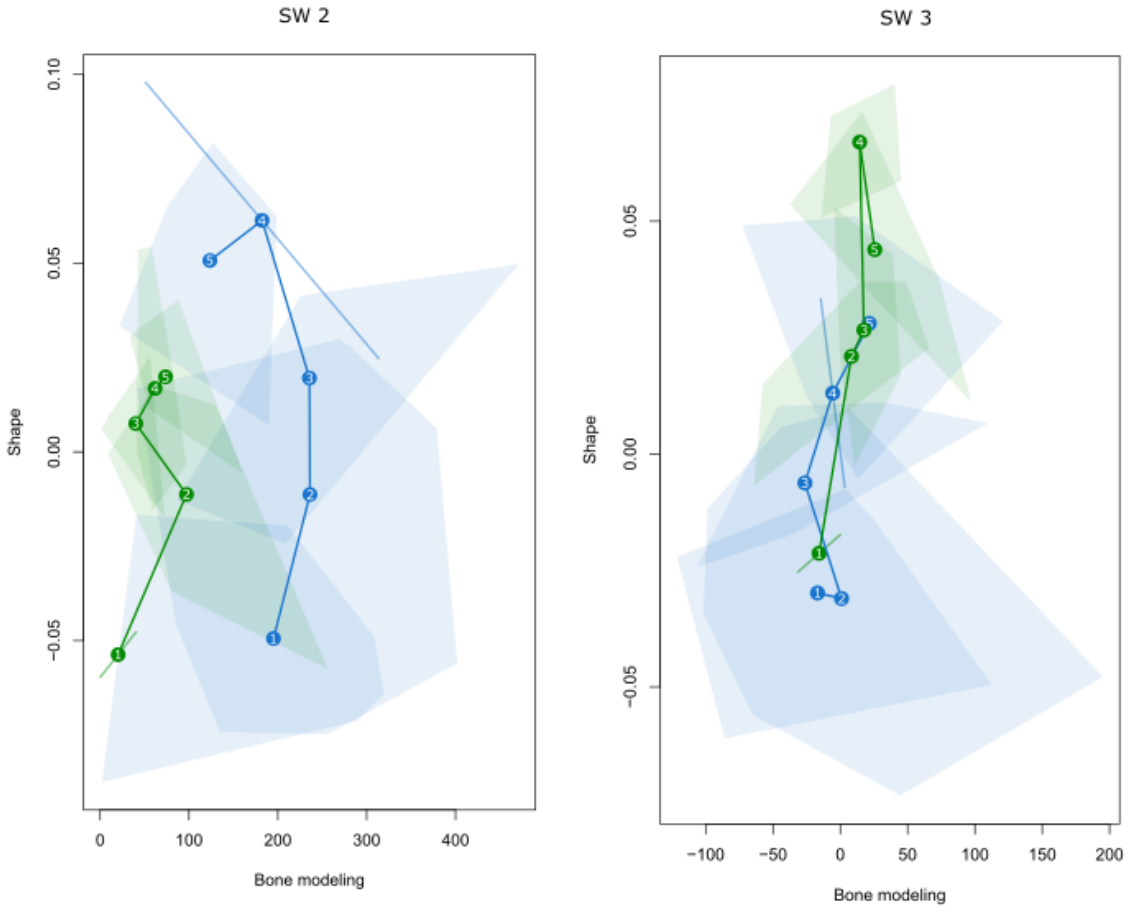

Author contributions

Alexandra Schuh

Quantification of maxillary ontogenetic processes using surface histology and geometrics morphometrics

---

Author contribution statement

Title: Ontogeny of the human maxilla: a study of intra-population variability combining surface bone histology and geometric morphometrics

Journal: Journal of Anatomy (Published)

Authors: Alexandra Schuh, Kornelius Kupczik, Philipp Gunz, Jean-Jacques Hublin, Sarah E. Freidline

---

Alexandra Schuh (First author):

- Study design
- Data collection
- Data analysis
- Writing of the manuscript

Kornelius Kupczik (Author 2):

- Study design
- Provided access to the necessary material
- Comments on the manuscript

Philipp Gunz (Author 3):

- Data analysis
- Comments on the manuscript

Jean-Jacques Hublin (Author 4):

- Funding acquisition

Sarah E. Freidline (Senior author):

- Project idea
- Study design
- Data collection
- Data analysis
- Comments on the manuscript

A. Schuh

Alexandra Schuh

Sarah E. Freidline

Alexandra Schuh

Quantification of maxillary ontogenetic processes using surface histology and geometrics morphometrics

---

Author contribution statement

Title: Intraspecific variability in human maxillary bone modeling patterns during ontogeny

Journal: American Journal of Physical Anthropology (Published)

Authors: Alexandra Schuh, Philipp Gunz, Chiara Villa, Kornelius Kupczik, Jean-Jacques Hublin, Sarah E. Freidline

---

Alexandra Schuh (First author):

- Project idea
- Study design
- Data collection
- Data analysis
- Writing of the manuscript

Philipp Gunz (Author 2):

- Data analysis
- Comments on the manuscript

Jean-Jacques Hublin (Author 5):

- Funding acquisition

Chiara Villa (Author 3):

- Data curation
- Provided access to the necessary material
- Comments on the manuscript

Kornelius Kupczik (Author 4):

- Provided access to the necessary material
- Comments on the manuscript

Sarah E. Freidline (Senior author):

- Project idea
- Study design
- Data analysis
- Comments on the manuscript

A. Schuh

Alexandra Schuh

Sarah E. Freidline

Alexandra Schuh

Quantification of maxillary ontogenetic processes using surface histology and geometrics morphometrics

---

Author contribution statement

Title: Quantifying maxillary development in chimpanzees and humans: an analysis of prognathism and orthognathism at the morphological and microscopic scales

Journal: Journal of Human Evolution (Submitted)

Authors: Alexandra Schuh, Philipp Gunz, Kornelius Kupczik, Jean-Jacques Hublin, Sarah E. Freidline

---

Alexandra Schuh (First author):

- Project idea
- Study design
- Data collection
- Data analysis
- Writing of the manuscript

Philipp Gunz (Author 2):

- Comments on the manuscript

.Kornelius Kupczik (Author 3):

- Provided access to the necessary material
- Comments on the manuscript

Jean-Jacques Hublin (Author 4):

- Funding acquisition

Sarah E. Freidline (Senior author):

- Study design
- Comments on the manuscript

A. Schuh

Alexandra Schuh

Sarah E. Freidline

Curriculum Vitae

Alexandra Schuh
Brandvorwerkstrasse, 32
04275 Leipzig, Germany

Tel. +49 (0)172 8492 166
@ alexandra_schuh@eva.mpg.de

CURRENT POSITION

May 2016 - **PhD candidate, Max Planck Institute for Evolutionary Anthropology, Leipzig School of Human Origins, Leipzig, Germany**

Project title: "Quantification of maxillary ontogenetic processes using surface histology and geometrics morphometrics"

Supervision: Sarah Freidline, Kornelius Kupczik, Jean-Jacques Hublin

UNIVERSITY EDUCATION

2012 – 2014 **University of Bordeaux, France**
Master degree in biological Anthropology and Prehistory, specialty: Human evolution

Master thesis: *The use of three dimensional imaging methods for the virtual reconstruction of the Qafzeh's 25 mandible (unpublished fossil, Middle Paleolithic, Israel)*.
Dir.: Tillier A.-m., Coqueugniot H., Dutailly B.

2011 – 2012 **University of Montreal, Quebec, Canada**
Bachelor in Biology, 3thd year; specialty: Cellular Biology and Physiology

2009 - 2011 **University of Strasbourg, France**
Bachelor in Biology, 1st and 2nd years; specialty: Cellular Biology and Physiology

ADDITIONAL TRAININGS

May/June 2020 **Bone histology – virtual sessions**
Resp.: J. Miszkiewicz

May 2017 **Advanced data visualization with R**
Resp.: C. Neumann

March 2016 **National Museum of Natural history, Paris, France**
1. *Comportements, anatomie des Primates Non Humains et évolution de l'Homme*
2. *Primates Non Humains et humains d'aujourd'hui : interactions et conservation*

Resp.: S. Krief

April 2015	**National Museum of Natural history, Paris, France** *Morphometry and forms analysis.* Resp.: M. Baylac
April 2013	**National Museum of Natural history, Paris, France** *Méthodes d'analyses en paléoanthropologie: du pourquoi au comment* Resp.: F. Detroit, M. Friess, A. Balzeau

SKILLS

Human evolution, Paleobiology, ontogeny, osteology, age/sex determination, archaeothanatology, 3D imaging, geometric morphometric techniques, virtual reconstruction, confocal microscopy

***Softwares*:** R, Geomagic, Viewbox, Avizo (VSG), Morphologica, Landmark app., MorphoJ, ImageJ

***Tools*:** MicroScribe, NextEngine; SmartZoom 5 digital microscope, Nanofocus confocal microscope

TEACHING

Oct. 2019	IMPRS – Leipzig School of Human Origins, Leipzig, Germany
May 2019	Molecular Anthropology Course, Leipzig, Germany
Oct. 2018	IMPRS – Leipzig School of Human Origins, Leipzig, Germany

FIELD WORK

June 2015	**Grotte de Sirogne**, Rocamadour, France. Middle Palaeolithic. *Dir.: P. Bayle*
July 2014	**La Colline du Château**, Nice, France. Middle Age. *Dir.: A. Civetta*
June 2013	**La Caune de l'Arago**, Tautavel, France. Middle Palaeolithic. *Dir.: A.-m. Moigne* **Amelestoy**, Pyrénées Atlantiques, France. Bronze Age. *Dir.: P. Courtaud*

LANGUAGES

French (native language)
English (fluent)
German (basic notions)

Publications and presentations

PUBLICATIONS

Schuh A., Kupczik K., Gunz P., Hublin J.-J., & Freidline S.E., 2021. Quantifying maxillary development in chimpanzees and humans: an analysis of prognathism and orthognathism at the morphological and microscopic scales. *Submitted*

Schuh, A., Gunz, P., Villa, C., Kupczik, K., Hublin, J. J., & Freidline, S. E., 2020. Intraspecific variability in human maxillary bone modeling patterns during ontogeny. *American Journal of Physical Anthropology*, 173, 655-670.

Schuh A., Kupczik K., Gunz P., Hublin J.-J., & Freidline S.E., 2019. Ontogeny of the human maxilla: a study of intra-population variability combining surface bone histology and geometric morphometrics. *Journal of Anatomy*, 235(2), 233-245.

Schuh A., Dutailly B., Coutinho Nogueira D., Santos F., Arensburg B., Vandermeersch B., Coqueugniot H., & Tillier A.-M., 2016. La mandibule de l'adulte Qafzeh 25 (Paléolithique moyen, Basse Galilée). Reconstruction virtuelle 3D et analyse morphométrique. *Paléorient*, 43, 49-59.

PRESENTATIONS

Podiums

Sept. 2019 — **Neanderthal maxillary ontogeny at the micro- and macroscopic scales: an integrative approach to study facial growth.** Schuh A., Maureille B., Toussaint M., Abrams G., Bonjean D., Gunz P., Hublin J.-J., Freidline S.
ESHE conference, Liege, Belgium

Jan. 2019 — **Variabilité intra-spécifique des processus de modelage osseux durant la croissance de l'os maxillaire chez Homo sapiens.** Schuh A., Kupczik K., Hublin J.-J., Freidline S.E.
Annual meetings of the Anthropological Society of Paris (SAP), Paris, France

Posters

Sept. 2018	**Ontogeny of the human maxilla: a study of intra specific variation using surface histology and geometric morphometrics.** Schuh A., Villa C., Kupczik K. and Freidline S. *ESHE conference, Faro, Portugal*
Apr. 2018	**Bone modeling patterns in the midface of modern humans during ontogeny: a study of intraspecific variability.** Schuh A. and Freidline S. *AAPA conference, Austin, USA*
Oct. 2017	**The relationship between maxillary bone growth and dental eruption in humans.** Schuh A., Kupczik K., Freidline S. *ISDM conference, Bordeaux, France*
Sept. 2017	**Ontogeny of the midface in H. sapiens: building an integrative growth model for paleoanthropological studies using bone modelling and geometric morphometrics.** Schuh A., kupczik K., Freidline S. *ESHE conference, Leiden, Netherlands*
Jan. 2016	**La mandibule de l'adulte Qafzeh 25 (Paléolithique moyen, Basse Galilée) et sa reconstruction virtuelle 3D. Implications anthropologiques. Schuh A.,** Dutailly B., Coqueugniot H., Santos F., Coutinho Nogueira D., Arensburg B., Vandermeersch B., Tillier A.-M. Annual meetings of the Anthropological Society of Paris (SAP), Lyon, France

Declaration of independence

Max-Planck-Institute
for evolutionary Anthropology
Department of Human Evolution
Deutscher Platz 6
04103 Leipzig

MAX-PLANCK-GESELLSCHAFT

DECLARATION OF INDEPENDENCE

I hereby declare that I have conceived and written the thesis "*Quantification of maxillary ontogenetic processes using surface histology and geometric morphometrics*" independently, without any inadmissible help and without using resources other than those stated. All direct and indirect quotations from the work of others have been clearly identified as such. I have not previously attempted to complete this or any other doctorate degree.

Leipzig, November 19, 2020

A. Schuh

Alexandra Schuh